To the Graduate Council:

I am submitting herewith a dissertation written by Michael Ray Caudill entitled "Paleoclimate, Burial Compaction, and Perched Water Tables; Carboniferous Vertic Paleosols, Ohio and Tennessee." I have examined the final copy of this dissertation for form and content and recommend that it be accepted in partial fulfillment of the requirements for the degree of Doctor of Philosophy, with a major in Geology.

Steven G. Driese

Steven G. Driese, Major Professor

We have read this dissertation
and recommend its acceptance:

Kenneth R. Walker

Claudia I. Mora

John T. Andrews

Accepted for the Council:

Carolyn Hodges

Associate Vice Chancellor and
Dean of The Graduate School

PALEOCLIMATE, BURIAL COMPACTION, AND PERCHED WATER TABLES; CARBONIFEROUS VERTIC PALEOSOLS, OHIO AND TENNESSEE

A Dissertation
Presented for the
Doctor of Philosophy
Degree
The University of Tennessee, Knoxville

Michael R. Caudill
December, 1996

DEDICATION

For Kim and Damian

I am forever indebted for the love, support, and sacrifice that made this undertaking possible.

ACKNOWLEDGMENTS

This research was supported by Petroleum Research Fund (PRF) Grant #25678-AC8-C-SF94 and by National Science Foundation (NSF) Grants #EAR-9206540 and EAR-9418183, awarded jointly to S. Driese and C. Mora. The Antoinette Lierman-Medlin Field Study Award, administered by the Coal Geology Division of the Geological Society of America (GSA), and a Southeastern Section GSA Student Research Grant, both awarded to Caudill, provided additional support.

I gratefully acknowledge the field assistance of members of the 1992 Graduate Seminar in Paleopedology; K. Tobin, and J. Dorsch., and F.W. Stapor (Tennessee Tech University) also assisted with field work on the Pennington paleosol (Chapter 2). In this regard, I am especially indebted to B.Glumac and S. Sherwood, who provided some of the thin section descriptions and photomicrographs. O. Kopp provided guidance with operation of the XRF. I am indebted to the Ohio Department of Natural Resources, Division of Geological Survey for unfettered access to their extensive core library.

Chapter 2 benefitted from the insightful comments of M. Kraus (*JSR* Associate Editor), R. Blodgett and T. Bown *(JSR* reviewers), and the careful editing of J. Southard (*JSR* Editor). Editorial comments from G. Plint (*Sedimentology* Associate Editor), and G. Retallack and B. Blodgett (*Sedimentology* reviewers) improved Chapter 3. Reviews by members of my research committee S. Driese, C. Mora, K. Walker, and T. Ammons) greatly improved the quality of this dissertation.

I am deeply indebted to S. Driese for sheperding my pursuit of a Ph.D. Sincerest thanks to my Mother and Father, Eula and Kirk, for the examples they set.

ABSTRACT

A Late Mississippian paleosol, in central Tennessee, satisfying all of the morphological criteria set forth in Soil Taxonomy for Holocene Vertisols provides quantitative paleoclimate information, in addition to the now commonplace interpretation of precipitation seasonality based on the presence of vertic features. Paleo-precipitation was estimated using the empirical relationship between depth to pedogenic carbonate horizon in Quaternary soils. Burial compaction, erosional truncation, and high paleoatmospheric CO_2 concentration, all factors which complicate paleo-precipitation estimates, are unusually well-constrained for this paleosol. Allowing for 10% compaction, the paleosol had a pre-burial depth of 100 cm for the pedogenic carbonate horizon, yielding a mean annual paleo-precipitation estimate of 648 mm $\pm$141. This is comparable to the mean annual precipitation for Brownsville, Texas, where similar soils are found today. A dolomicrite crust, developed in gilgai micro-lows, is well-preserved in the paleo-Vertisol. Higher Late Mississippian paleotemperatures and rates of evapotranspiration associated with a lower latitude paleogeography for central Tennessee during the Late Mississippian may explain in part why Holocene coastal Vertisols in the Brownsville region lack surficial crusts. The Late Mississippian climate of central Tennessee is qualitatively defined as semi-arid.

Burial compaction is one of several major obstacles to estimating paleo-precipitation from depth to pedogenic carbonate in favorably preserved paleosols. Paleosols must be decompacted and pre-burial depth to pedogenic carbonate obtained. Vertic paleosols may be particularly good candidates for paleoprecipitation estimates,

because of an increased likelihood of preserving clastic dikes, one of the best features for estimating burial compaction. Compaction estimates from clastic dikes and literature - based depth of burial estimates suggest that vertic paleosols undergo significantly less burial compaction than may be commonly assumed. Late Carboniferous vertic paleosols, buried to 2.5 to 3.0 km, compacted to 93% of their original thickness. In contrast, clastic dikes in a non-pedogenic shale directly underlying one of the Late Carboniferous paleosols records compaction to 70% of original thickness. Similarly obtained burial compaction and burial depth estimates for Early Carboniferous, Ordovician, and Proterozoic vertic paleosols are used to test a burial compaction curve and equation specific for vertic paleosols. Results suggest that this "vertic-calibrated" curve and equation can be used to estimate burial compaction for vertic paleosols lacking clastic dikes, but additional testing is needed. Naturally high bulk densities may have limited the compactability of vertic paleosols. Likewise, high initial bulk density and an abundance of swelling-clays may have severely limited the transmissivity of vertic paleosols as they passed from pedogenic to burial environments. Thus, upon burial vertic paleosols may have behaved as closed systems, which has implications for understanding their diagenetic modification. Additional efforts to understand burial compaction of vertic paleosols also promise to improve our understanding of aquifer/aquiclude and hydrocarbon/reservoir relationships in sedimentary basins containing intercalated paleosols.

The Harlem coal (Upper Pennsylvanian) is genetically related to the underlying, vertic, sub-Ames paleosol complex. Color patterns in the paleosol complex appear to

have survived burial diagenesis and provide sensitive data on soil drainage and redox conditions. Catenary relationships preserved by the paleosol complex, indicate that soil drainage setting, largely a reflection of subtle topographic differences on the paleo-landscape, controlled initiation of the Harlem coal swamp. In the study area, paleotopography reflected the presence of an abandoned fluvial channel tract, or perhaps a marginal-marine bar complex (distributary mouth bar?) stranded on a broad, newly exposed surface created by withdrawal of the pre-Ames sea from the Appalachian basin. The Harlem peat accumulated in isolated topographic lows following local establishment of saturated zones in the top of the paleosol complex. Development of perched water tables was facilitated by formation of clay-enriched subsoil intervals. The clay-enriched intervals record the onset of long-wet/short-dry seasonality in precipitation and a corresponding decrease in the intensity of churning in the soil body. As the new, wetter climate became established, perched zones of saturation grew upwards to intersect the soil surface and initiated coal swamps. During the subsequent "Ames" transgression, the paleolandscape influenced deposition such that marine limestones were deposited on local topographic highs. The casual, routine invocation of a transgression-driven, broad, ubiquitous, uniformly rising regional water table to explain the initiation of coals swamps is not compatible with the gross color patterns preserved in the paleosol complex. Rather, the incipient Harlem coal swamp, feed by saturated zones in the top of the paleosol complex, records the onset of a wetter climate nourished by a new source of surface moisture, made available by expansion of the "Ames" sea.

TABLE OF CONTENTS

CHAPTER		PAGE
I.	INTRODUCTION	1
II.	PRESERVATION OF A PALEO-VERTISOL AND AN ESTIMATE OF LATE MISSISSIPPIAN PALEO-PRECIPITATION	5
	Introduction	5
	Location and Methods	7
	Stratigraphy and Depositional Setting	10
	Outcrop Descriptions	11
	Profile Descriptions	11
	Subjacent and Superjacent Strata	18
	Micromorphology	18
	Paleosol Matrix	18
	Concretions and Nodules	19
	Dolomicrite Crust	22
	Mineralogy	25
	Interpretations and Discussion	26
	Local Paleogeography	26
	Claystone Paleo-Vertisol	26
	Origin of Dolomitic Carbonate Nodules	31
	Origin of Dolomitic Crust	33
	Estimate of Paleo-Precipitation	36
	Precipitation and Depth-to-Carbonate Data Set	36
	Obstacles	37
	Erosional Truncation	38
	Late Mississippian Atmospheric CO_2 Level	38
	Burial Compaction	39
	Depth to Pedogenic Carbonate	41
	Estimate of Late Mississippian Paleo-precipitation	41
	Conclusions	43
III.	PHYSICAL COMPACTION OF VERTIC PALEOSOLS: IMPLICATIONS FOR BURIAL DIAGENESIS AND PALEO-PRECIPITATION ESTIMATES	45
	Introduction	45
	Location and Stratigraphy	47

Methods..... 47
Vertic Paleosols..... 52
Clastic Dikes..... 57
Paleosol Compaction Equations..... 60
Solidity and Burial Compaction..... 60
Shale Compaction Curves and Equations..... 63
Sandstone Compaction Curves and Equations..... 64
"Vertic-Calibrated" Sandstone Compaction Curve and Equation..... 65
Discussion..... 68
Implications..... 71
Conclusions..... 71

IV. VERTIC PALEOSOLS, PERCHED WATER TABLES, AND INCIPIENT LATE PENNSYLVANIAN COAL SWAMPS; CONEMAUGH GROUP, APPALACHIAN BASIN..... 73
Introduction..... 73
Location and Stratigraphy..... 75
Methods..... 79
Profile Characteristics..... 80
Low-chroma Units..... 83
High-chroma Units..... 85
Cumulative Thickness and Superjacent Strata..... 88
Spatial Variations..... 90
Interpretations and Discussion..... 96
The Paleosol Complex..... 96
Significance of color..... 96
Soil structure, slickensides, carbonate nodules..... 99
Geochemistry..... 100
Paleoclimate..... 107
Perched Water Table and the Harlem Coal..... 107
Ames Marine Unit..... 111
Stimuli..... 112
Pre-Ames Paleolandscape and Its Genesis..... 115
Conclusions..... 117

V. GENERAL CONCLUSIONS AND SUGGESTIONS FOR FURTHER RESEARCH..... 119
General Conclusions..... 119
Suggestions for Further Research..... 121

REFERENCES..... 124

APPENDICES..... 135

VITA

LIST OF TABLES

Table 2.1 Comparison of Soil Taxonomy criteria with features in paleo-Vertisol 32

Table 3.1 Dike measurements for estimation of physical compaction..... 58

Table 4.1 Comparison of %LCU relative to lithology of overlying strata..... 89

Table 4.2 Ca/Sr for the uppermost profile units sampled, relative to lithology of overlying strata..... 105

LIST OF FIGURES

FIGURE		PAGE
2.1	Location map of study area near Monterey, Tennessee	8
2.2	Generalized stratigraphic column for Upper Mississippian and Lower Pennsylvanian rocks in east-central Tennessee	9
2.3	Macroscale features of paleo-Vertisol	12
2.4	Schematic profiles of paleo-Vertisol	14
2.5	Macromorphologic features in paleo-Vertisol	15
2.6	Large vertical crack, filled with laminated silt, in core of pseudo-anticline	16
2.7	Micromorphology of claystone paleosol	20
2.8	Silt fillings in vertical crack and clay linings of micro-crack	21
2.9	Micromorphology of pedogenic carbonate	23
2.10	Micromorphology of dolomicrite crust	24
2.11	Diagrammatic reconstruction of local paleogeography and paleoenvironments in study area during Late Mississippian time	27
2.12	Conceptual model for formation of dolomicrite crust at top of paleosol	35
3.1	Location of drill core sites for Late Pennsylvanian paleosols containing clastic dikes	48
3.2	General stratigraphy of the Upper Pennsylvanian in Ohio	49
3.3	Measurement method of clastic dikes for use in calculating compaction	51
3.4	Schematic profile of sub-Portersville paleosol and preserved clastic dike	53
3.5	Schematic profile of sub-Ames paleosol and preserved clastic dike	54

3.6 Schematic profile of sub-Brush Creek paleosol with clastic dikes preserved in the paleosol and in the underlying shale 55

3.7 Burial curve diagrams plotting depth of burial versus compaction as a percent of original thickness 62

4.1 Map showing location of study area, drill-cores, and stratigraphic cross-sections 76

4.2 Stratigraphy of the Upper Pennsylvanian Conemaugh Group 77

4.3 Schematic profiles of the sub-Ames paleosol complex at sites interpreted to have been poorly drained 81

4.4 Schematic profiles of the sub-Ames paleosol complex at sites interpreted to have been well-drained 82

4.5 Selected morphological features from polished slabs of low-chroma units 84

4.6 Selected morphological features from polished slabs of high-chroma units 87

4.7 Stratigraphic cross-section A-A' 91

4.8 Stratigraphic cross-section B-B' 92

4.9 Stratigraphic cross-section C-C' 93

4.10 Stratigraphic cross-section D-D' 94

4.11 Stratigraphic cross-section E-E' 95

4.12 Contour map of percentage of profile thickness composed of high-chroma units, and distribution of Harlem coal bodies 97

4.13 Plot of clayeyness ratio 101

4.14 Plot of leaching ratio 103

4.15 Plot of weathering ratio 106

CHAPTER I

INTRODUCTION

THEME, PERSPECTIVE, GOALS, APPROACHES AND IMPLICATIONS

In recent years, paleosols have been recognized as significant repositories of physical and chemical evidence that can be used to interpret paleoclimate. Paleosols can play a significant role in constraining the general circulation models (GCMs) that are presently being used to study pre-Cenozoic paleoclimate. Pre-Cenozoic climatic interpretations derived from studies of paleosols are generally restricted to qualitative statements that depend on broad analogies to climatically sensitive orders of modern soils such as Vertisols and Oxisols. Quantitative interpretation of various aspects of paleoclimate remains an elusive goal.

This dissertation concerns the uses of vertic paleosols as evidence for paleoenvironmental interpretations. It focuses on a Late Mississippian vertic paleosol in central Tennessee and on several Late Pennsylvanian examples from southeastern Ohio. Paleoprecipitation is the recurring theme of each of the three chapters. An example of quantifying paleoprecipitation using depth to pedogenic carbonate in vertic paleosols is offered in Chapter 2. Chapter 3 seeks to improve the reliability of paleoprecipitation estimates from vertic paleosols. Chapter 4 assesses whether the initiation of some Late Pennsylvanian coal swamps necessarily records increased levels of paleoprecipitation compared with that suggested by the vertic paleosols that underlie them. The goals of

Chapters 2, 3, and 4 are summarized below.

A case study quantifying Late Mississippian paleoprecipitation in east-central Tennessee using depth to pedogenic carbonate in a vertic paleosol is presented in Chapter 2. The primary goal of this chapter is to show that in situations where vertic paleosols have been favorably preserved, they can be employed to estimate mean annual paleoprecipitation. Obstacles to arriving at such estimates are examined and approaches to overcoming them are explained. In addition, the genesis of a dolomitic crust capping the paleosol is interpreted. The contribution of this crust to preservation of the nearly complete profile of the vertic paleosol is considered. Finally, the general paleoclimatic setting of the paleosol is compared to modern climates of regions with similar ranges of mean annual precipitation and geographic settings.

In Chapter 3, vertic soils, and by extension vertic paleosols, are considered from the perspective of their compactability upon burial, compared with the burial compactability of argillaceous sediment and other types of soils/paleosols. The goal of this chapter is to develop a means of reliably estimating burial compaction for vertic paleosols, thereby improving the accuracy with which paleoprecipitation can be estimated using the decompacted depth to pedogenic carbonate in vertic paleosols. To achieve this, clastic dikes preserved in three Late Pennsylvanian vertic paleosols were measured and used to calculate burial compaction. These data were compared to burial compaction estimates obtained from compaction equations for argillaceous sediment, sandstones, and non-vertic soils/paleosols. These estimates are shown to be poor approximations of the known burial compaction recorded by the clastic dikes in the Late Pennsylvanian

paleosols. Burial compaction estimates from examples of Proterozoic, Ordovician, and Mississippian vertic paleosols and the dike-based compaction data from the Late Pennsylvanian vertic paleosols are employed to develop a burial compaction equation and curve calibrated specifically for vertic paleosols. This "vertic-calibrated" equation and curve can be used to estimate burial compaction for vertic paleosols lacking clastic dikes.

Chapter 4 concerns the association of thick vertic paleosols with some Late Pennsylvanian coals in southeastern Ohio. The work presented here focuses on the region's most widespread vertic paleosol-coal couplet, the sub-Ames paleosol complex/ Harlem coal association. The pairing of vertic paleosols with overlying coals has been interpreted by other workers as evidence of paleoclimate change, specifically increased paleoprecipitation. Previously, I and other workers suggested that the sub-Ames paleosol complex records the development of a perched, saturated zone, that facilitated initiation of a coal swamp. Thus, the goals of this chapter are to further assess formation of the perched zone and whether or not increased paleoprecipitation was a requirement for its production and eventually that of the coal swamp. Catenary relationships preserved in the sub-Ames paleosol complex are used to assess paleolandscape, specifically soil drainage setting, and its role in the formation of the coal swamp. Geochemical data and soil morphology provide evidence of the pedogenic processes that facilitated growth of the perched zones, which bears on the stimulus for coal swamp initiation.

In addition to points mentioned above, Chapter 4 speaks to several broader issues. Foremost among these, it illustrates that interpretations of depositional histories of stratigraphic intervals containing paleosols should include thorough appraisals of the

potential roles of paleolandscape/soilscape. Furthermore, this chapter demonstrates that paleosol color, in spite of all the negative "press", does survive burial diagenesis in some, and perhaps many, situations and can provide sensitive data on soil drainage and redox conditions. Finally, pitfalls of the casual, routine invocation of a broad, ubiquitous and uniformly rising regional water table to explain coal swamp initiation are exposed.

CHAPTER 2

PRESERVATION OF A PALEO-VERTISOL AND AN ESTIMATE OF LATE MISSISSIPPIAN PALEO-PRECIPITATION

INTRODUCTION

In recent years, paleosols have been recognized as significant repositories of paleoclimate information. Interpretations of this information in pre-Cenozoic paleosols are generally restricted to qualitative statements that depend on broad analogies to climatically sensitive orders of modern soils such as Vertisols and Oxisols. Quantitative interpretation of various aspects of paleoclimate remains an elusive goal.

Paleo-precipitation is one of the most important facets of paleoclimate. On the basis of Quaternary soils of known rainfall, Retallack (1994) defined the relationship long known to exist between depth to carbonate in soils and mean annual rainfall (Jenny and Leonard 1935) and applied it to paleosols (e.g., Retallack 1994, Retallack and Mindszenty 1994). Obviously, there is great potential for misinterpretation of paleo-precipitation if this relationship is applied to ancient paleosols without constraining other major factors influencing the depth to carbonate in paleosols. Retallack (1994) identified several major obstacles to estimation of paleo-precipitation based on the depth to carbonate: (1) erosional truncation of paleosol profiles, (2) compaction of paleosols during burial, and (3) levels of atmospheric carbon dioxide different from today. Inadequately accounting for the first two factors leads to underestimation of paleo-

precipitation, whereas higher levels of atmospheric CO_2 results in overestimation.

Furthermore, application of this approach to paleosols seems best restricted to pedogenic carbonate horizons preserved in paleosols that formed well above the water table (Blodgett, pers. comm. 1994). Smith (1994) and Aslan et al. (1993) have reported alluvial and fluvio-deltaic soils containing nodular carbonate formed in response to water-table fluctuations. Aslan et al. (1993) specifically noted that depth to carbonate nodules in hydromorphic soils should not be used as a measure of rainfall.

Recently, several vertic paleosols intercalated with marginal marine deposits in the Upper Mississippian (Chesterian) Pennington Formation of central Tennessee were identified (Caudill et al. 1992b, 1996). The thickest of these paleosols formed well above the water table and preserves a horizon of pedogenic carbonate. This paleosol contains an array of pedogenic features sufficient for its interpretation as a direct analogue to Holocene Vertisols (i.e., a *paleo-Vertisol* versus a *vertic paleosol*; Caudill and Driese 1994, Caudill et al. 1996). By analogy to the Vertisol soil order (Soil Survey Staff 1990), paleo-Vertisols yield tighter qualitative constraints on paleoclimate than generic vertic paleosols. Holocene Vertisols are present in areas as climatically diverse as equatorial Indonesia and the frigid piedmonts of Montana (Dudal 1989), but approximately 90% of all Vertisols form in dry, tropical to subtropical settings, including the 70% of Vertisols in the semiarid tropics (Blokhuis 1989, Dudal 1989). Vertic paleosols include paleosols that are vertic intergrades of other soil orders, and consequently reveal little about paleoclimate other than a predominance of seasonal precipitation.

The Late Mississippian paleo-Vertisol identified here permits quantitative

estimation of paleo-precipitation because factors such as erosional truncation, compaction, atmospheric pCO_2, and the relative position of the water table can be unusually well constrained. This paleosol contains a pervasive horizon of pedogenic carbonate and preserves a nearly complete soil profile in gilgai micro-lows. I describe circumstances that limited erosion of the soil profile in gilgai micro-lows of the paleo-Vertisol. Vertical, pedogenic micro-cracks are also preserved and provide a reliable means of constraining burial compaction. Late Mississippian levels of atmospheric carbon dioxide have been estimated for time-equivalent paleosols (Mora and Driese 1993, Mora et al. 1996) using the soil carbonate paleobarometer of Cerling (1991). Lack of low-chroma mottles in the claystone matrix of the pedogenic carbonate unit argues against formation of the nodules due to fluctuations of the water table.

LOCATION AND METHODS

The Pennington Formation is exposed in roadcuts along Interstate 40, just west of Monterey, Tennessee (Fig. 2.1). At the study locality, paleosols are present in two stratigraphic intervals separated by approximately 20 m of unexposed section (Fig. 2.2). Paleosols of the upper stratigraphic interval range in thickness from 0.5 to 1.8 m. The thickest and best developed of these paleosols contains a pedogenic carbonate horizon and is the focus of this paper.

The macromorphology of the paleosol was described following the approach outlined by Retallack (1988). Colors were described from wetted samples using the Munsell Rock-Color Chart. Profiles were described both within pseudo-anticlines and in the intervening areas. The depth to the pedogenic carbonate horizon was measured

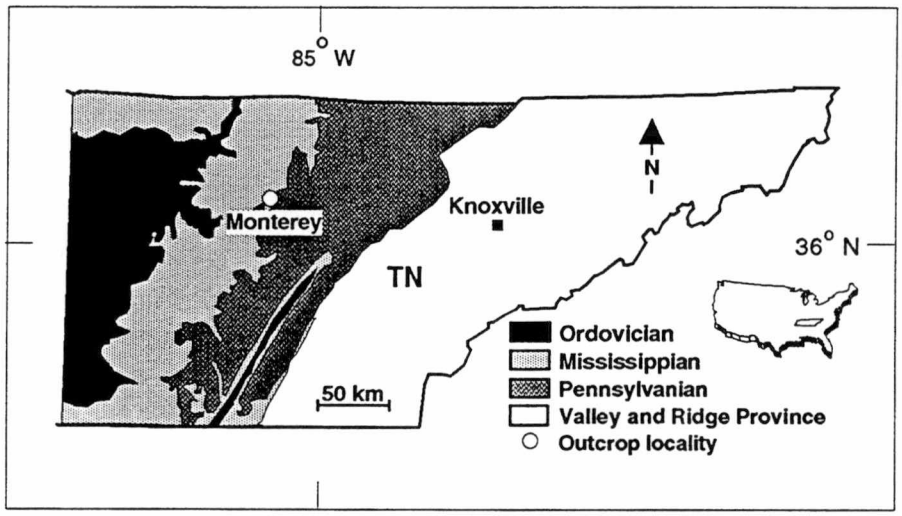


Figure 2.1 - Map showing location of study area near Monterey, Tennessee.

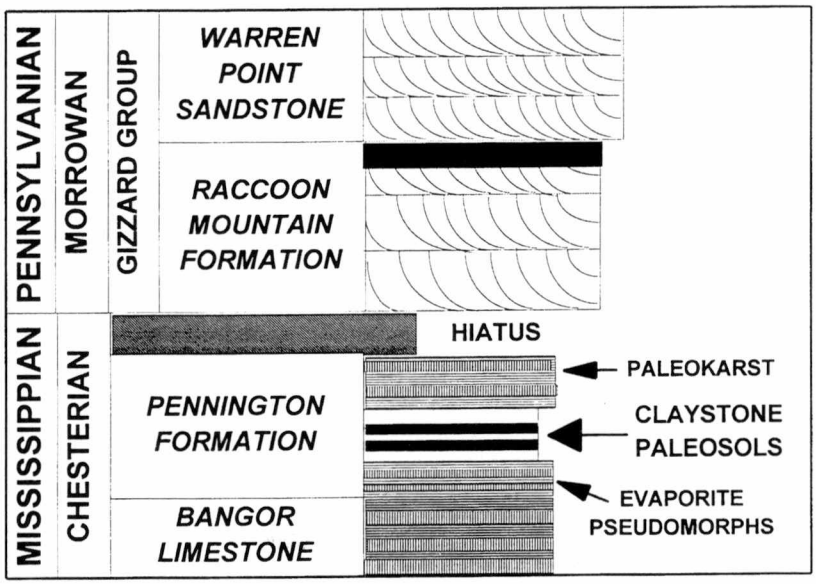


Figure 2.2 - Generalized stratigraphic column for Upper Mississippian and Lower Pennsylvanian rocks in east-central Tennessee. Paleosol discussed in this paper is in the middle of the Pennington Formation. (not to scale)

halfway between pseudoanticlines. Length ratios of ptygmatically folded micro-cracks used to estimate compaction were measured using a planimeter on enlarged photographs. The micromorphology of the claystone matrix and carbonate nodules and rhizocretions was examined in thin section and described according to Brewer (1976) and Wright (1990), respectively. Petrographic analyses of carbonate nodules/rhizocretions and the dolomicrite crust were conducted on stained (combination stain) thin sections using plane light and cathodoluminescence. Whole-rock samples of the paleosol matrix were collected from each unit (horizon), as well as superjacent and subjacent strata, focusing on the profile between pseudo-anticlines. The bulk mineralogy of the matrix samples and of the carbonate nodules and rhizocretions was analyzed in hand-packed mounts using a Siemens D500 X-ray Diffractometer. The clay mineralogy of the < 2 μm size fraction of the paleosol matrix was determined using elutriated mounts, glycolation, and routine heat treatments.

STRATIGRAPHY AND DEPOSITIONAL SETTING

The Pennington Formation is Chesterian (Crawford 1985) and ranges from 30 to 150 m in thickness in Tennessee (Milici et al. 1979). It consists of a mixed siliciclastic-carbonate sequence composed of dolomite, limestone, fine-grained sandstone, pebbly sandstone, and red, green, and gray shale (Milici 1974; Milici et al. 1979). Also present, previously grouped with the shales, are several red and gray-green mudstones that lack fissility and have the hackly appearance of paleosols (Caudill et al. 1992b, 1996).

The Formation thins from east to west, with terrigenous clastic rocks becoming more abundant in the east and carbonate rocks progressively more abundant towards the

west. On the Cumberland Plateau of Tennessee, the Pennington Formation is underlain by the Mississippian Bangor Limestone and overlain by the Mississippian/ Pennsylvanian Gizzard Group (Fig. 2.2). The contact between the Gizzard Group and the Pennington Formation varies from unconformable to gradational to intertonguing (cf. Milici 1974), with some evidence for formation of paleokarst (Driese et al. 1994).

In Tennessee, the Pennington Formation comprises nondeltaic littoral deposits underlain by offshore carbonates and overlain by coal-bearing deltaic deposits (Milici 1974). Carbonates dominate the lower part of the formation, with interbedded terrigenous clastics becoming more abundant upward, paralleling the larger regressive trend defined by the transition from Mississippian offshore carbonates to Pennsylvanian deltaic deposits (Milici et al. 1979). An array of depositional environments have been ascribed to the Pennington Formation and lithostratigraphically equivalent strata, including: offshore sandbars (Milici et al. 1979), a variety of peritidal environments (Bergenback et al. 1972), barrier-beach and marsh environments (Milici 1974), carbonate tidal island-barrier bar complexes and low-energy, terrigenous, offshore environments (Ferm et al. 1972; Ferm 1974), and tidally influenced, terrigenous clastic environments (Sedimentation Seminar 1981).

OUTCROP DESCRIPTIONS

Profile Descriptions

The outcrop shown in Figures 2.3A and B shows the defining characteristics of the paleosol. The paleosol is approximately 1.5 m thick and contains four morphological units roughly equivalent to horizons. Schematic profiles (Fig. 2.4A, B) illustrate the

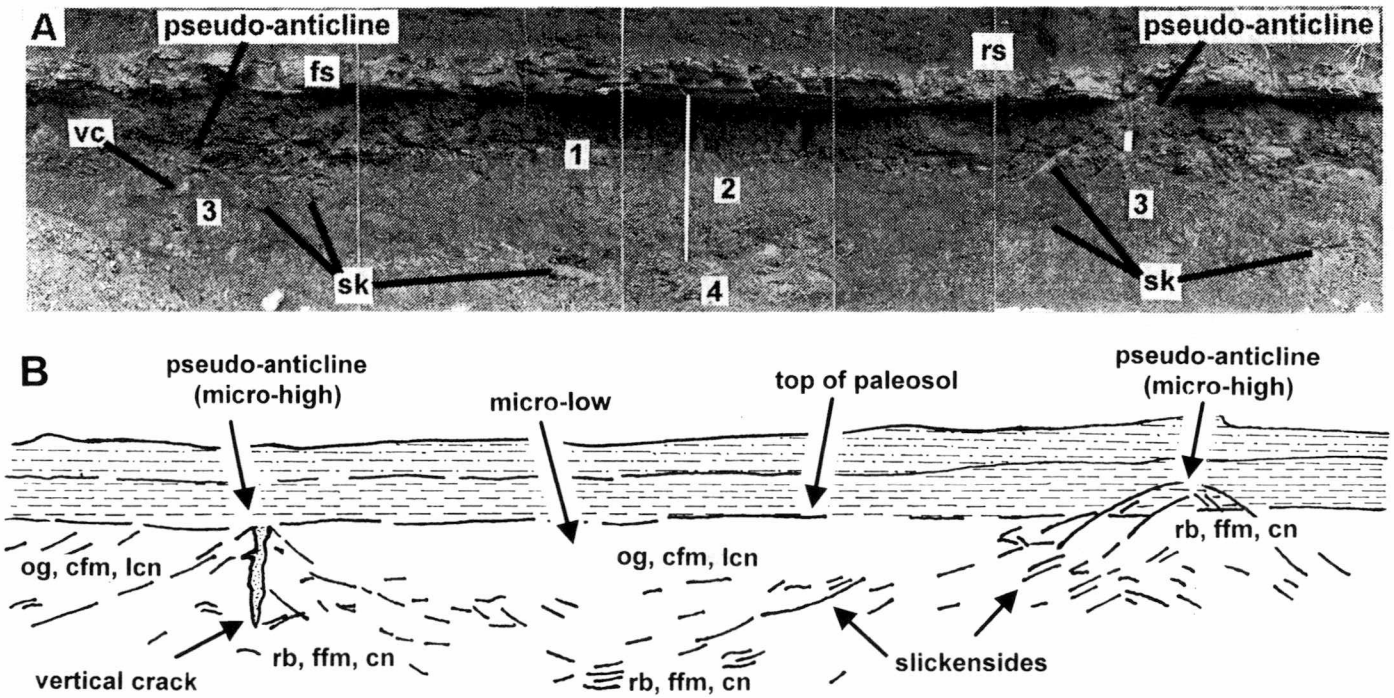


Figure 2.3 - Macroscale features of paleo-Vertisol exposed in outcrop at Monterey, Tennessee. A) Photomosaic of main outcrop of paleosol showing selected macromorphologic features and lateral variation of paleosol Units delineating mukkara. Numbers refer to units constituting paleosol. Key: rs = red shale; fs = fine-grained sandstone; vc = silt-filled vertical crack; sk = pedogenic slickensides. Vertical Jacob's staff at center is 1.2 m long. B) Schematic tracing of photomosaic in A showing pedogenic slickensides, pseudo-anticlines, soil color pattern (og = olive gray, rb = red brown), and distribution of Fe-Mn concretions (cfm = common Fe-Mn concretions, ffm = few Fe-Mn concretions) and carbonate nodules (cn = carbonate nodules present, lcn = lacks carbonate nodules), which collectively delineate mukkara.

marked lateral variation in horizonation from pseudo-anticlines to areas between pseudo-anticlines. The morphological units/horizons are described below, in descending order:

Unit 1: 0-15 cm thick; dolomicrite; dark greenish gray (5GY3/1), hard, massive; contact clear and wavy (Fig. 2.5A).

Unit 2: 0-80 cm thick; silty claystone; dark olive gray (5Y3/1); weak, fine to medium, blocky structure; common, Fe-Mn concretions (Fig. 2.5B), 0.1-1 cm in diameter; common, small slickensides; noncalcareous; contact gradual and wavy.

Unit 3: 0-85 cm thick; silty claystone; dark reddish brown (10R3/4); moderate, medium, blocky structure with common wedge-shaped structural aggregates (Fig. 2.5C); common, small slickensides and many large, arcuate slickensides, some with dark greenish gray (G4/1) diffuse margins; few to common, disorthic, tuberous, dolomicrite nodules; very weakly calcareous; contact gradual and wavy.

Unit 4: 20-70 cm thick; silty claystone; dark reddish brown (10R3/4); moderate, coarse, blocky structure with few wedge-shaped structural aggregates; common, small and many large, arcuate slickensides (Fig. 2.4D), many of which are subhorizontal in thin zone (10 cm) at top of unit; common, disorthic, tuberous, dolomicrite nodules and few, stacked, dolomicrite rhizocretions (Fig. 2.5E); few Fe-Mn concretions (<0.5 cm in diameter); weakly calcareous; contact gradual and wavy.

Unit 5: 0-45 cm thick; interlaminated claystone and shale; dark reddish brown(10R3/4) with thin beds of dark greenish gray (5G4/1); scattered zones of thin, platy peds and disrupted sedimentary layering (Fig. 2.5); few small slickensides; common, disorthic, tuberous, dolomicrite nodules and few, stacked, dolomicrite rhizocretions (Fig. 2.5F); very weakly calcareous; contact gradual and smooth.

In addition to the features described above, Unit 3 of the paleosol contains a macro-scale feature seldom reported from Paleozoic vertic paleosols: a large, vertical crack. The crack is filled with dark greenish gray (5G4/1) silt and is preserved in a pseudo-anticline (Figs. 2.3A, B; 2.6). The crack varies from 5 to 10 cm in width and exceeds 85 cm in length. It is intersected by a few large arcuate slickensides and has several thin (2 cm) layers of silt extending up to 10 cm laterally from the crack.

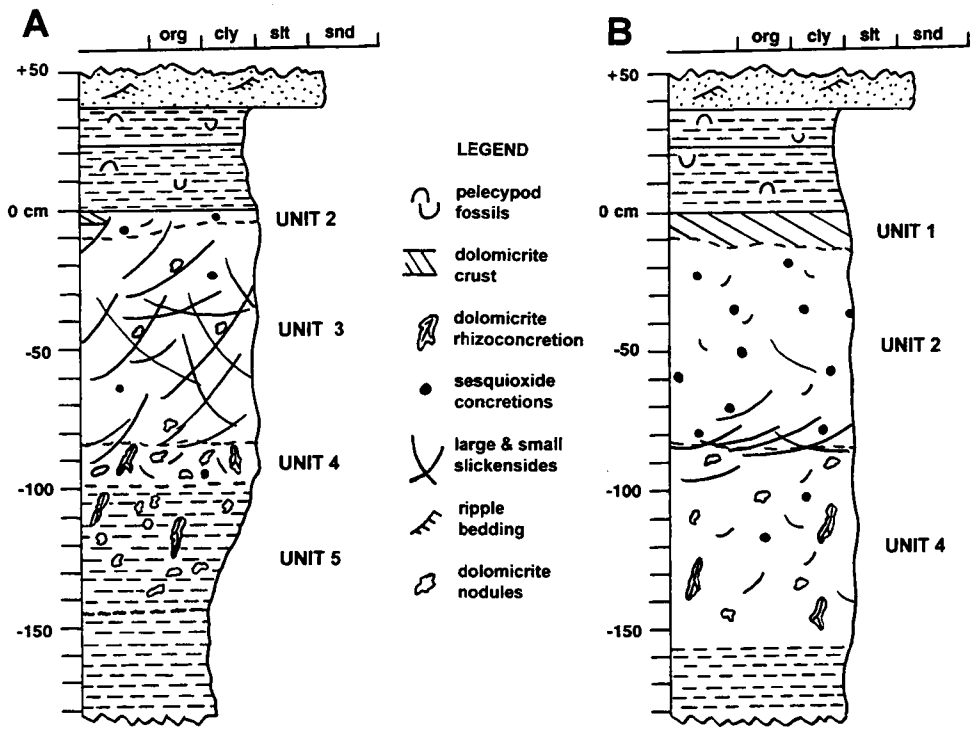


Figure 2.4 Schematic profiles of paleosol. A) Profile of paleosol at pseudo-anticlines. Note that Units 1 and 2 are thin to absent, Unit 5 is present, and Unit 3 is very thick and thoroughly slickensided. B) Profile of paleosol in areas between pseudo-anticlines. Note greater thickness of Units 1, 2, and 4, whereas Units 3 and 5 are absent.

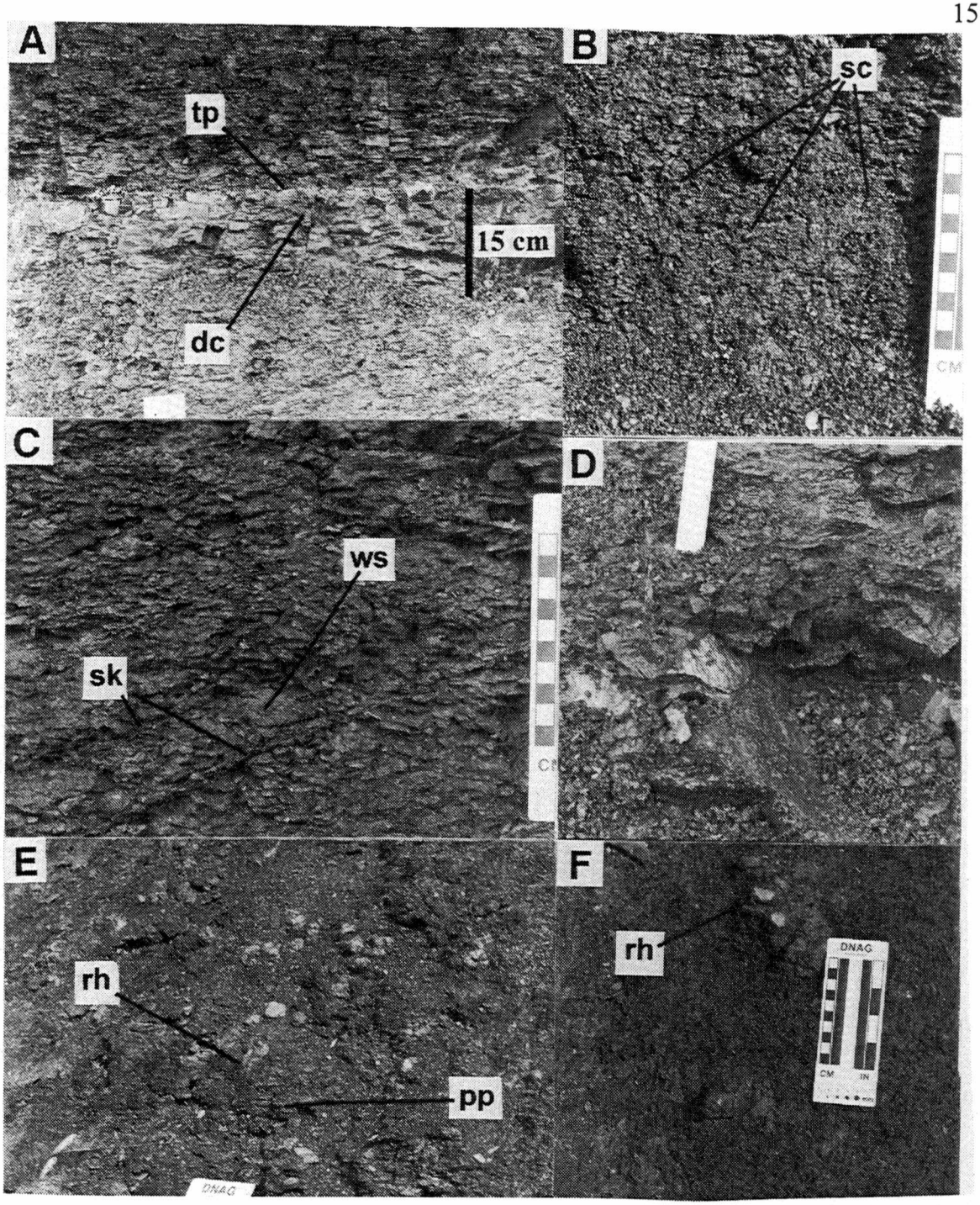


Figure 2.5 - Macromorphologic features in paleosol. A) Unit 1, consisting of dolomicrite crust (dc) at top of paleosol (tp), sharply overlain by red shale, and underlain by Unit 2. Note transitional lower contact with Unit 2. B) Unit 2, Fe-Mn concretions (sc) are common. C) Unit 3, showing wedge-shaped structural aggregates (ws) formed by intersection of pedogenic slickensides (sk). D) Polished surface on large pedogenic slickenside within Unit 3 (ruler is 10 cm long). E) Unit 4, showing platy ped structure (pp) and scattered, disorthic carbonate nodules and rhizoconcretions (rh). F) Unit 4, containing large, tuberose rhizoconcretions (rh) composed of vertically stacked nodules.

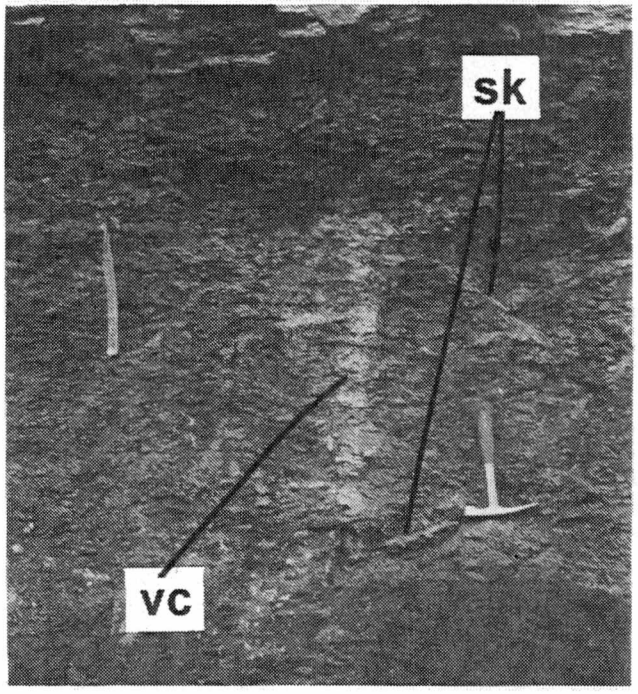


Figure 2.6 - Large vertical crack (vc), filled with laminated silt, in core of pseudo-anticline; note that crack crosscuts pedogenic slickensides (sk; see also Figure 2.3A). Hammer is 30 cm long. Tape and pin mark top of paleosol.

Lateral thickness variations in the morphological units (i.e., horizons) constituting the paleosol are very distinctive (Fig. 2.3). The most obvious variation is in Unit 2, which is dark olive gray and contrasts sharply with the reddish brown that dominates the rest of the profile. Unit 2 thins from a maximum thickness of 80 cm between pseudo-anticlines to 0-5 cm at crests of pseudo-anticlines. This trend of thinning towards pseudo-anticlines is paralleled by Unit 1, the dolomicrite at the top of the paleosol. Conversely, Units 3 and 5 are developed only in the pseudo-anticlines and are absent from the profile in areas between pseudo-anticlines. The lateral thinning of Unit 2 and the preferential development of Unit 3 in pseudo-anticlines delineate *mukkara structure*. The mukkara is best recognized based on the following: (1) the color pattern of the paleosol, wherein the dark olive-gray Unit 2 is underlain by the dark reddish brown Unit 4 and is situated between pseudo-anticlines composed of the dark reddish brown Units 3, 4, and 5; and (2) the distribution pattern of carbonate nodules and Fe-Mn concretions in the paleosol, wherein Unit 2 contains abundant Fe-Mn concretions, but lacks carbonate nodules, and the laterally adjacent and underlying dark reddish brown Units (3, 4 and 5) contain carbonate nodules, but few Fe-Mn concretions. Although the specific colors in the paleosols are products of burial gleying in Unit 2 and diagenetic recrystallization of hematite (cf., Blodgett et al. 1993) in Units 3, 4, and 5, the color patterns, if not the actual colors, are pedogenic. The horizonation, color patterns, and distribution of pseudo-anticlines that define the mukkara in the paleosol compare very well with mukkara in modern clay-rich soils (Stace et al. 1968; Lynn and Williams 1992).

Subjacent and Superjacent Strata

The paleosol is underlain and overlain by shale. The subjacent strata comprise approximately 1 m of semifissile, dark greenish gray (5G4/1), clay shale that becomes interlaminated downwards with dark reddish brown shale (10R3/4). This unit passes downwards into 1 m of olive gray (5Y4/1), silty shale containing thin (< 5 cm) siltstone layers. The silty shale is underlain by 2.8 m of medium to coarse, gray (N5), calcareous sandstone. The sandstone has an erosional base and contains hummocky, micro-hummocky, and medium-scale trough cross-stratification. Scattered throughout the lower part of this unit are a few pebble- and cobble-size claystone clasts, along with inarticulate brachiopods and small echinoderm ossicles.

Between pseudo-anticlines, the dolomicrite (Unit 1) at the top of the paleosol is abruptly overlain by approximately 40 cm of clay shale, which passes upward from very dark reddish brown (10R3/2) to dark greenish gray (5GY4/1). Pectenid pelecypods are scattered throughout this unit. Where pseudo-anticlines are developed, Unit 1 is typically absent and Unit 3 is directly overlain by the clay shale. Some of the large arcuate slickensides that define pseudo-anticlines in the paleosol extend upwards into the overlying shale. These extensions have shallower dips than contiguous parts of the slickensides within the paleosol, which tend to steepen towards the top of the paleosol.

MICROMORPHOLOGY

Paleosol Matrix

The claystone matrix of the paleosol is dominated by sepic-plasmic (bright-clay) fabric defined by segregations of clay minerals with preferred orientations and congruent

extinction patterns (Brewer 1976). The sepic-plasmic fabric can be subdivided into masepic (one preferred direction of alignment), bimasepic (two directions), vosepic (cavity-lining), and skelsepic (grain-encircling) varieties. Masepic (Fig. 2.7A, B) and bimasepic (Fig. 2.7C) fabrics are present throughout the paleosol, whereas the less prevalent vosepic fabric (Fig. 2.7F) bounds micro-peds, some of which are brecciated due to displacive precipitation of carbonate (Fig. 2.7D). The skelsepic fabric surrounds a few of the Fe-Mn concretions and some of the sand and coarse silt grains.

Silt-size mineral grains are scattered throughout the dense clay-rich matrix of the paleosol to form a porphyroskelic (floating grain) fabric. Most grains consist of monocrystalline quartz, but unoriented, coarse, elongated grains of illite are also present. Channel-like and planar voids (< 0.25 mm in diameter) are present in intrapedal and interpedal configurations and are filled with combinations of carbonate, ferric material, and quartz silt grains. Some of the channel-like voids are tubular and appear to be micro-rhizoliths (Fig. 2.7E).

The large, vertical crack in Unit 3 is filled with quartz silt and minor amounts of clay minerals. The silt infill contains subhorizontal laminae and numerous vertical micro-cracks (Fig. 2.8A). These micro-cracks are lined with thin bands of dark clay, which appear to be coatings of infiltrated soil material (Fig. 2.8B).

Concretions and Nodules

Dense, red, Fe-Mn concretions (1-5 mm in diameter) are common and few, respectively, in morphological Units 2 and 4. In addition, two types of carbonate nodules, both dominated by the alpha fabrics of Wright (1990), were identified in the

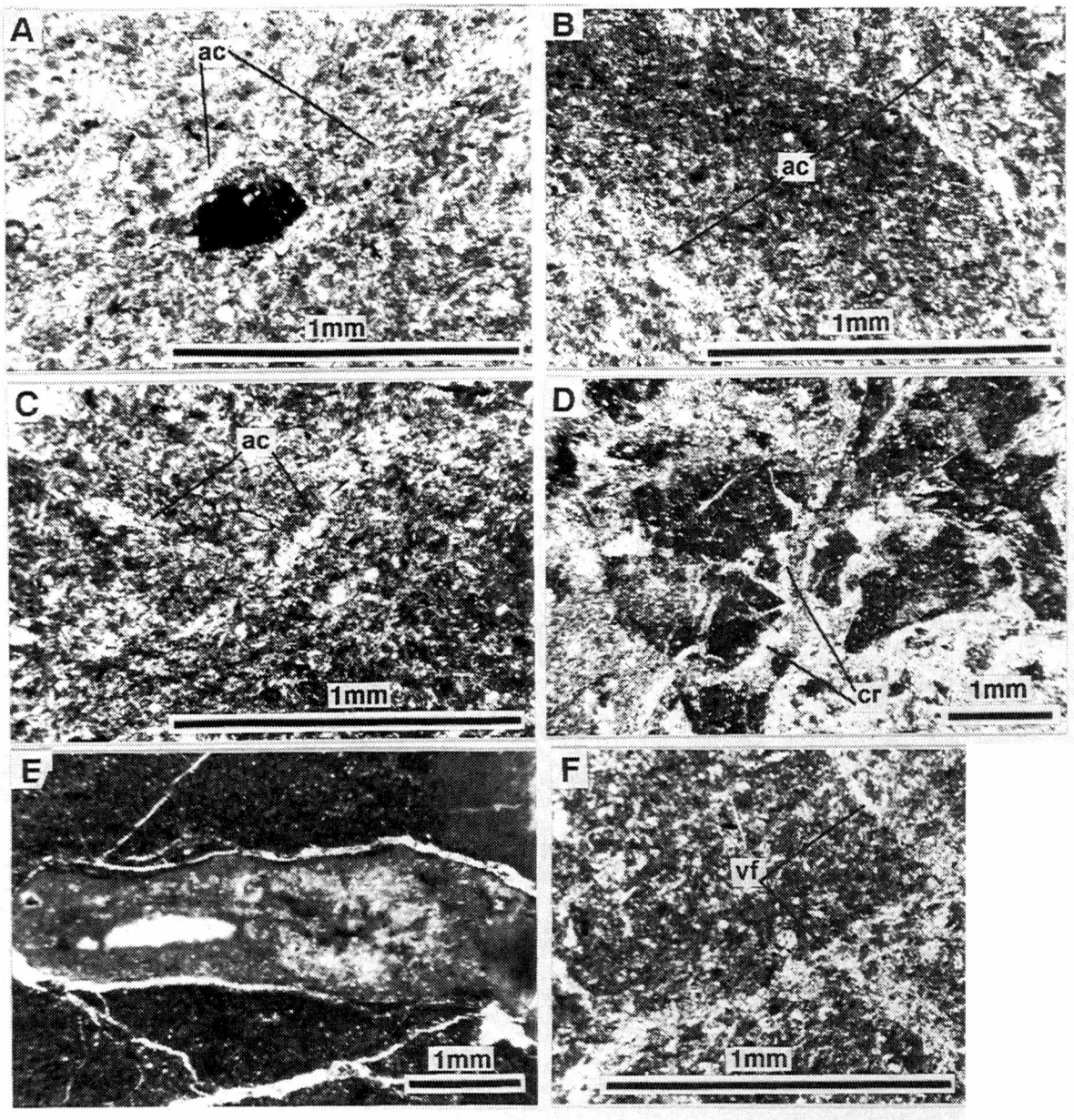


Figure 2.7 - Micromorphology of claystone paleosol. All photos under crossed polarizers except for E. A, B, C) Sepic-plasmic micro-fabrics characterized by one (masepic; A, B) or two (bimasepic; C) preferred orientations of aligned clays (ac) in the paleosol matrix. D) Peds brecciated by displacive precipitation of carbonate (cr) in paleosol matrix. E) Micritic rhizolith showing central pore occluded by calcite spar cement. Plane-polarized light. F) Vosepic micro-fabric (vf) characterized by clays aligned in voids between peds.

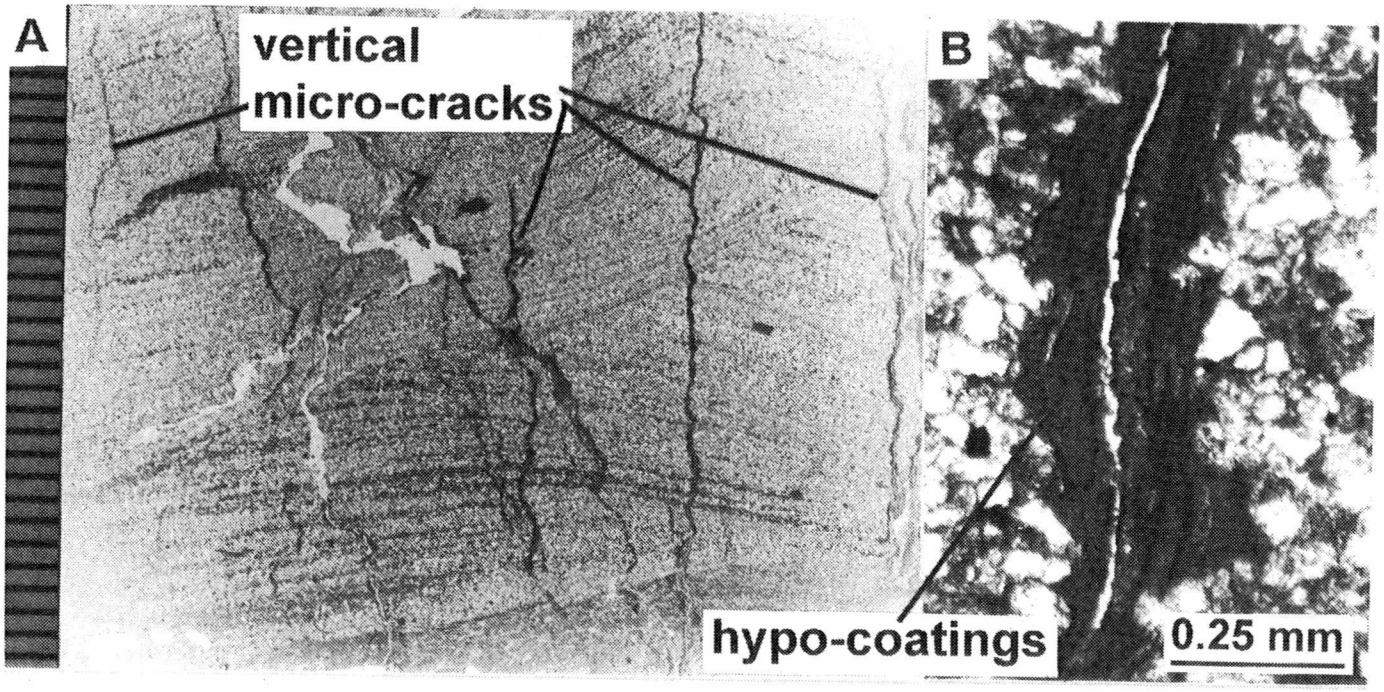


Figure 2.8 - Silt fillings in vertical crack. A) Whole thin-section photograph (ordinary incident light) showing vertical micro-cracks in siltstone filling a large vertical crack. Scale bar in mm. B) Thin-section photomicrograph, in plane-polarized light, showing dark laminated clay lining micro-cracks interpreted as coatings of infiltrated soil material.

paleosol. Type 1 nodules consist of homogeneous, dense, fine-grained carbonate (Fig. 2.9A) with scattered skeletal (i.e., detrital sand and silt) grains and few small Fe-Mn nodules. Circumgranular and irregular fractures filled with clay minerals, and, less commonly, calcite spar cement are found in some Type 1 nodules (Fig. 2.9B). Type 2 nodules have more complex fabrics. They typically contain many carbonate spar-filled fractures and voids, have a brecciated appearance (Fig. 2.9D), and preserve clay-filled, tubular cavities interpreted as rhizoliths; a few have cores formed of Fe-Mn concretions (Fig. 2.9C). Cathodoluminescence microscopy indicates that the spar infilling fractures in Type 2 nodules precipitated in three distinct phases. Both types of carbonate nodules have distinct, sharp margins.

Dolomicrite Crust

The carbonate crust (i.e., Unit 1) contains many large pellets, 1-2 mm long (Figs. 2.10A, B), set in a silty, very fine-grained carbonate matrix, but typically containing little or no silt themselves. The large pellets are also found filling horizontally oriented, bulbous burrows with meniscate backfilling (Fig. 2.10C). Tubular, vertical burrows, 0.5 mm in diameter and 3 mm long, are filled with smaller pellets and in one instance crosscut a larger bulbous burrow. In some areas, the carbonate matrix is organized into fine, soil-like aggregates of small (< 0.2 mm) peloids and commonly contains planar voids lined with oriented clays forming a vosepic fabric (Fig. 2.10E). Many irregularly shaped grains of silty claystone, 0.1-2 mm in diameter, are scattered throughout the crust (Fig. 2.10D). A few of the claystone grains contain root channels filled with the very fine-grained carbonate matrix material (Fig. 2.10F). The lower part of the crust consists

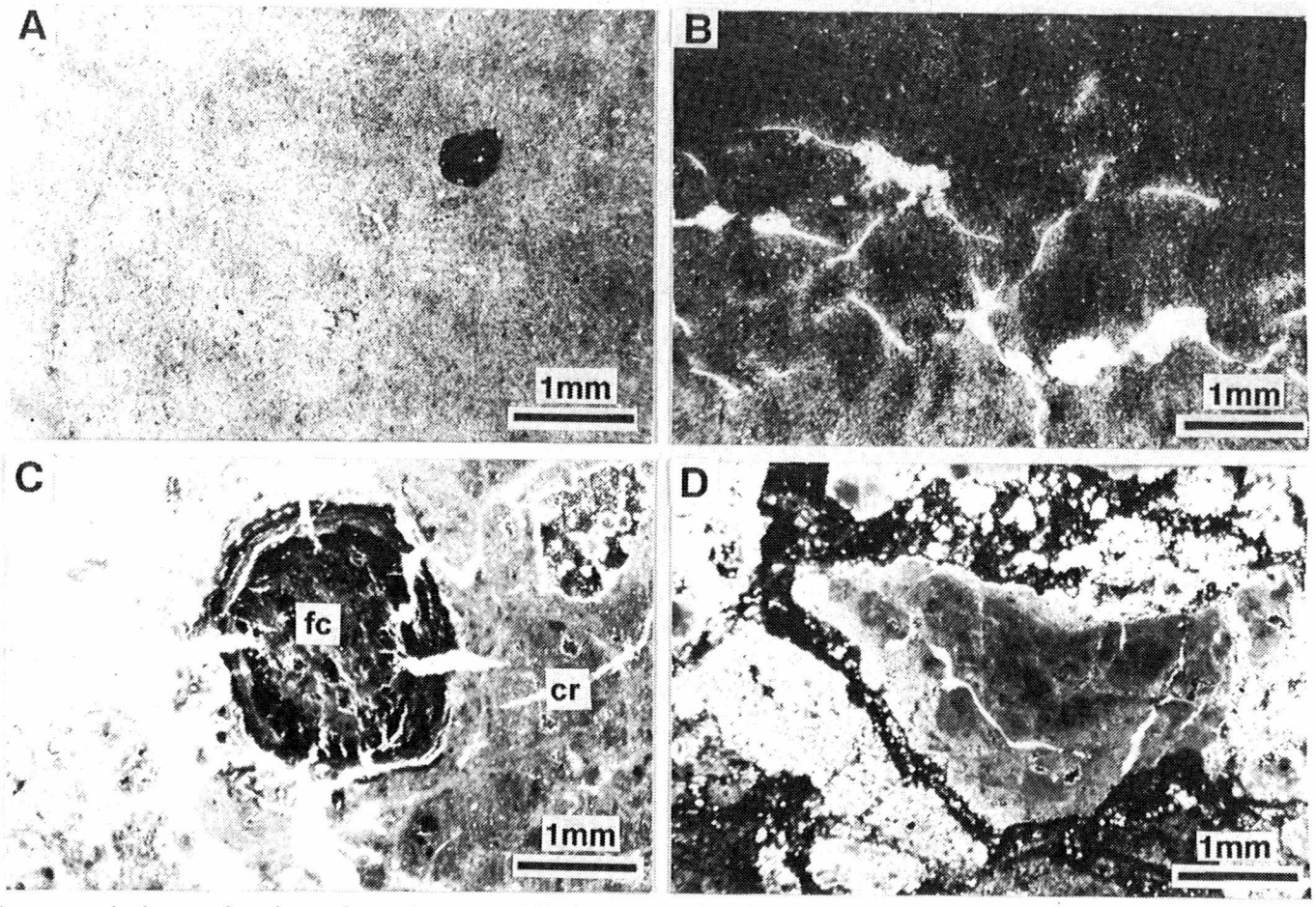


Figure 2.9 - Micromorphology of pedogenic carbonate. All photos are in plane-polarized light. A) Homogeneous micrite nodule containing sparse opaque Fe-Mn nodule. B) Micrite nodule with circumgranular cracks and irregular voids filled by calcite spar cement and clays. C) Micrite nodule containing ferruginous concretion (fc) at nodule core and septarian cracks filled with calcite spar cement (cr). (D) Micrite nodule with brecciated fabric. Clays and opaque Fe-oxides fill cracks between breccia clasts.

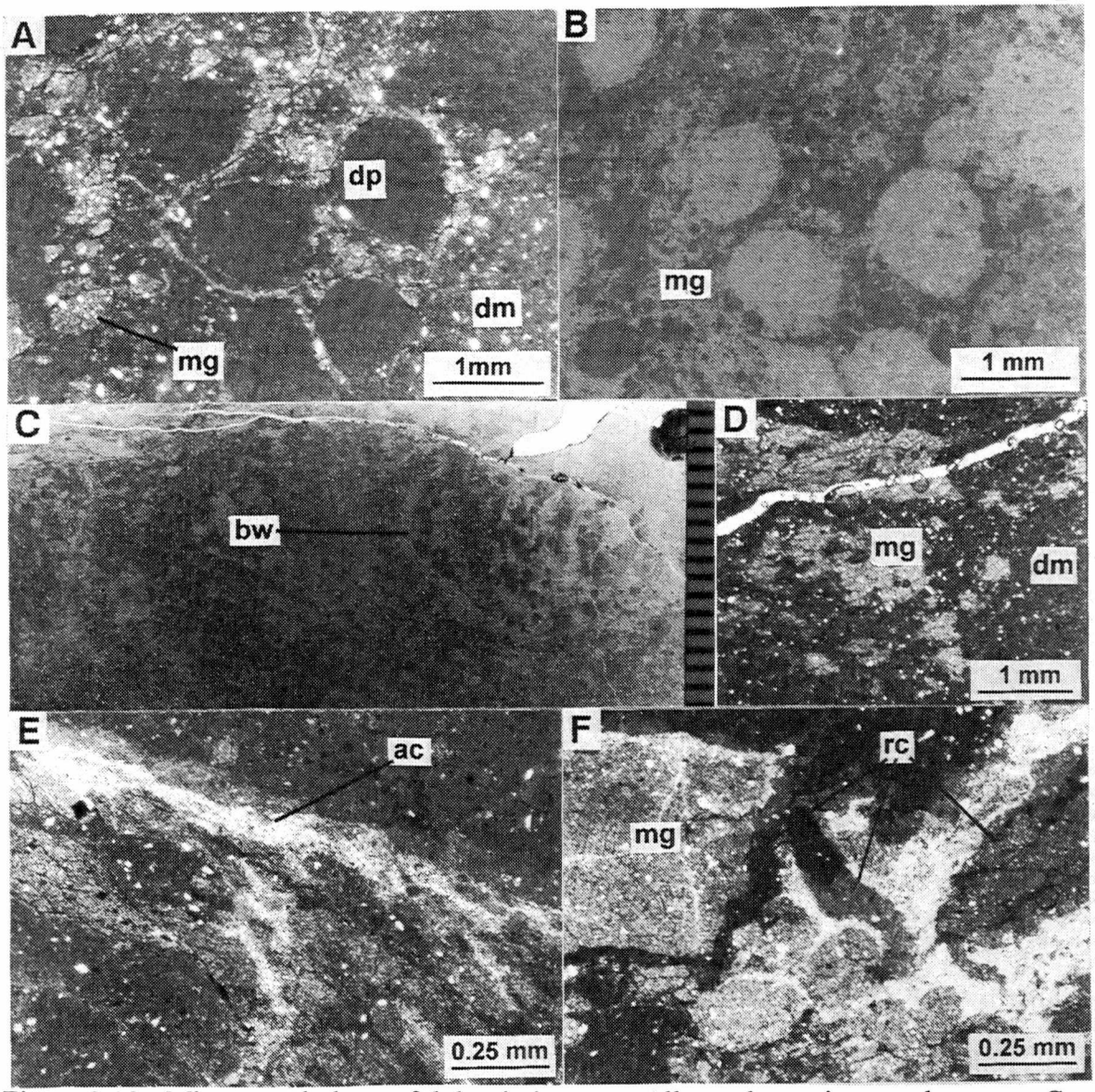


Figure 2.10 - Micromorphology of dolomicrite crust. All are photomicrographs except C, which is a whole thin-section photograph. A) Large dolomitized fecal? pellets (dp) preserved in crust composed of dolomicrite (dm) and mudstone grains (mg) derived from the paleosol. Plane-polarized light. B) Approximately same field of view as in A, under cathodoluminescence. Note uniform bright luminescence of pellets and dolomicrite matrix. Dark, nonluminescent areas are terrigenous clay, silt, and mudstone grains. C) Large bulbous burrow with meniscate backfilling (bw) composed of pellets, dolomicrite, and mudstone grains (scale bar in millimeters; ordinary incident light). D) Clotted soil-like aggregates (fine peds) produced by pedogenic reworking of crust composed of dolomicrite (dm) and mudstone grains incorporated from the paleosol (mg). Plane-polarized light. E) Aligned clays (ac) filling planar void (vosepic fabric; crossed polarizers). F) Root channels lined with bright clay hypocoatings. Centers of root channel (rc) are filled with dolomicrite. Note large mudstone grain (mg; crossed polarizers).

mainly of homogeneous silty claystone containing minor, discontinuous, horizontally disposed masses of very fine-grained carbonate. Upward in the crust, these carbonate masses become progressively more abundant and coalesce to eventually constitute the matrix of the crust.

MINERALOGY

Matrix Mineralogy

Illite/smectite containing less than 10% interlayered smectite is the dominant clay mineral in the clay-size fraction (< 2 μm) of the paleosol matrix. Chlorite and quartz are far less abundant, and the presence of a kaolinite component is not ruled out. First-order approximations of Sheldon (1995) indicated that R3 ordered illite/smectite with < 10% interlayered smectite constitutes > 80% of the < 1 μm size fraction, which contains only illite/smectite and chlorite.

Carbonate nodules within the paleosol consist chiefly of dolomite (80-90%), the balance consisting of quartz, illite, chlorite, and kaolinite(?). Sheldon (1995) noted that detrital 2M illite is preserved in the nodules. Calcite was not detected in any of the nodules. Unit 1 of the paleosol is a crust composed predominantly of dolomite. Stained thin sections suggest that the dolomite is micritic and ferroan. Cathodoluminescence microscopy reveals that the dolomicrite has a uniform bright luminescence (Fig. 2.10A, B), suggesting that the manganese concentration in the dolomicrite is sufficient to overcome the quenching effect of iron.

INTERPRETATIONS AND DISCUSSION

Local Paleogeography

The Pennington Formation is a mixed siliciclastic-carbonate sequence of nondeltaic littoral deposits (Milici 1974). My interpretation of the local paleogeography is based on: (1) paleoenvironmental interpretations of the Pennington Formation offered by other workers (cited above), (2) the strata above and below the paleosol in the study area, and (3) the tendency of Vertisols to form on relatively flat topography (cf. Ahmad 1983). I suggest that the paleosol formed on a flat, low-lying coastal plain adjacent to a clastic lagoon, which was separated from an offshore area of carbonate production by a barrier or tidal bar complex (Fig. 2.11). Given this distribution of environments, a minor drop followed by a similar rise in relative sea level could have produced the vertical lithologic succession shown by the units immediately overlying and underlying the paleosol and have exposed clastic lagoonal sediments to pedogenesis.

Claystone Paleo-Vertisol

Soil Taxonomy (Soil Survey Staff 1990) defines a soil as "collections of natural bodies on the earth's surface, ..., containing living matter and supporting or capable of supporting plants out-of-doors". Given this definition, the presence of rhizocretions and micro-rhizoliths in the mudstone we examined in the Pennington Formation indicates colonization by plants and supports a paleosol interpretation. Additional evidence includes: (1) a hackly soil-like macro-fabric (Fig. 2.5), (2) the gradual nature of the boundaries between units constituting the claystone (Fig. 2.3, 2.4), and (3) the presence of soil-like micro-fabrics (i.e., sepic-plasmic) of birefringent clay (Fig. 2.7).

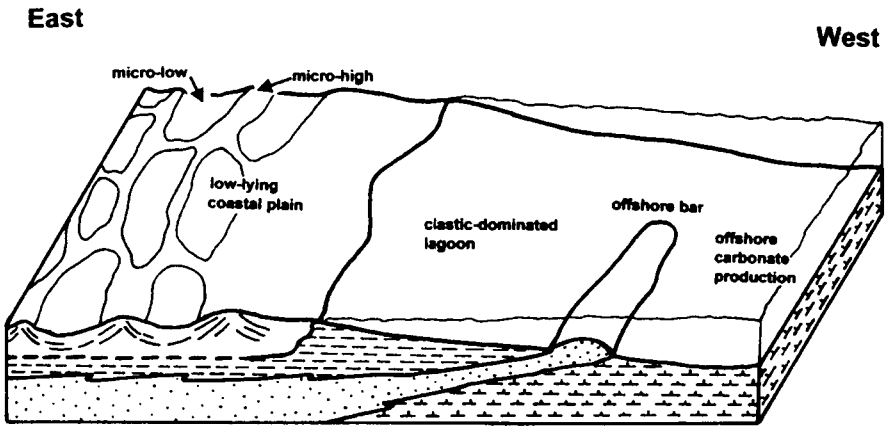


Figure 2.11 - Highly diagrammatic reconstruction of local paleogeography and paleoenvironments in study area during Late Mississippian time. View to south. No scale intended.

The claystone also contains mukkara (Fig. 2.3), which is a sub-soil feature commonly associated with gilgai micro-topography (Paton 1974). The presence of mukkara in the paleosol, taken in tandem with the preferential development of the dolomicrite crust in areas between pseudo-anticlines, suggests that the surface of the soil was patterned with the micro-highs and lows of gilgai. Unit 2 appears to correspond to the micro-lows of gilgai, whereas the pseudo-anticlines, which consist largely of Unit 3, represent the micro-highs. Thus, the pseudo-anticlines correspond to local micro-topographic divides that shed water into adjacent micro-lows where increased plant growth and accumulation of organic matter were favored (Lynn and Williams 1992). The micro-lows lay between the pseudo-anticlines and episodically became saturated and reducing, whereas the micro-highs and the lower parts of the paleosol (Units 4 and 5) remained oxygenated.

The paleosol preserves a nearly complete profile in the micro-low where depth to pedogenic carbonate was measured. Erosion associated with formation of Unit 1, the dolomicrite crust, removed and reworked a thin, surface horizon. Much of the eroded material was not transported from the area, but was immediately redeposited and subsequently incorporated into the dolomicrite crust. The following observations support our contention that the thickness of the soil profile in micro-lows was not significantly reduced by erosion: (1) erosion was probably more intense at micro-highs than in micro-lows (cf., Newman 1986), where entrained soil material appears to have been trapped; (2) erosion of the soil surface was not sufficient to suppress gilgai micro-relief, the presence of which is inferred from the preferential development of the dolomicrite crust between

pseudo-anticlines we equate with micro-highs; (3) numerous grains of silty claystone scattered throughout the dolomicrite crust suggest deposition of eroded soil material in concert with formation of the crust; (4) some silty claystone grains in the crust contain dolomicrite-filled, fine root channels compatible with derivation from surface horizons; and (5) the paleosol is directly overlain by shale, recording drowning of the soil surface during transgression of a low-energy environment.

The most prominent macro features in the paleosol, such as large arcuate slickensides, wedge-shaped structural aggregates (i.e., parallelepipeds), pseudo-anticlines, and mukkara (Figs. 2.3, 2.4, 2.5), suggest that alternating periodic expansion and contraction of the soil body were dominant pedogenic processes. These processes were driven by stresses comparable to those produced in modern clay-rich soils containing abundant expandable clays and subjected to periodic wetting and drying, such as Vertisols. Expandable clays are rare in the paleosol due to extensive illitization. On the basis of oxygen isotope compositions of illite/smectite and pedogenic carbonate, Mora et al. (in review) suggested that illitization in the paleo-Vertisol was initiated in the pedogenic environment and continued in the shallow burial environment. The presence of 2M illite in the carbonate nodules indicates that some of the illite in the paleosol is detrital.

Alternating wet and dry conditions are also compatible with the presence of Fe-Mn concretions and carbonate nodules, and the septarian and circumgranular cracks present in some of the carbonate nodules (Fig. 2.11; cf. Brewer 1976, Freytet and Plaziat 1982, Blokhuis et al. 1990). Banding in the Fe-Mn concretions, common in the claystone matrix of Unit 2, suggests episodic fluctuations in oxygenation of parts of the paleosol.

Although a consensus is lacking, several workers have suggested that micro-lows experience a seasonal fluctuation in moisture content greater than in micro-highs (Wilding et al. 1990). This may explain why Fe-Mn concretions are most abundant in Unit 2, which developed preferentially in micro-lows.

In addition to the features cited above, Lynn and Williams (1992) noted that the morphological expression of the stresses produced by soil expansion during wetting is enhanced in soils containing carbonate horizons. Material from the carbonate horizons can be progressively thrust along pedogenic slickensides into pseudo-anticlinal areas. The carbonate nodules disseminated throughout Unit 3, a unit present only in pseudo-anticlines, probably originated in Unit 4 and were pedoturbated and translocated in this way into the pseudo-anticlines so as to form Unit 3. Wilding et al. (1990) documented a similar modern scenario for the Vertisols of coastal Texas.

Some of the slickensides in the pseudo-anticlines of the paleosol appear to have been loci for the propagation of nonpedogenic slickensides into the overlying shale during burial compaction. Pedogenic slickensides characteristically have steepening dips as they near the soil surface and encounter decreasing vertical stress. The greater vertical stress that accompanies burial results in flatter dips for any slickensides that form. The marked decrease in dip of parts of the slickensides extending from the paleosol into the shale overlying the paleosol suggest that this part of the slickenside formed during burial compaction, under greater vertical stress than the portions of the slickensides lying within the paleosol.

Mack and others (1993) have produced a classification scheme for paleosols. It remains controversial and we see no need in applying it here, because the array of features preserved in the paleosol from the Pennington Formation meets the morphological requirements set forth in Soil Taxonomy (Soil Survey Staff 1990) for the Holocene order Vertisols. Therefore, in this rare circumstance, we interpret the paleosol as a paleo-Vertisol, that is, a direct analogue to Holocene Vertisols. Table 2.1 compares the features required of modern Vertisols by Soil Taxonomy (Soil Survey Staff 1990) to those found in the paleosol.

Origin of Dolomitic Carbonate Nodules

Accumulations of pedogenic carbonate ("calcretes"), composed predominantly of low-magnesium calcite, are widespread in fossil and modern soils (cf. Wright and Tucker 1991). Dolomitic calcretes ("dolocretes") have been reported in a variety of settings, including: (1) Quaternary dolocretes flanking the southern Australian coast (Hutton and Dixon 1981, Milnes and Hutton 1983, Phillips and Milnes 1983), (2) within thick Quaternary calcretes of the Kalahari Desert (Watts 1980), and (3) associated with Lower Carboniferous paleosols developed in marginal marine deposits in South Wales (Wright and Robinson 1988; Searl 1988) and Belgium (Muchez and Viaene 1987). In the Australian examples, pedogenic calcite cementation of preexisting dolomite forms indurated hard-pans. In the other studies, primary precipitation of dolomite in the pedogenic environment is called upon. In the Lower Carboniferous paleosols, dolomite is interpreted to be essentially a coastal pedogenic equivalent to calcrete development in a more fully emergent soil (Searl 1988).

Table 2.1. Summary of Soil Taxonomy criteria (Soil Survey Staff 1990) for Holocene Vertisols compared to features in paleo-Vertisol from the Pennington Formation.

Soil Taxonomy Criteria	Features in Paleo-Vertisol
1) No lithic or paralithic contact, petrocalcic horizon, or duripan within 50 cm of surface; **and**	Not present in paleosol
2) 30% or more clay in all subhorizons to a depth of 50 cm; **and**	> 30% clay based on estimates from thin sections
3) Open cracks at a depth of 50 cm that are at least 1 cm wide and extend upward to the surface; **and**	Silt-filled vertical crack > 85 cm long and approximately 7 cm wide at 50 cm depth
4) Must have one or more of the following features:	
a) gilgai; **or**	Inferred by presence of mukkara and thickness trend in crust
b) at a depth of 25-100 cm, slickensides close enough to intersect; **or**	Common in Unit 3 and few in Unit 4
c) at a depth of 25-100 cm, wedge-shaped structural aggregates with long axes tilted 10-60° from horizontal	Common in Unit 3 and few in Unit 4

Dolomitic carbonate nodules in the paleo-Vertisol of the Pennington Formation retain many petrographic features consistent with a pedogenic origin, including disorthic fabric and root tubules (Fig. 2.5E, F). There is no apparent destruction of pedogenic fabrics associated with dolomite precipitation (Figs. 2.7E, 2.9). The more complex nodules retain cathodoluminescence zonations similar to those observed in calcitic pedogenic nodules from other vertic, Paleozoic claystone paleosols (Driese and Mora 1993). Micro-crystalline dolomite is restricted to nodules, and the clay matrix of the paleosol is essentially devoid of carbonate. Carbon and oxygen stable isotope compositions of dolomite scatter between values typical of pedogenic calcite and dolomite precipitated in shallow, evaporative environments (Caudill et al. 1992b). Collectively, these observations suggest that the dolomite precipitated in a pedogenic environment, most likely during very early postpedogenic dissolution and recrystallization of pedogenic calcium carbonate. We favor a *per descensum* (Goudie 1973) origin for the dolomite. A capillary fringe origin seems unlikely, because the paleosol and the nodular carbonate unit lack low-chroma mottles and thus appear to have formed well above the water table, which was lowered in response to the drop in base level that exposed the area to pedogenesis. In modern soils, accumulation of carbonate by capillary rise in not thought to be widespread (Birkeland 1984).

Origin of the Dolomicrite Crust

The origin of the dolomicrite crust is intimately related to the presence of gilgai micro-relief on the surface of the paleosol during active pedogenesis. The subsurface expression of the micro-relief is preserved as mukkara, which is revealed by lateral

thickness variation in Unit 2 (Fig. 2.3, 2.4). Unit 2 is up to 80 cm thick in areas corresponding to gilgai micro-lows and thins to 0-5 cm near prominent pseudo-anticlines, which correspond to gilgai micro-highs. Thickness trends in the dolomicrite crust parallel those of Unit 2 such that the crust is thickest in micro-lows. Both the crust and Unit 2 are characteristically absent in the micro-high areas represented by pseudo-anticlines. This suggests that gilgai micro-relief was indeed present on the soil surface during formation of the dolomicrite crust and that the crust formed preferentially in the micro-lows (Fig. 2.12). The top of the paleosol, which we place at the top of the dolomicrite crust, is now flat because of infilling of the micro-lows by the crust.

The crust may have formed as a result of sporadic inundation of the gilgai-bearing soil surface by storm tides (Fig. 2.12). The paleosol occupied a coastal setting closely adjacent to the Chesterian epeiric sea, just a meter or so above normal tidal level (Fig. 2.11). Sporadic inundation by storm tides may have delivered carbonate mud from offshore environments to the surface of the paleo-Vertisol, where surficial soil material was eroded and entrained. As the storm tides receded, the carbonate mud and much of the eroded soil material accumulated in micro-lows on the soil surface.

Storm tides would also have ponded marine waters in micro-lows. Normal marine waters have a Mg/Ca ratio sufficiently high to cause dolomitization if the competing ion effect of SO_4^{2-} can be overcome (Baker and Kastner 1981). Dolomite may also form (at slow rates of crystallization) from freshwater with Mg/Ca ratios as low as 1:1, because of the lack of competing ions (Land 1973). The dolomicrite crust may thus have formed as rainfall diluted marine waters ponded in the micro-lows on the soil

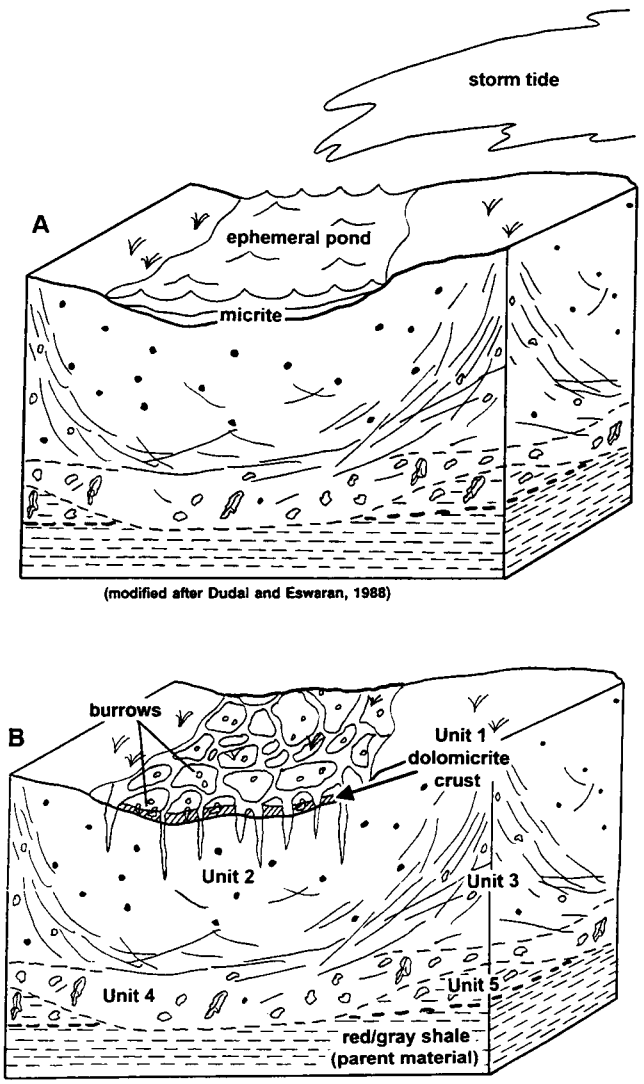


Figure 2.12 - Conceptual model for formation of dolomicrite crust at top of paleosol. A) Ponding of marine water in gilgai micro-relief following inundation of soil surface by storm tide. B) Pedogenic modification of crust. See legend in Figure 2.4.

surface. The introduction of rain water reduced salinity, thereby diminishing the effect of competing ions (principally SO_4^{2-}) in the ponded marine water. Because of the very small amount of Ca and Mg in rainwater, the Mg/Ca ratio in the ponded water may not have changed significantly. Thus, we favor a primary or penecontemporaneous recrystallization origin for the dolomicrite forming the crust at the top of the paleo-Vertisol.

Pedogenic modification of the crust occurred during its sporadic formation (Fig. 2.12B). The effects of soil-forming processes are recorded in the crust by the following features: (1) the clotted soil-like structure of the dolomicrite matrix (Figs. 2.10A, B, D) and (2) birefringent, illuvial clay fillings in planar voids and pores (Fig. 2.10E). Pedogenesis welded the crust onto the preexisting surface of the paleosol, as is indicated by the gradual transition from the claystone lithology of the paleosol "proper" to the dolomicrite crust (Fig. 2.5A). Abundant claystone grains scattered throughout the crust reflect entrainment and redeposition of surficial soil material by storm tides. Evidence of significant transport and erosion is lacking.

ESTIMATE OF PALEO-PRECIPITATION

Precipitation and Depth-to-Carbonate Data Set

The data base compiled by Retallack (1994) and used to quantify the precipitation and depth-to- carbonate relationship includes a significant number of vertic soils (cracking soils), as well as Vertisols from Australia and India (Retallack, pers. comm. 1995). The following are some of the ground rules used by Retallack to select soils for the data set compilation :

(1) all soils are Pleistocene or Holocene and situated on freely draining, low-lying or rolling terrains;

(2) target horizons are those with the most abundant, in-place, micritic carbonate nodules;

(3) carbonate horizons consisting of "veins" or "cements" are not included, because they could be of ground-water rather than pedogenic origin; and

(4) carbonate horizons massive enough to qualify as "K horizons" are not included, because of the complex history and great antiquity they indicate.

Retallack's compilation is global in scale and literature-based. Given the nature of the data set, it is unlikely that the following possible influences on depth to carbonate were evaluated on a soil-by-soil basis: (1) variations in depth of carbonate accumulation or leaching due to Late Quaternary fluctuations in precipitation; and (2) the possibility that in soils where the water table was close to or within the pedon, carbonate accumulation may have been more a function of rates of evapotranspiration than of mean annual precipitation (Blodgett, pers. comm. 1994). These problems probably contribute to the relatively large spread of the data set.

Obstacles

Retallack (1994) identified three primary obstacles that impede efforts to quantify paleo-precipitation using depth to pedogenic carbonate in paleosols: the effects of erosional truncation, compaction, and atmospheric CO_2 concentration on the depth to pedogenic carbonate. Where the carbonate horizon of interest is preserved in a vertic paleosol, every effort should be made to assure that depth to pedogenic carbonate in vertic paleosols is measured in parts of the profile that have not been subjected to vertical,

physical redistribution of pedogenic carbonate along slickensides. In addition, nodular carbonate horizons in hydromorphic paleosols are not suitable candidates for estimating paleo-precipitation, because they may have formed in response to water-table fluctuations (Aslan et al. 1993). My interpretation of the paleo-Vertisol in the Pennington Formation indicates that it formed following a drop in relative sea level and a corresponding drop in the water table. The lack of low-chroma mottles in the paleosol, particularly the claystone matrix of the nodular carbonate horizon, indicates that the paleosol and the carbonate nodules formed well above the water table. The remaining primary obstacles to estimating paleoprecipitation from depth to pedogenic carbonate are considered in the following sections.

Erosional Truncation

The effect of erosional truncation on my estimate of paleoprecipitation is minimal. The paleosol has undergone, at most, minor erosional stripping, and a nearly complete soil profile is preserved in the micro-low where depth to pedogenic carbonate was measured. The potential effect of minor erosional truncation on paleoprecipitation estimates is further minimized by the inclusion of some eroded soils in Retallack's data set, thereby offsetting this potential bias.

Late Mississippian Atmospheric CO_2 Level

At any given precipitation level, elevated concentrations of atmospheric CO_2 acidify soils and increase the depth at which carbonate horizons form (Retallack 1994). Therefore, Retallack's method may overestimate paleo-precipitation for soils formed during periods of elevated atmospheric pCO_2. During the Late Mississippian,

atmospheric pCO_2 may have been 2-4 times greater than present levels (600-1200 ppmV), judging from measured $\delta^{13}C$ compositions of pedogenic carbonate and coexisting organic carbon from the Pennington paleo-Vertisol (Mora and Driese 1993, Mora et al. 1996), and assuming soil CO_2 values of 3000-7000 ppmV. These estimates are in close agreement with those predicted by long-term carbon cycle models (Berner 1993). Slightly elevated Late Mississippian atmospheric pCO_2 concentration may lead to slight overestimation of paleo-precipitation.

Burial Compaction

Burial compaction reduces the depth to pedogenic carbonate horizons in paleosols and therefore leads to underestimation of paleo-precipitation. Retallack (1991) noted that perhaps the most reliable evidence for determining compaction in paleosols is ptygmatic folding of vertical cracks filled with soil material. The paleo-Vertisol in the Pennington Formation contains a large, vertical, silt-filled crack, which in outcrop shows little indication of ptygmatic folds (Fig. 2.6). The vertical micro-cracks present in the silt filling the large crack (Fig. 2.8A) are better evidence for evaluating compaction, however. These micro-cracks are lined with bands of oriented clay interpreted as coatings of infiltrated soil material (Fig. 2.8B). Measuring the length of the micro-cracks around their few convolutions and comparing this to their straight-line length yields a compaction ratio of less than 10%. Implicit in this estimate, however, is the assumption that the claystone body of the paleosol and the silt-infilling in the large, vertical crack compacted equally; differential compaction of the paleosol and vertical crack is considered below.

The bulk densities of sediments strongly influence their compactability and are widely known to be directly related to grain density and fluid content, the latter being a function of porosity and degree of saturation. The grain densities for quartz, the dominant mineral in the silt-filled crack, and illite, the most abundant mineral in the claystone matrix of the paleosol, are essentially equal (2.65 and 2.66 g/cm^3, respectively; Olhoeft and Johnson 1989). Thus, the contrasting mineralogies of the paleosol matrix and the silt-filled crack would not contribute significantly to differential compaction of the two materials. Blodgett (1985) suggested that Vertisols may undergo little burial compaction because of their naturally high initial bulk densities. A mean oven-dry bulk density of 1.8 g/cm^3 was reported for U.S. Vertisols (380 samples; Eswaran et al. 1989), whereas 2.3 g/cm^3 was reported for a Trinidad Vertisol (Ahmad 1983). Fox (1964) and Berndt and Coughlan (1977), however, have shown that the higher the moisture content of Vertisols, the lower their bulk densities. Accordingly, oven-dry bulk densities may be of limited use in assessing the propensity of Vertisols to compact upon burial, because Vertisols may encounter and absorb significant amounts of water as they are buried. Any differences in compactability due to differing bulk densities must therefore derive from the fluid content of the silt-filled crack versus that of the claystone matrix of the paleosol. Trask (1931) found that saturated coarse and fine silt with estimated water contents of 52% and 66%, respectively, had bulk densities of 1.26 and 0.88 g/cm^3. Ahmad (1983) cited bulk densities from Trinidad Vertisols ranging from 1.30 g/cm^3 at 40% moisture content to 0.80 g/cm^3 at 80% moisture content. The higher permeability of silt and the green color of the silt filling in the large vertical crack suggest that it was saturated with

water. The bulk density can be estimated to have been between 1.26 and 0.88 g/cm^3, by comparison with the data of Trask (1931). The paleosol appears to have been unsaturated, judging from the prominence of red coloration, and therefore may have had a bulk density similar to or slightly greater than the silt-filled crack (Ahmad 1983). As such, compaction in the crack probably equalled or exceeded compaction in the paleosol, and it seems reasonable to use the length ratios of the ptygmatically folded micro-cracks in the siltstone to estimate maximum compaction in the claystone matrix of the paleosol.

Depth to Pedogenic Carbonate

The paleo-Vertisol in the Pennington Formation contains a pedogenic carbonate horizon at a depth of 90 cm within the profile measured in a gilgai micro-low. This gives a maximum decompacted depth to the pedogenic carbonate horizon of 100 cm. We measured depth to pedogenic carbonate in a micro-low to minimize the possibility that the pedogenic carbonate had been vertically translocated during soil formation. The large arcuate slickensides typical of Vertisols are avenues along which physical mixing of the soil takes place, and can translocate soil carbonate nodules to higher levels in the soil profile (Lynn and Williams 1992). Such slickensides are horizontally oriented in gilgai micro-lows, but become progressively more steeply inclined as they approach micro-highs, where they coalesce to form pseudo-anticlines (Fig. 2.3B). Therefore, the potential for vertical transport of soil carbonate nodules is greatly diminished in micro-lows.

Estimate of Late Mississippian Paleo-precipitation

Retallack (1994) compiled data from Quaternary soils and used it to derive an equation for calculating mean annual precipitation from depth to soil carbonate horizon:

$$P = 139.6 - 6.388D - 0.01303D^2,$$

which has a correlation coefficient r of 0.79 and standard error σ of ± 141 mm, where P = mean annual precipitation (mm) and D = depth (cm) to soil carbonate horizon. Note that D is measured from the top of the soil downward and by convention is always negative. Using this equation and a decompacted depth to soil carbonate of 100 cm, we calculate a mean annual paleo-precipitation of 648 ± 141 mm for central Tennessee during the Late Mississippian. The upper and lower ends of this range are comparable to present-day mean annual precipitation at Alice Springs, Australia (726 mm) and Amarillo, Texas (502 mm), whereas our calculated mean is similar to present day mean annual precipitation at Brownsville, Texas (670 mm) (Muller 1982).

In addition to precipitation, numerous factors interact to produce climate. It is interesting to note that in the Troll and Paffen climate classification, all of the sites mentioned above are in steppe and semi-desert climates, whereas in the Koppen classification Amarillo and Alice Springs lie in steppe climates and Brownsville lies at the dry margin of a zone of warm humid temperate climate (see Muller 1982). Brownsville, which has a mean annual precipitation very near that calculated from the Mississippian paleo-Vertisol, lies at a latitude of ~ 25 °N. A more tropical setting is envisioned for the paleo-Vertisol on the basis of paleogeographic reconstructions indicating a 5-10 °S paleolatitude for Tennessee during the Late Mississippian (Scotese et al. 1979). All other things being equal, mean annual temperature increases with decreasing latitude, and thus the climate in which the paleo-Vertisol formed was probably warmer than that of Brownsville, which has a mean annual temperature of 23.2 °C

(Muller 1982). This is important, because higher temperatures produce higher rates of evapotranspiration. Holocene Vertisols of the Lomalta and Benito series occupy sites less than a meter above normal tide level along Laguna Madre on the southeastern coast of Texas, near Brownsville (Williams et al. 1977). Although calcareous, and occupying a coastal setting similar to that envisioned for the paleo-Vertisol, these Holocene Vertisols lack the carbonate crust and carbonate nodules characteristic of the paleo-Vertisol. Akin (1990) noted that an annual rainfall of 630 mm produces a humid climate in northwestern Europe, but results in semiarid conditions in the lowland tropics. Using the same logic, we suggest that, in spite of similarities in mean annual precipitation, the paleo-Vertisol formed under a drier climate, which we qualitatively define as semiarid, than that of present-day Brownsville. This may help explain why the paleo-Vertisol contains a carbonate crust and nodules, which are notably lacking in the Holocene coastal Vertisols near Brownsville.

CONCLUSIONS

(1) The Pennington Formation contains a paleo-Vertisol, i.e., one that meets morphological criteria set forth in Soil Taxonomy (Soil Survey Staff 1990) for Holocene Vertisols. The paleo-Vertisol is capped by a dolomicrite crust that is interpreted to have formed as a result of episodic inundation of the gilgai-bearing soil surface by storm tides, causing accumulation of carbonate mud and marine water preferentially in gilgai micro-lows. The crust thins over micro-highs, suggesting that a nearly complete soil profile is preserved in micro-lows.

(2) A deep, vertical, silt-filled crack is preserved in the paleo-Vertisol. It contains

vertical, clay-lined micro-cracks, which were used to estimate less than 10% burial compaction of the paleo-Vertisol. This observation supports the contention of Blodgett (1985) that Vertisols undergo little burial compaction due to high initial bulk densities and allows determination of the uncompacted depth to pedogenic carbonate in the paleosol. Note that depth to pedogenic carbonate in vertic paleosols should be measured in areas between pseudo-anticlines so as to minimize the possibility that carbonate nodules, etc., have been vertically translocated along major slickensides.

(3) The equation of Retallack (1994), relating depth to pedogenic carbonate in Late Quaternary soils to mean annual precipitation, was used in tandem with the decompacted depth to pedogenic carbonate in the paleo-Vertisol to calculate a mean annual precipitation of 648 mm for the Late Mississippian in central Tennessee. This level of annual precipitation is comparable to that of present-day Brownsville, Texas, a site of modern Vertisol development. On the basis of paleogeographic reconstructions, however, the paleo-Vertisol formed at lower latitudes (5-10 °S vs. 25 °N) and possibly higher mean annual temperatures (i.e., > 23.2 °C) than Holocene Vertisols in the vicinity of Brownsville. Higher mean temperatures and rates of evapotranspiration may partially account for the development of the carbonate crust and nodules in the paleo-Vertisol, and the concommitant lack of carbonate crusts and significant development of carbonate nodules in Holocene Vertisols near Brownsville. Qualitatively, the Late Mississippian climate of central Tennessee is defined as semiarid.

CHAPTER 3

PHYSICAL COMPACTION OF VERTIC PALEOSOLS: IMPLICATIONS FOR BURIAL DIAGENESIS AND PALEO-PRECIPITATION ESTIMATES

INTRODUCTION

Empirical burial curves and equations available for argillaceous sediments and sandstone deposits are useful because they facilitate depth of burial or burial compaction estimates (Baldwin and Butler, 1985). Empirical burial curves and equations specific to paleosols, however, do not exist. In a little known publication, Retallack (1993) suggested that in spite of the generally clayey nature of soils, and by extension paleosols, the standard burial curve and equation for argillaceous sediments are not suitable proxies for estimating burial compaction in paleosols. He further argued that due to soil structural elements, the Slater-Christie sandstone burial curve and equation given in Baldwin and Butler (1985) produce better burial compaction estimates for paleosols. In this paper, we test Retallack's assertion using a burial compaction estimate based on clastic dikes preserved in Late Carboniferous (Pennsylvanian) vertic paleosols of southeastern Ohio, U.S.A., and suggest a more suitable proxy burial curve and equation for vertic paleosols in general.

Burial compaction is one of the major obstacles to estimating paleoprecipitation from depth to pedogenic carbonate in paleosols (Retallack 1994). Modern Vertisols undergo seasonal cracking, and thus vertic paleosols may be particularly good candidates

for paleoprecipitation estimates, because of an increased likelihood of preserving filled cracks as clastic dikes. Clastic dikes are one of the best features for estimating burial compaction. Due to filling of cracks with material similar to the soil matrix and the limitations of ourcrop exposure, clastic dikes will not be available in many vertic paleosols. Therefore, an empirically based burial curve for vertic paleosols would be of great use to sedimentary geologists interested in reconstructing basin history, thereby allowing for estimation of burial compaction in vertic paleosols lacking clastic dikes. The proxy curve and equation for paleosol compaction that I presented and offer a preliminary test of, in this paper, is the Slater-Christie sandstone burial curve and equation given in Baldwin and Butler (1985); modified to reflect the high initial bulk densities typical of modern Vertisols (c.f. Blodgett 1985).

In the sections which follow I briefly describe three Late Carboniferous (Pennsylvanian) vertic paleosols and the clastic dikes preserved within them. Furthermore, I outline a new method for measuring the length of clastic dikes along their convoluted traces and calculate burial compaction for the paleosols using the preserved dikes. Several different potential proxy burial curves are then assessed. A preliminary test of the favored proxy burial curve is conducted using clastic dike based compaction estimates and literature-based depth of burial estimates for Proterozoic, Ordovician, Early Carboniferous (Mississippian), and Late Carboniferous (Pennsylvanian) vertic paleosols. A brief discussion of some of the factors which may influence the compaction of vertic paleosols relative to compaction of sandstone and argillaceous sediment is also offered.

LOCATION AND STRATIGRAPHY

The clastic dikes that provided the impetus for this study are preserved in drill cores of Late Carboniferous (Pennsylvanian) paleosols from three sites in southeastern Ohio, U.S.A. (Fig. 3.1). The paleosols lie in the lower part of the Conemaugh Group (roughly time-equivalent to the Glenshaw Formation of West Virginia and Pennsylvania) and formed during the Early to Middle Stephanian (roughly equivalent to the Missourian stage); (Fig. 3.2). The paleosols closely underlie major marine marker units of the region, specifically, the Brush Creek, Portersville and Ames marine zones, which span a stratigraphic interval of approximately 65 m. The paleosols are, in places, separated from the overlying marine zones by relatively thin coal beds and/or non-marine to marginal-marine clastic deposits. Throughout this paper the paleosols will be referred to as the sub-Ames paleosol, sub-Brush Creek paleosol, etc., reflecting their stratigraphic proximity to marine marker units. Stratigraphic studies (see Chapter 4) indicate that the sub-Ames marine-zone intervals of ancient soil formation identified here are, in general, widely distributed throughout southeastern Ohio. Joeckel (1995) has documented the widespread nature of the sub-Ames paleosol in outcrop.

METHODS

The macromorphology of each paleosol was described following the approach outlined by Retallack (1988). Colors were described from wetted samples using the Munsell Rock-Color Chart (Munsell Color 1984). Thin sections of the paleosols, and the clastic dikes in particular, were examined using standard petrographic techniques. Preliminary analyses of the bulk mineralogy of paleosols matrices were conducted using

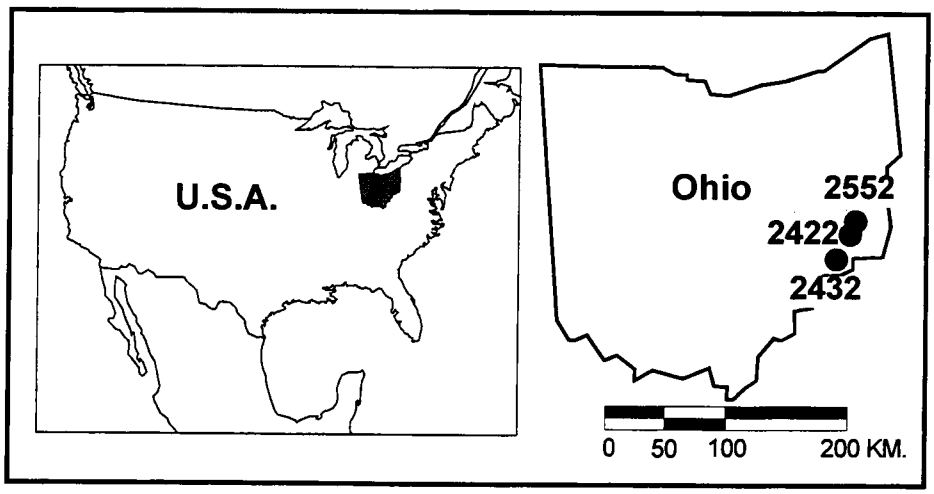


Figure 3.1 Location of drill core sites. Sub-Brush Creek, sub-Portersville, and sub-Ames paleosols described from cores 2552, 2422, and 2432, respectively.

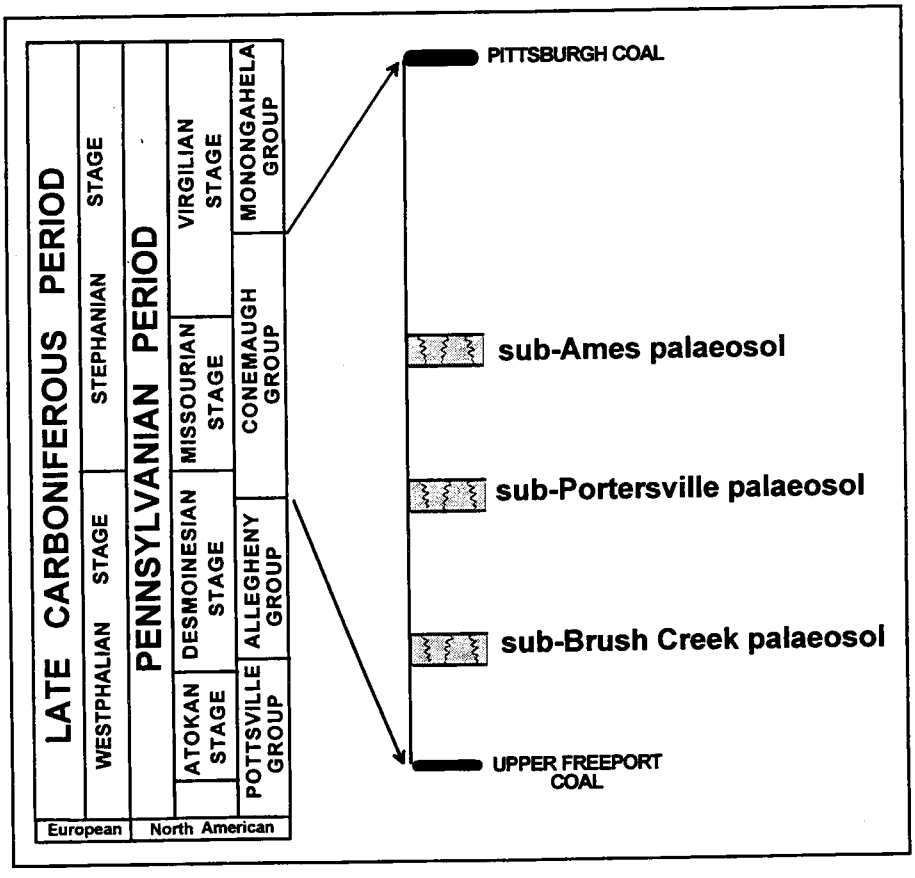


Figure 3.2 General stratigraphy of the Upper Pennsylvanian in Ohio. Stratigraphic positions of the paleosols are approximate.

hand-packed mounts and a Siemens D500 X-ray Diffractometer.

Core samples containing clastic dikes were slabbed, polished, and photographed. Photographic negatives of the clastic dikes were digitally scanned and stored on CD-ROM. Bit-map images of the clastic dikes were pasted onto a page in a graphics software package. The distance along the convoluted trace of a clastic dike was then measured by: 1) dividing the trace into short, straight-line segments, 2) using the diagonal dimension command of the graphics software to obtain the length of each straight-line segment, and 3) summing the lengths of the straight-line segments (Fig. 3.3). The vertical length of the compacted clastic dike was measured along a straight line using the vertical dimension command in the graphic software (Fig. 3.3). Burial compaction of the paleosol, expressed as a percentage of its original thickness, was calculated using the following formula;

$$\% \text{ Compaction} = (\sum \text{straight-line segments} / \text{ total length of dike}) \times 100. \quad (1)$$

Each dike was measured three times and compaction calculated from the average of the three measurements. The burial compaction estimate for the Late Carboniferous paleosols is, in turn, the average of that calculated from each of the four clastic dikes described in this paper. The burial compaction estimate for the Lower Carboniferous paleosol reported in Caudill et al. (1996) was recalculated from measurements obtained using the method described above.

Only vertically oriented dikes were considered for analysis, which prevented underestimation of compaction. It was assumed that the cracks that were filled to produce the clastic dikes were originally straight and vertical.

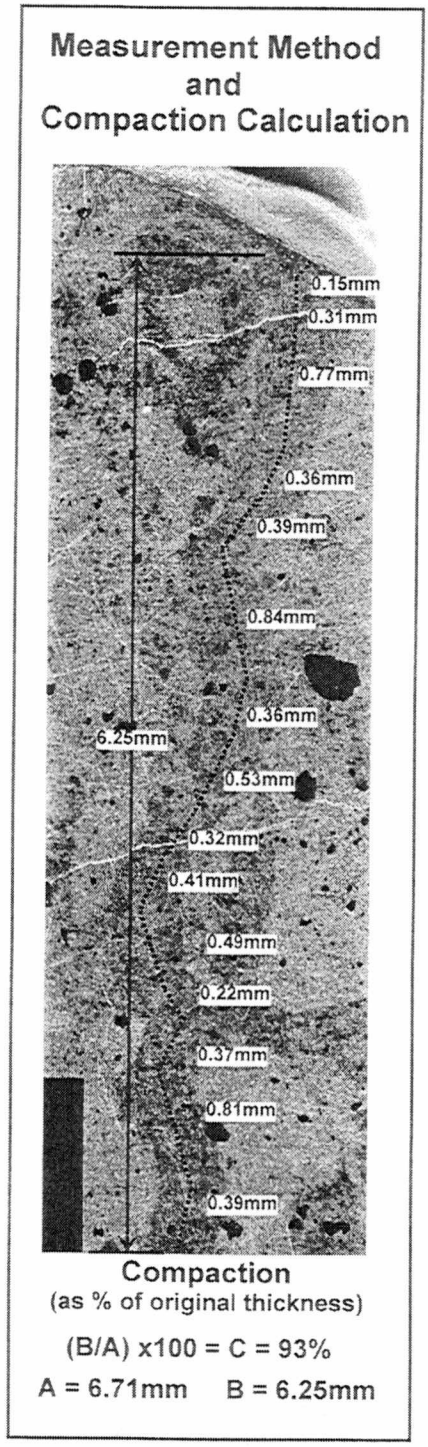


Figure 3.3 Measurement of clastic dikes and calculation of compaction as % of original thickness, where A = distance around convoluted trace of clastic dike and B = vertical straight-line length.

VERTIC PALEOSOLS

Clastic dikes are preserved in three core samples (2432, 2422, 2552), one each from the sub-Brush Creek, sub-Portersville, and sub-Ames paleosols. The paleosols are alluvial in nature and formed on a Late Pennsylvanian fluvio-deltaic landscape (c.f. Donaldson 1985). The paleosols are treated collectively in the descriptions, because our goal is simply to prove that they are indeed paleosols and of vertic affinity. Schematic profiles of the sub-Brush Creek (2552) and sub-Portersville (2422) paleosols, and one example of the sub-Ames paleosol (2432), are shown in Figures 3.4, 3.5 and 3.6. The sub-Brush Creek and sub-Portersville paleosols are 2.7 and 3.7 m thick, whereas the sub-Ames paleosol is almost 11m thick. The great thickness of the sub-Ames paleosol is characteristic (c.f Joeckel 1995) and points to welding of successive soil horizons to produce this complex paleosol. Inclined, polished and grooved, slickensided surfaces that cross-cut the paleosols (in core) are common and mark the presence of large, arcuate, pedogenic slickensides, which are typical of Holocene Vertisols (Soil Survey Staff 1990). Portions of wedge-shaped structural aggregates are preserved in core where the slickensides mutually intersect. The paleosols contain a variety of root-related features, including both horizontal and vertical carbonized root traces, carbonized root traces on the surfaces of large slickensides, red, olive-gray, and yellow-brown mottles associated with clay-filled root channels, and rhizocretions. Some units of the paleosols preserve weak to moderate, blocky soil structure. In thin section, masepic clay fabrics (Brewer 1976) are common, as are micro-peds displaying redoximorphic features such as Fe-depleted margins (Vepraskas 1992). Carbonate nodules are present in all of the

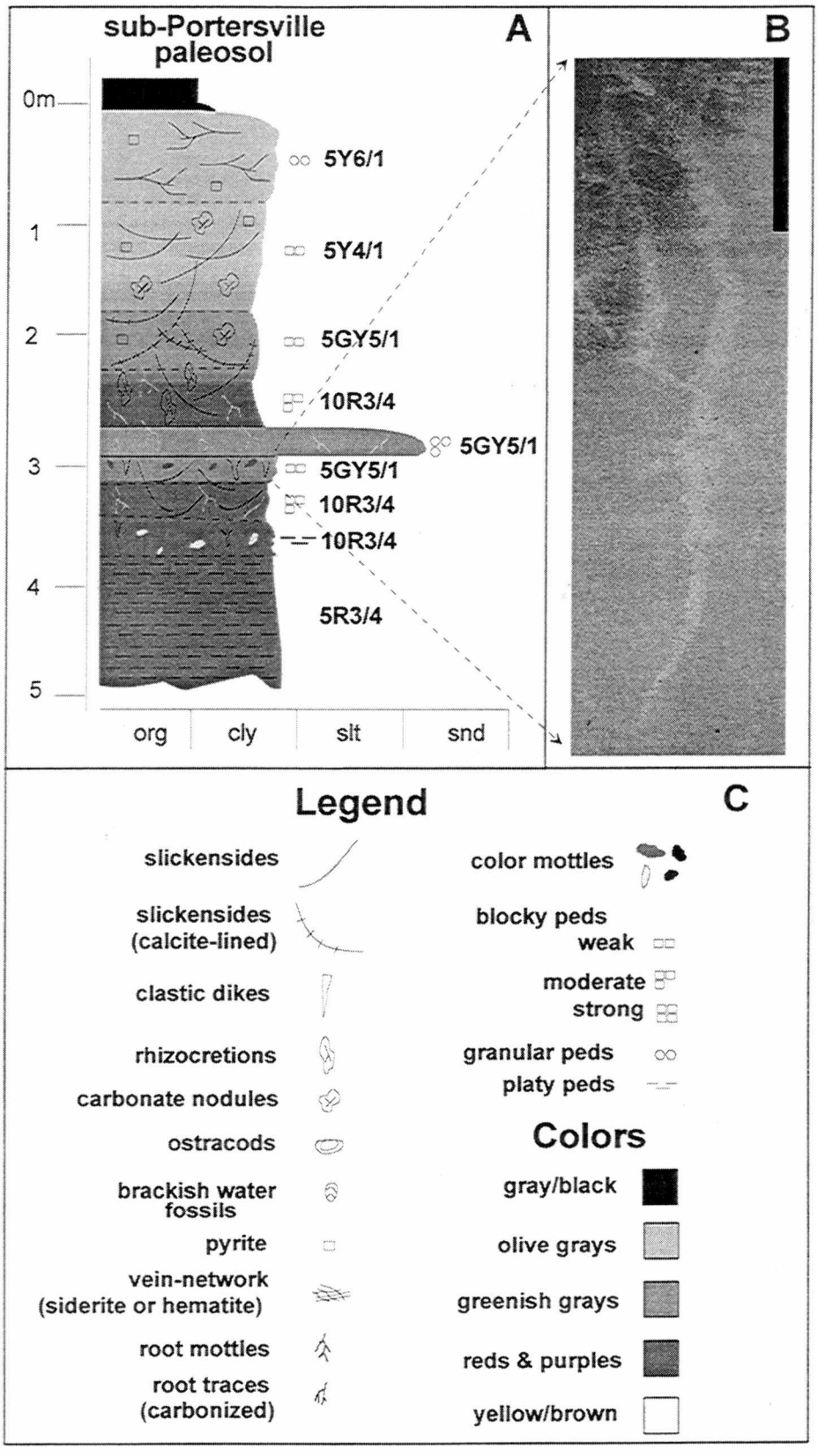


Figure 3.4 (A) Schematic profile of sub-Portersville paleosol in core 2422. (B) Clastic preserved in sub-Portersville paleosol (scale bar is 1 cm in length). (C) Symbols and colors used in schematic profiles of paleosols.

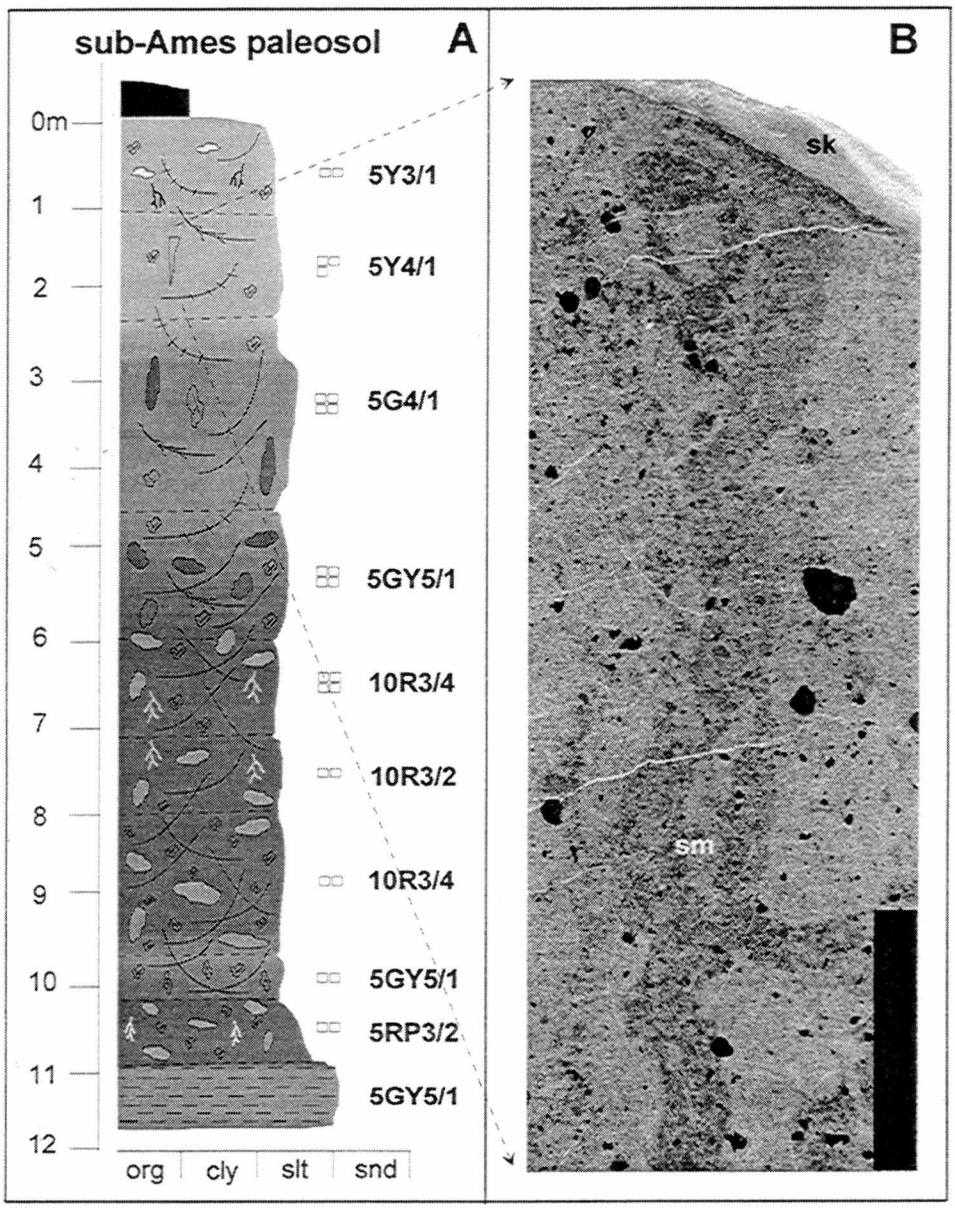


Figure 3.5 (A) Schematic profile of sub-Ames paleosol in core 2432. (B) Clastic dike preserved in sub-Ames paleosol (scale bar is 1 cm in length). Slickenside cross-cutting core indicated by "sk". Fragment of paleosol matrix spalled from wall of clastic dike indicated by "sm".

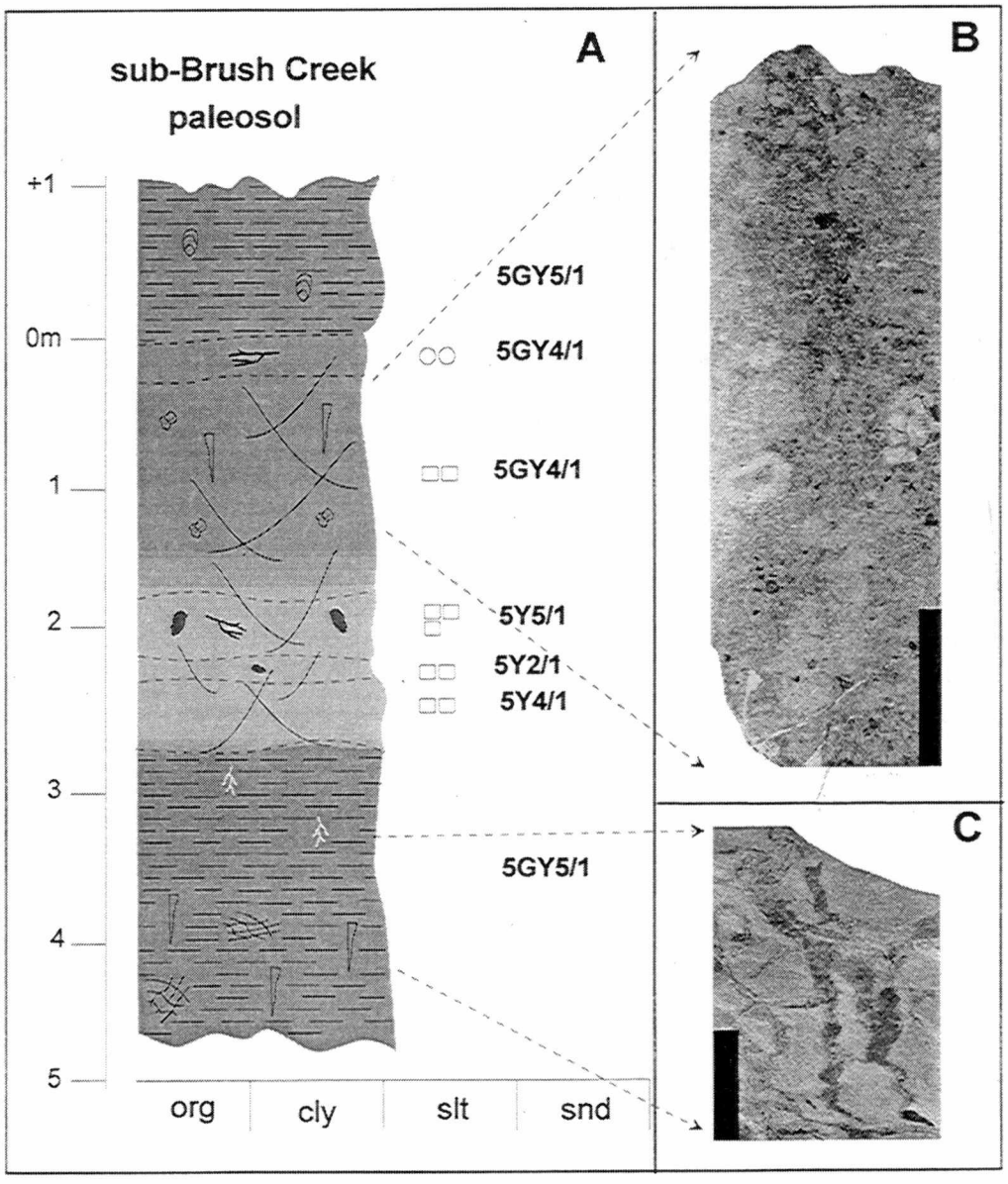


Figure 3.6 (A) Schematic profile of sub-Brush Creek paleosol in core 2552. (B) Clastic dike preserved in sub-Brush Creek paleosol (scale bar is 1 cm in length). (C) Convoluted clastic dikes preserved in shale underlying sub-Brush Creek paleosol indicate greater degree of compaction in shale than that observed in paleosol.

paleosols, but are most common in the profile from the sub-Ames paleosol (compare Figs. 3.4A, 3.5A, and 3.6A). Both alpha (abiotic) and beta types (biologically influenced) are present (Wright and Tucker 1991), with the alpha type typically ranging from 1-15 mm in diameter and the beta type generally larger, ranging from 20-60 mm in diameter.

Claystone matrices of paleosol units containing the clastic dikes are weakly calcareous. The clastic-dike bearing units of the sub-Brush Creek and sub-Ames paleosols contain small (< 15mm), tuberous, disorthic, carbonate nodules. These alpha-type nodules consist of dense, homogenous micrite that is interrupted by rare to common septarian cracks filled with microspar. Carbonate nodules are absent in the dike-bearing unit of the sub-Portersville paleosol.

The paleosols are clay-rich, and preliminary x-ray diffraction analysis reveals that they consist largely of illite, illite/smectite, kaolinite and/or chlorite (?). Red and purple portions of the clay matrix contain abundant hematite, whereas yellowish mottles are colored by goethite. The large arcuate slickensides and parallelepipeds (wedge-shaped structural aggregates) present in the paleosols are characteristic of the Holocene soil order Vertisol (Soil Survey Staff 1990). The vertic affinity of the paleosols suggests that they originally contained a significant component of smectitic clays and underwent argillipedoturbation in response to substantial seasonal variation in precipitation (c.f. Buol et al. 1989).

CLASTIC DIKES

The sub-Portersville paleosol in drill core 2422 contains a well-preserved clastic dike (Figs. 3.4A, B), the entire length of which appears to be included in the sample core slab. The clastic dike is approximately 35 mm in length (straight-line) and a maximum of 2.5 mm in width. It is filled with a grain-supported mass of angular quartz silt and very fine-grained sand. Using measurements from this dike, I estimate that the sub-Portersville paleosol was compacted to 93% of its original thickness during burial (Table 3.1).

The sub-Ames paleosol in drill core 2432 contains a well preserved clastic dike, but only a portion of its full length is contained in the sample core slab (Figs. 3.5A, B). The length of the dike in the sample is approximately 60 mm and the width is 5 mm. The clastic dike is filled with material similar to that of the surrounding clay matrix, but is darker (olive black (5Y 2/1)) in color. About two-thirds of the way along its length, the dike bifurcates around a large block of paleosol matrix that became incorporated into the fill material of the dike due to spalling along dike walls (Fig. 3.5B). Based on the portion of the dike preserved in the sample core slabs, it is estimated that the sub-Ames paleosol was compacted to 93% of its original thickness (Table 3.1).

As in the case described above, the full length of the clastic dike in the sub-Brush Creek paleosol is not present in the sample core slab. The portion of the dike contained in the sample measures approximately 70 mm in length and 7 mm in width (Fig. 3.6B). The dike is filled with clay similar to that comprising the matrix of the paleosol, but is darker in color (dark olive gray (5Y 3/1)) due to the greater abundance of opaque grains.

Table 3.1. Dike measurement data used for estimation of physical compaction of paleosols.

PALEOSOL	DIKE LENGTH	SUM OF STRAIGHT-LINE SEGMENTS	COMPACTION	AVERAGE COMPACTION
PENNSYLVANIAN				
(SUB-AMES)	61.5 mm	66.6 mm	92 %	
	62.0	66.9	93	92 %
	62.0	66.7	92	
(SUB-PORTERSVILLE)	36.1	39.8	91	
	37.3	41.3	90	91 %
	36.9	40.7	91	
(SUB-BRUSH CREEK)	68.8	74.1	93	
	69.0	75.9	91	92 %
	68.8	7.56	91	
(SUB-BRUSH CREEK SHALE)	41.7	60.1	69	
	40.6	58.1	70	70 %
	41.8	59.8	70	
MISSISSIPPIAN (PENNINGTON FM.)	70.8 mm	77.5 mm	91 %	
	71.1	77.3	92	92 %
	71.3	77.0	93	
ORDOVICIAN (POWELL MTN.) dike 1	23.2 mm	28.1mm	83 %	
	23.3	28.5	82	82 %
	23.5	29.4	80	
ORDOVICIAN (POWELL MTN.) dike 2	25.0 mm	29.4 mm	85 %	
	25.1	30.6	82	83 %
	25.0	30.0	83	

The margins of this dike are less distinct than those of the previously described dikes. Measurements indicate that the sub-Brush Creek paleosol compacted to 92% of its original thickness during burial (Table 3.1).

Some might consider the accuracy of the compaction estimates from the sub-Ames and sub-Brush Creek paleosols to be questionable, because full-length samples of the clastic dikes were not available for measurement. I admit that it is possible that the unmeasured parts of the dikes are more convoluted than the measured parts, implying that I could have underestimated burial compaction for these paleosols. However, the striking similarity of estimates derived from these paleosols and the estimate from the sub-Portersville, where estimates are based on measurements of the full length of the clastic dike, seems too consistent to be pure coincidence. Thus, I contend that the portions of the clastic dikes measured from the sub-Ames and sub-Brush Creek paleosols have yielded reasonable burial compaction estimates for these paleosols.

Finally, the non-pedogenic shale underlying the sub-Brush Creek paleosol also contains clastic dikes. These dikes have markedly convoluted traces (Fig. 3.6C) and in that sense bear little resemblance to the clastic dikes observed in the paleosols. Our measurements of the clastic dikes preserved in the non-pedogenic shale indicate that it compacted to 70% of it original thickness (Table 1), a very significant departure from the compaction estimated for the paleosols. These results support previous contentions of original high bulk density for vertic paleosols (Blodgett 1985; Caudill et al. 1996).

PALEOSOL COMPACTION EQUATIONS

Solidity and Burial Compaction

Clastic dikes are clearly some of the best evidence for estimating burial compaction, but they are not routinely preserved. Estimating burial compaction for paleosols lacking clastic dikes is problematic. Retallack (1991a; 1993; 1994) made use of compaction curves given in Baldwin and Butler (1985) to estimate compaction in paleosols. The equations for these curves relate the "solidity" (complement of porosity) of strata to depth of burial and must be solved for burial compaction.

Retallack (1993) solved for burial compaction "as percent of original thickness", which is the inverse of Baldwin's (1971) "decompaction number" (i.e., the number by which the compacted thickness is multiplied to obtain pre-compaction thickness). I favor Retallack' s definition of compaction, because it is easier to visualize. Burial compaction (C) "as percent of original thickness" is given by the following equation, in which S_i = initial solidity (i.e., pre-compaction solidity) and S_b = burial solidity:

$$C = S_i / S_b . \qquad (2)$$

To obtain burial compaction, equations for the compaction curves given in Baldwin and Butler (1985) are solved for " burial solidity" as shown in the example below using the shale compaction curve, in which D = depth of burial (in km):

$$D = 6.02 S_b^{6.35} \qquad (3)$$

$$\text{and ...} \quad S_b = (D/6.02)^{1/6.35}. \qquad (4)$$

Then both sides of the equation are divided into "initial solidity" as follows to yield burial compaction (C):

$$C = S_i/S_b = S_i/(D/6.02)^{1/6.35} . \quad (5)$$

"Initial solidity" is obtained by reading directly from the plot of compaction curves in Baldwin and Butler (their Figure 3). Burial depth (D) commonly can be obtained from the literature, in which estimates are based on studies of regional stratigraphy and structure, conodont alteration, vitrinite reflection, moisture content of coals, etc.

Figure 3.7A shows the geologically significant portion (D>1 km) of the standard Baldwin-Butler compaction curves, as well as "vertic-calibrated" curves for shale and sandstone. The "vertic-calibrated" curves were derived from the standard curves by incorporating higher "initial solidities" (i.e., S_i = 70%) in the equations for the standard curves. This was done to accommodate the naturally high bulk densities of Vertisols, which Blodgett (1985) noted may limit the compactability of vertic paleosols. Eswaran et al. (1989) calculated a mean dry bulk density of 1.8 gm/cm^3 (n=380) for U.S. Vertisols. Using this value and the equation of Roberts (1967) for "solid-grain proportion" (i.e. solidity), I calculate an average "initial solidity" of 70% for Vertisols and extend this value to vertic paleosols: so that

$$S_i = \rho_{bd}/\rho_s , \quad (6)$$

ρ_{bd} = grain bulk density (i.e., 2.6 for montmorillonite) and ρ_s =dry bulk density.

The suitability of the various curves and equations as a method for estimating compaction in vertic paleosols lacking clastic dikes is illustrated in Figure 3.7A. Clastic dikes preserved in the Pennsylvanian vertic paleosols indicate compaction to approximately 93% of original thickness. For illustrative purposes let us assume a maximum burial depth of approximately 3 km (Beaumont et al., 1987). Plotting

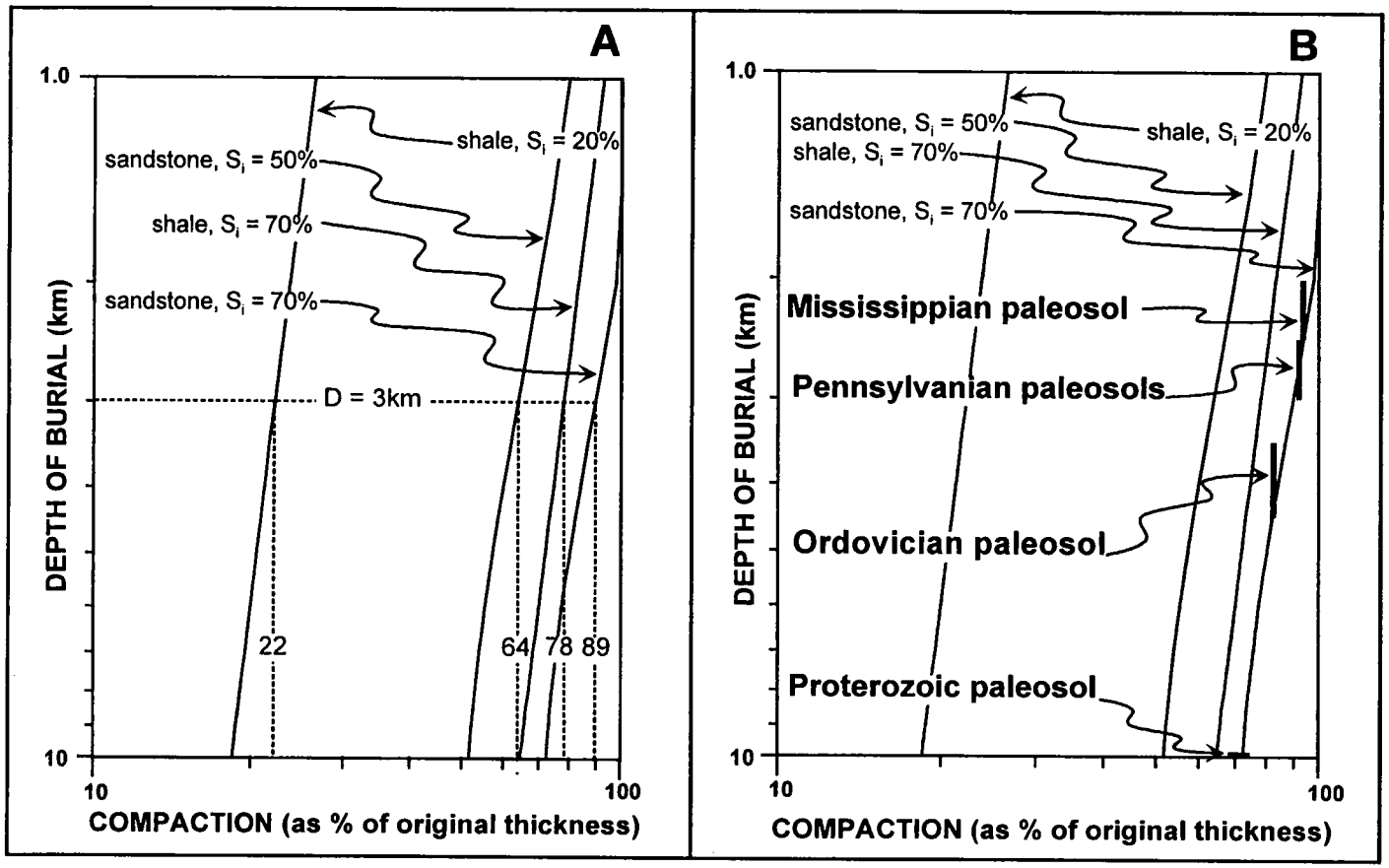


Figure 3.7 Burial curve diagrams plotting depth of burial versus compaction as % of original thickness (modified from Baldwin and Butler (1985) to reflect compaction instead of solidity). Burial curves were produced using equations indicated in text. (A) Compaction estimates from various burial curves for an assumed burial depth of 3 km. (B) Clastic-dike based compaction estimates for various paleosols compared to compaction estimates of various burial curves\equations. Note, dike-based estimates fall along the "vertic-calibrated" sandstone curve (i.e., sandstone curve with S_i (initial solidity) = 70%).

intersection points of this depth with each of the curves in Figure 3.7A, or setting D (i.e., burial depth) equal to 3 km and using the equations for the various curves yields compaction estimates, which can be compared to the known compaction of the Pennsylvanian vertic paleosols. Results of such comparisons are discussed below.

Shale Compaction Curves and Equations

For a burial depth of 3 km the standard shale curve indicates compaction to 22% of original thickness, which compares poorly to the 93% compaction estimated from clastic dikes in vertic paleosols buried to a similar depth. It is no surprise that the standard shale curve, based on compaction studies of "soupy" argillaceous sediments, grossly overestimates compaction in vertic paleosols. The departure emanates in large part from the low "initial solidity" of approximately 20% that is implicit in this equation.

To offset the low "initial solidity" of the standard shale curve/equation I follow Retallack's (1991b) lead and "calibrate" the standard shale equation to an "initial solidity" more characteristic of soils. Holocene Vertisols, and by extension vertic paleosols, differ from other soils and paleosols in several important ways, not least among them bulk density. Therefore, unlike Retallack I "calibrate" the standard shale curve/equation specifically for vertic paleosols by assuming an "initial solidity" of 70%. By examining Figure 3.7A, it is obvious that the "vertic-calibrated" shale curve yields significantly better results than the standard shale curve. For a burial depth of 3 km, our "vertic-calibrated" shale curve estimates burial compaction as 78% of original paleosol thickness, which is a significantly better estimate of the known value (93%) than that given by the standard shale equation.

Sandstone Compaction Curve and Equation

Recognizing the potential influence of soil structure on paleosol compaction, Retallack (1993) suggested that the Slater and Christie (1980) formula favored by Baldwin and Butler (1985) for sandstone compaction might more accurately calculate compaction in paleosols than the shale equation. Solving the Slater-Christie equation for sandstone compaction Retallack (1993) obtained the following expression:

$$C = -S_i/[0.49/(e^{(D/3.7)}) - 1]. \quad (7)$$

Retallack noted that the 50% "initial solidity" (S_i) implicit in the Slater-Christie formula was a more realistic average value for soils than the 20% implied by the Baldwin-Butler equation for compaction of argillaceous sediment. To support this contention Retallack cited 1.3 gm/cm^3 as the average bulk density of soils, which implies a soil solidity of 50% assuming a grain density of approximately 2.6 gm/cm^3. The standard sandstone compaction curve and equation estimates burial compaction as 64% of original thickness, for a burial depth of 3 km. Although this estimate is a significant improvement over that of the standard shale equation, it does not compare as well with the known compaction of 93% as does the "vertic-calibrated" shale curve and equation estimate.

In this paper, the 50% "initial solidity" (S_i) Retallack used in calculating paleosol compaction is replaced with 70% to yield an equation calibrated specifically to calculate burial compaction in vertic paleosols. The following "vertic-calibrated" equation is obtained:

$$C = -.70/[0.49/(e^{(D/3.7)}) - 1]. \quad (8)$$

Using this equation inconjunction with burial depth of 3 km, a burial compaction estimate of 89% of original thickness is obtained (Fig. 3.7A). This value compares very favorably with the known compaction of 93% and, for a burial depth of 3 km, yields significantly more accurate estimates than any of the curves and equations visited earlier. The following section examines, in greater detail, the applicability of the "vertic-calibrated" sandstone equation to estimating vertic paleosol compaction.

"Vertic-Calibrated" Sandstone Compaction Curve and Equation

The applicability of the "vertic-calibrated" sandstone curve and equation for estimating compaction in vertic paleosols lacking clastic dikes can be more critically evaluated by comparing measured compaction (i.e., clastic-dike derived) and burial depth range with calculated compaction, over the same depth range. Graphical comparisons of this type are shown in Figure 3.7B. In this figure, the measured compaction and burial depth range for examples of Pennsylvanian, Mississippian, Upper Ordovician, and Lower Proterozoic vertic paleosols are plotted, and can be readily compared to "vertic-calibrated" sandstone curve, as well as to the various other curves previously discussed.

The Pennsylvanian paleosols examined in this paper contain clastic dikes that record an average burial compaction to 93% of original thickness. Taking into consideration the total Pennsylvanian and Permian sediment thicknesses in southeastern Ohio indicated by Beaumont and others (1987), and the stratigraphic position of the paleosols within these successions, I estimate that the Pennsylvanian vertic paleosols were buried to a depth of 2.5 to 3 km. The calculated burial compaction for this range of burial depth is 89 to 93% of original soil thickness, which compares very well with the

measured compaction of 93%. This is demonstrated in Figure 3.7B by the intersection of the depth range-measured compaction plot with the "vertic- calibrated" sandstone curve.

Caudill and others (1996) have estimated maximum burial compaction to approximately 90% of original thickness for a Late Mississippian vertic paleosol exposed on the western margin of the Cumberland Plateau in Tennessee. Application of the improved measurement technique described previously in this paper to this paleosol indicates a burial compaction of 93%. Based on Beaumont and others (1987), this paleosol is estimated to have been buried to a depth of 2 to 2.5 km, which is compatible with the findings of Sheldon (1995) and Mora et al. (in review). Using this depth range and the "vertic-calibrated" sandstone equation, a burial compaction of 92 to 98% of original thickness is calculated. This compares well with the measured compaction of 92%, and as seen in Figure 3.7B, the depth range-measured compaction plot for this paleosol intersects the "vertic-calibrated" sandstone curve.

Driese and Foreman (1992) described Late Ordovician vertic paleosols in northeastern Tennessee and southwestern Virginia. On further examination, one of the paleosols exposed at the Powell Mountain locality was found to contain clastic dikes. Using the approach I described earlier in this paper, the vertic paleosol containing the clastic dike was compacted to 83% of its original thickness. Based on Conodont Alteration Indices presented in Harris (1979) and preserved stratigraphic thicknesses of Paleozoic rocks, a burial depth of 3 to 4.5 km is estimated for this vertic paleosol. For this depth range the "vertic-calibrated" sandstone curve and equation yields a compaction estimate of 82 to 89%, which compares well with the measured compaction (i.e., clastic-

dike derived) of 83%. The plot of burial depth versus measured compaction for this paleosol is shown in Figure 3.7B, in which it is shown to intersect the "vertic-calibrated" sandstone curve.

Retallack (1986) described an Lower Proterozoic (2.2 Ga) vertic paleosol near Waterval Onder, South Africa. It contains clastic dikes, from which Retallack estimated burial compaction to 67 to 73% of original thickness. The paleosol closely overlies the Hekpoort Basalt and is overlain by 7 km of sedimentary rocks of the Pretoria Group, 3 km of the Rooiberg Felsite, and 7 km of the intrusive Bushveld Complex, which includes 1-2 km of mafic sills within the sedimentary cover. Retallack suggested that the paleosol is no more than a few tens of millions of years younger than the Hekpoort Basalt. Radiometric dates for the Hekpoort Basalt and the Bushveld Complex suggests that the paleosol is approximately 100 million years older than the Bushveld Complex. Based on this information it is suggested that the paleosol was well lithified before emplacement of the Bushveld Complex and underwent little, if any, additional compaction as a result. Therefore, it isl justifiable to assume that the compaction recorded in the paleosol occurred in response to burial by Pretoria Group and Rooiberg Felsite to a depth of 10 km. Using the "vertic-calibrated" sandstone equation and a burial depth of 10 km a compaction to 72% of original thickness is calculated. This compares quite well with the compaction estimate of 67 to 73% that Retallack (1986) obtained from clastic dikes in the Waterval Onder vertic paleosol (Fig. 3.7B).

In summary, measured compaction (i.e., clastic-dike derived) and burial depth ranges for Pennsylvanian, Mississippian, Upper Ordovician, and Lower Proterozoic

examples of vertic paleosols correspond best to compaction calculated via the "vertic-calibrated" sandstone equation. This is demonstrated in Figure 3.7B, in which measured compaction-burial depth range plots for the various paleosols fall along the "vertic-calibrated" sandstone compaction curve. At this point there is insufficient empirical evidence to test the entire 1 to 10 km depth range over which the curve extends. Nonetheless, these preliminary results strongly suggest that the "vertic-calibrated" sandstone curve can be used to estimate burial compaction in vertic paleosols over a fairly broad range of burial depths (i.e., approximately 2 to 10 km). Therefore, in the absence of a paleosol compaction curve and more specifically a vertic paleosol compaction curve, the "vertic-calibrated" sandstone curve is favored for estimating compaction in vertic paleosols lacking clastic dikes or other preserved features used to derive burial compaction. Some preliminary considerations as to why the modified sandstone curve and equation produces better results than the other curves examined in this paper are discussed in the following section.

DISCUSSION

Intuitively, it seems unlikely that a sandstone compaction curve would predict compaction in vertic paleosols more favorably than a shale compaction curve. This bias may stem largely from the greater similarity in grain-size and mineralogy between argillaceous sediment and vertic soils versus that between sand and vertic soils. Obviously, the very low "initial solidity" (20%) of the argillaceous sediment, on which the standard shale curve is based, precludes its use for estimating compaction in high solidity (70%) vertic paleosols. Given the similarity of grain-size and mineralogy,

however, it would seem that a shale compaction curve calibrated to accommodate the high "initial solidity" of vertic paleosols would produce better results than the standard shale curve or sandstone compaction curve. It has been shown that the "vertic-calibrated" shale curve produces much better results than either the standard shale or standard sandstone curve. Surprisingly, the preliminary empirical evidence I present also shows that the "vertic- calibrated" sandstone curve produces even better results than the "vertic-calibrated" shale curve. Apparently, calibrating the standard shale curve to a high "initial solidity" is not sufficient to offset the differences in the burial compaction of argillaceous sediment versus vertic soils, as is indicated by the "measured compaction-burial depth" plots in Figure 3.7B. Retallack (1993) first suggested that soil structural elements (peds) cause soils to compact at rates more akin to sandstone than shale. The proxy curve that is proposed here for estimating burial compaction in vertic paleosols incorporates both the influence of high "initial solidity" and soil structure (peds).

As a result of their sheet-like form, clay minerals in argillaceous sediment tend to orient their basal planes perpendicular to overburden pressure during burial compaction (Rieke and Chilingarian, 1974). Development of preferred orientation by clay mineral particles is the main physical change accompanying consolidation of argillaceous sediments, along with the slow expulsion of pore fluids and corresponding progressive increase in solidity (i.e., decrease in porosity) (Allen, 1985). The degree of orientation increases with increasing overburden pressure, which enhances the development of fissility in shale. Although some vertic paleosols display limited fissility, the absence of fissility in the vertic paleosols considered in this paper suggests that reorientation of clay

mineral particles did not contribute significantly to compaction during burial. This observation, and the overestimates of burial compaction that the "vertic-calibrated" shale curve produces, suggest that the ease with which preferred orientation develops in argillaceous sediment renders them more compactible than vertic soils.

Many soils, Vertisols among them, contain well-developed soil structural elements (i.e., peds). In structured soils compaction proceeds in a fashion akin to the repacking of sand grains in sandstone, such that soil peds are packed more closely together (Hillel, 1980) and the contact area between peds increases, as peds begin to deform (Harris, 1971). Once the soil peds start to deform, overburden stress can then act on the clay mineral grains within the soil peds so as to initiate development of preferred orientation. Prior to burial, vertic soils are in a "semi-compacted" state from the standpoint of their naturally high bulk density and "initial solidity", as Figure 3.7B implies, and appear to be largely unaffected by compaction at burial depths of less than 1.5 km or so. Therefore, the propensity for vertic soils to develop oriented clay mineral particles may be diminished by their naturally high bulk density and "initial solidity", as well as the presence of soil peds, to the point that vertic soils compact more like sandstone than like argillaceous sediment. The disparity in the amount of compaction experienced by the Pennsylvanian vertic paleosols (compacted to 93% of original thickness) versus that recorded by the coeval, nonpedogenic shale (compacted to 70% of original thickness) directly underlying the sub-Brush Creek paleosol, is difficult to discount.

IMPLICATIONS

The "vertic-calibrated" sandstone compaction curve and equation presented in this paper improves the accuracy of estimates of burial compaction for vertic paleosols, improving in turn, the reliability of paleoprecipitation estimates. Furthermore, if vertic paleosols have high initial bulk density and undergo little compaction to burial depths of 1.5 km or so, as this study suggests, they will have very limited transmissivity, even at the onset of burial. This suggests that upon burial vertic paleosols may operate as closed systems, which has major implications for understanding their diagenetic modification. Additionally, efforts to quantify and understand the nature of burial compaction for vertic paleosols also promises to improve our understanding of aquifer/aquiclude and hydrocarbon reservoir/seal relationships in sedimentary basins containing intercalated paleosols.

CONCLUSIONS

The sub-Brush Creek, sub-Portersville, and sub-Ames paleosols from drill cores 2552, 2422, and 2432, respectively, are Vertisol-like. Clastic dikes preserved in these paleosols indicate burial compaction to approximately 93% of original thickness. Using a literature-derived burial depth of 3 km, standard burial curves for argillaceous sediment and sandstone both significantly overestimate burial compaction for these paleosols. The standard argillaceous sediment burial curve, calibrated to an initial solidity of 70% to reflect the naturally high bulk density of modern Vertisols, produces somewhat better estimates of burial compaction (i.e., 78% vs. 93%). However, the sandstone burial curve calibrated to 70% initial solidity produces the best results (i.e., 89% vs. 93%).

Preliminary assessment of the suitability of the "vertic-calibrated" sandstone burial curve and equation for predicting burial compaction in vertic paleosols is encouraging, but requires additional testing using other vertic paleosols. Clastic dikes preserved in vertic paleosols of Mississippian, Ordovician, and Lower Proterozoic age indicate burial compaction amounts compatible with compaction estimates obtained using the "vertic-calibrated" sandstone curve. Large portions of the curve, however, remain untested and well-preserved clastic dikes from vertic paleosols buried to depths between 5 and 10 km would be useful in this regard.

Finally, the "vertic-calibrated" sandstone curve and equation improve the accuracy of burial compaction estimates for vertic paleosols. More accurate estimates of burial compaction increases the reliability of paleoprecipitation estimates based on depth to pedogenic carbonate in vertic paleosols. Their high initial bulk density suggests that vertic paleosols had limited transmissivity at the onset of burial and so, may have functioned as closed systems during burial diagenesis. Further efforts to quantify and understand the nature of burial compaction for vertic paleosols promise to improve our understanding of aquifer/aquiclude and hydrocarbon reservoir/seal relationships in sedimentary basins containing intercalated paleosols.

CHAPTER 4

VERTIC PALEOSOLS, PERCHED WATER TABLES, AND INCIPIENT LATE PENNSYLVANIAN COAL SWAMPS; CONEMAUGH GROUP, APPALACHIAN BASIN

INTRODUCTION

Historically, the Conemaugh Group (Upper Pennsylvanian) of the central Appalachian basin is noted for prominence of fine-grained lithologies and red-green color banding. It has been informally referred to as the "Barren Measures" and, not surprisingly, the coals of this Group have received much less research emphasis than the thicker, more widely distributed, and more economically significant coals of the underlying and overlying Allegheny and Monongahela Groups (c.f., Merrill 1986). Conemaugh coals are of considerable paleoenvironmental and paleoclimatic interest, however, as noted in several recent studies (e.g., Cecil 1990, Joeckel 1995, Heckel 1995). Conemaugh coals are unique in that they record coal swamp development during a time that, overall, appears to have been the driest interval of the Pennsylvanian Period (Cecil 1990, Winston 1990). According to Cecil's (1990) model, Conemaugh coals record short-term climatic cyclicity that consisted of alternations from long-wet/short-dry to short-wet/long-dry. Intervals of short-wet/long-dry seasonality were marked by development of abundant vertic paleosols in upland areas and deposition of lacustrine limestones in basinal sites, whereas long-

wet/short-dry seasonality produced coals in basinal settings and leached soils in upland areas.

Heckel (1995) described a means by which global-scale, glacio-eustatic sea level fluctuations could have produced cyclic, regional-scale changes in the Late Pennsylvanian climate of the Appalachian basin on a temporal scale compatible with changes in climatic seasonality of Cecil (1990). Heckel suggested that cyclic expansion of the Midcontinent epeiric sea into the Appalachian region would have provided a broad expanse of marine water as a nearby source of atmospheric moisture. This, in turn, would lead to the cyclic production of moist climates and coal swamps (i.e., coals of the Conemaugh and Monongahela Groups) during what, otherwise, appears to have been the driest interval (i.e., the Late Pennsylvanian) of the Pennsylvanian Period.

In Cecil's model, vertic paleosols and coals indicate divergent paleoenvironments in that coals are the basinal expression of long-wet/short-dry climatic seasonality, whereas vertic paleosols are the upland expression of short-dry/long-wet seasonality. Caudill and Driese (1995) reported the common association of several Conemaugh coals (most importantly, the Harlem and Anderson coals) with vertic paleosols, in southeastern Ohio. Prior to this, in a site-specific study of a coal-vertic paleosol association, Caudill and others (1992a) suggested a genetic link between the vertic sub-Ames paleosol and the overlying Harlem coal. They noted the dominance of gray-green colors (nearly all of which were low chroma, i.e. ≤ 2) in the upper part of the paleosol and reddish colors (nearly all of high chroma, i.e. > 2) in the lower part of the profile. They interpreted this color distribution as recording development of a perched water table in the upper part of

the vertic paleosol and related its eventual intersection of the soil surface to growth of the "Harlem coal swamp". In a regional study of the sub-Ames paleosol complex, Joeckel (1995) came to a somewhat similar conclusion, suggesting a genetic link between the Harlem coal and sub-Ames paleosol complex.

This study further examines the significance of the coal-vertic paleosol association for development of Conemaugh coals. Utilizing data from closely spaced drill core, it demonstrates the influence that soils/soil landscapes can exert on subsequent deposition, in this instance, the formation of a coal swamp via water table perching, Furthermore, it evaluates several possible stimuli for growth of a perched water table in the upper part of the sub-Ames paleosol complex and initiation of the "Harlem coal swamp", including 1) changes in climatic seasonality as implied by Cecil (1990) and 2) drainage modification in response to rise of base level in advance of the "Ames transgression", as suggested by Joeckel (1995).

LOCATION AND STRATIGRAPHY

The study area spans Belmont, Monroe, Noble, and parts of Jefferson and Washington counties of southeastern Ohio (Fig. 4.1). Drill core locations are keyed to the lithology of the strata directly overlying the sub-Ames paleosol complex. Figure 1 also shows the location of five cross-sections constructed through the "sub-Ames paleosol complex-Harlem coal-Ames marine unit (SAHA)" stratigraphic interval.

The SAHA stratigraphic interval is situated towards the center of the Conemaugh Group (Upper Pennsylvanian) (Fig. 4.2). Subsurface correlation of this stratigraphic interval was guided by the thicknesses of the Ames-Pittsburgh coal and Ames-Middle

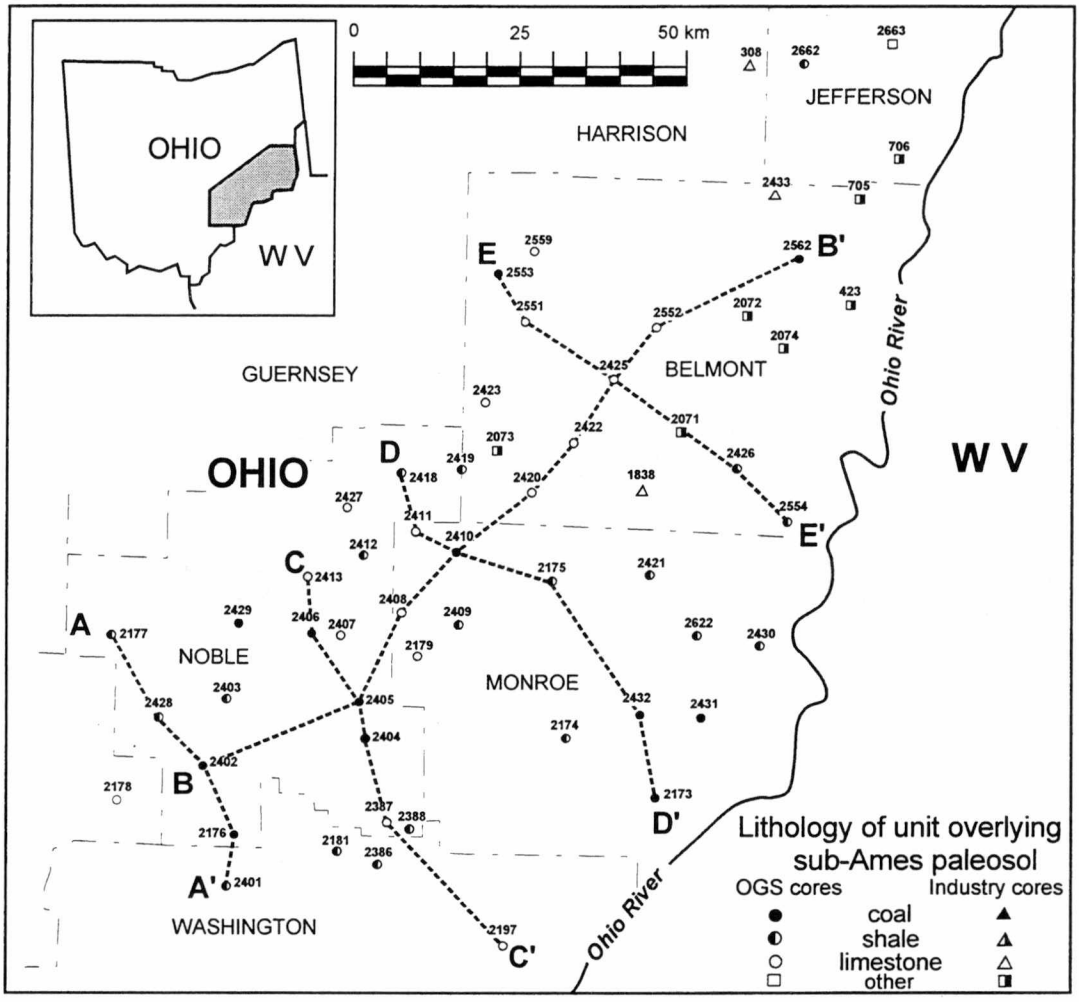


Figure 4.1 - Map showing location of study area, drill-cores, and stratigraphic cross-sections. Each core location is labeled with the core file number designated by the Ohio Geological Survey.

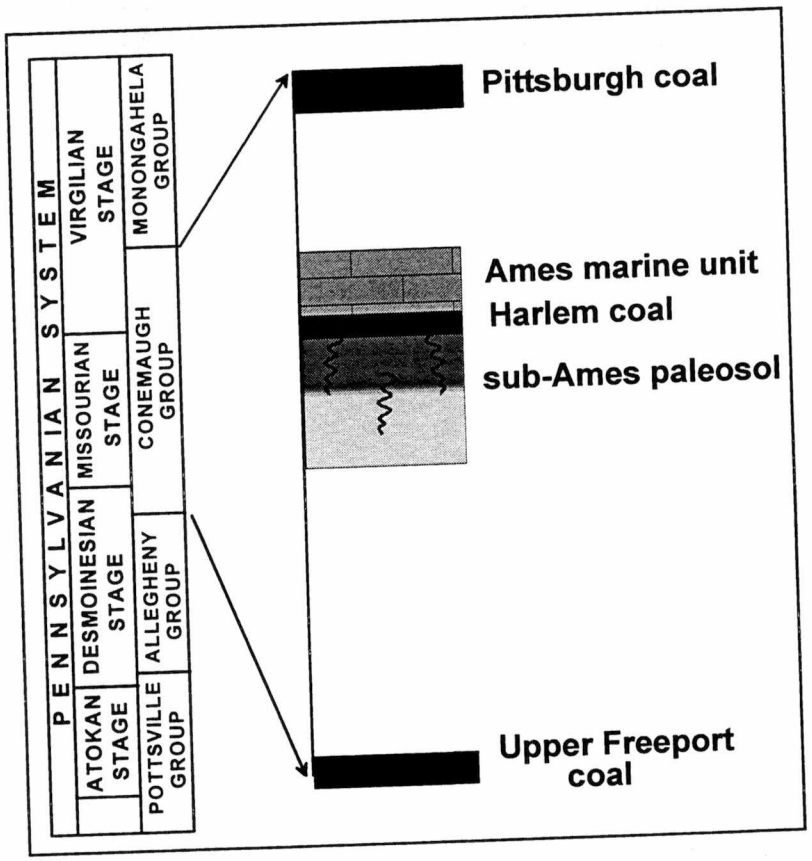


Figure 4.2 - Stratigraphy of the Conemaugh Group (Upper Pennsylvanian) (schematic not to scale).

Kittaning coal intervals. In retrospect, the upper boundary of the sub-Ames paleosol complex may be a better choice for correlation, but it is best recognized based on its proximity to the Ames marine unit.

The Ames marine unit is routinely regarded as the most widely distributed Pennsylvanian marine unit in the Appalachian basin. Al-Qayim (1983) mapped the lithologic variability of the Ames marine unit at a basin-wide scale. Our data, however, suggest significantly greater lateral lithologic variation than he envisioned, as will be discussed later.

In the study area, the sub-Ames paleosol complex varies from 5 to nearly 17 m in thickness. The paleosol complex is equivalent to the Round Knob shale (stratigraphically equivalent to Pittsburgh redbeds) of Condit (1912). Based on studies of outcrop (Joeckel 1995) and subsurface mapping presented here, the paleosol complex appears to be as widely distributed as the Ames marine unit.

In contrast to the Ames marine unit and the sub-Ames paleosol complex, the Harlem coal is highly discontinuous and thin, varying from 0 to 47 cm in thickness (cores 2553, 2404) and averaging 30 cm in the study area. There has been some debate over correlation of the Harlem coal beyond the type area (Carroll County, Ohio), where the stratigraphic relationship, top to bottom, of the Harlem coal, a light- to medium-gray clay, and a calcareous, red, variegated mudstone referred to as the Round Knob shale, was described by Delong (1969). The gray clay and red mudstone, collectively, compare very well to the green-gray low-chroma units overlying reddish high-chroma units in the paleosol complex of the study area. We suggest that the Harlem coal is best recognized

and correlated based on its position directly atop the sub-Ames paleosol complex, rather than the "traditional" practice of focusing on the position of the coal with respect to the Ames marine unit, which varies significantly in its stratigraphic proximity to the coal. The marine unit can lie directly atop the coal (Joeckel 1995, this study), but also commonly lies 3-8m above the coal (Al-Qayim 1983). Defining the Harlem coal based on its position relative to the paleosol reflects their genetic linkage (Joeckel 1995).

METHODS

This study is based on drill core samples and records obtained from the Ohio Geological Survey. Description of the macromorphology of the six profiles examined in detail was supplemented using polished slabs of each unit in a given profile, and followed the format outlined in Retallack (1988). The geochemistry of bulk samples of each soil unit in these six profiles was analyzed using pressed pellets and an energy-dispersive, EG&G Ortec x-ray fluorescence analyzer.

To better understand the processes that contributed to the formation of the paleosol complex selected molar ratios were calculated from raw geochemical data. The calculation and use of molar ratios are described in Retallack (1990), Mora et al. (1993), and applied in Retallack (1983, 1991, 1994), Feakes and Retallack (1988), and Retallack and Mindszenty (1994). Other techniques of data manipulation such as concentration ratios or the mass-balance approach offer better quantitative assessments, but require that the geochemical composition of the parent material be known. The great thickness and obvious genetic complexity of the sub-Ames paleosol complex, combined with its presence in cyclothemic deposits, which by definition include both marine and terrestrial

deposits, preclude the use of these techniques.

Based on examination of the data and comparison of the morphological characteristics of the sub-Ames paleosol complex with the many paleosols Retallack and coworkers (see references above) have analyzed using this method, three molar ratios were examined. These ratios and the characteristic/process that they are intended to gauge are: 1) SiO_2/Al_2O_3, "clayeyness", 2) SiO_2/Fe_2O_3, "weathering", and 3) Ba/Sr, "leaching". An additional ratio, Ca/Sr, was calculated for the uppermost sample of each profile. The ratio is used to assess "marine hydromorphism", as discussed later. To my knowledge this ratio has not been used in analysis of pre-Pleistocene paleosols.

The percentage of total profile thickness comprised by low-chroma units (%LCU) was calculated for each of the 48 drill cores. In those cores not described in detail, lithologic descriptions in drill core records were used. Although these descriptions do not specify chroma, experience has shown that units variously and routinely described as greenish gray, gray-green, and the like are characteristically low-chroma, whereas those described as red, reddish gray, red-gray, etc. are typically high chroma. No doubt there are exceptions to these assumptions, but the correlations appear to be strong enough to emerge from the noise inherent in this approach.

PROFILE CHARACTERISTICS

Profiles of the paleosol complex were described in detail in the following cores; 2402, 2405, 2408, 2428, 2432, and 2552 (Fig. 4.1). Morphological features of the profiles examined are schematically illustrated in Figures 4.3 and 4.4. Similar to the approach of Joeckel (1995), profile units, approximating horizons, are grouped into two

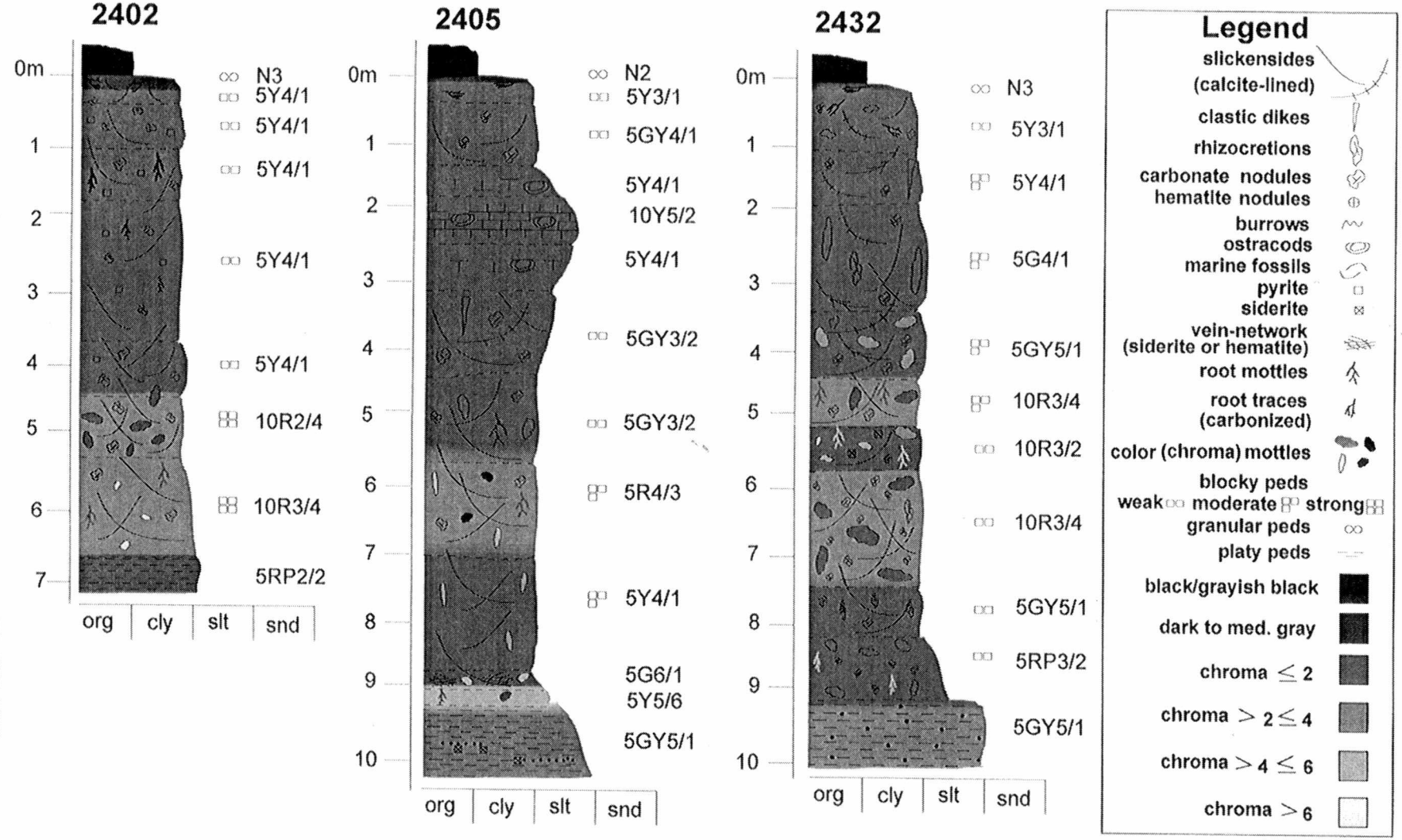


Figure 4.3 - Schematic profiles of the sub-Ames paleosol complex at sites interpreted to have been poorly drained.

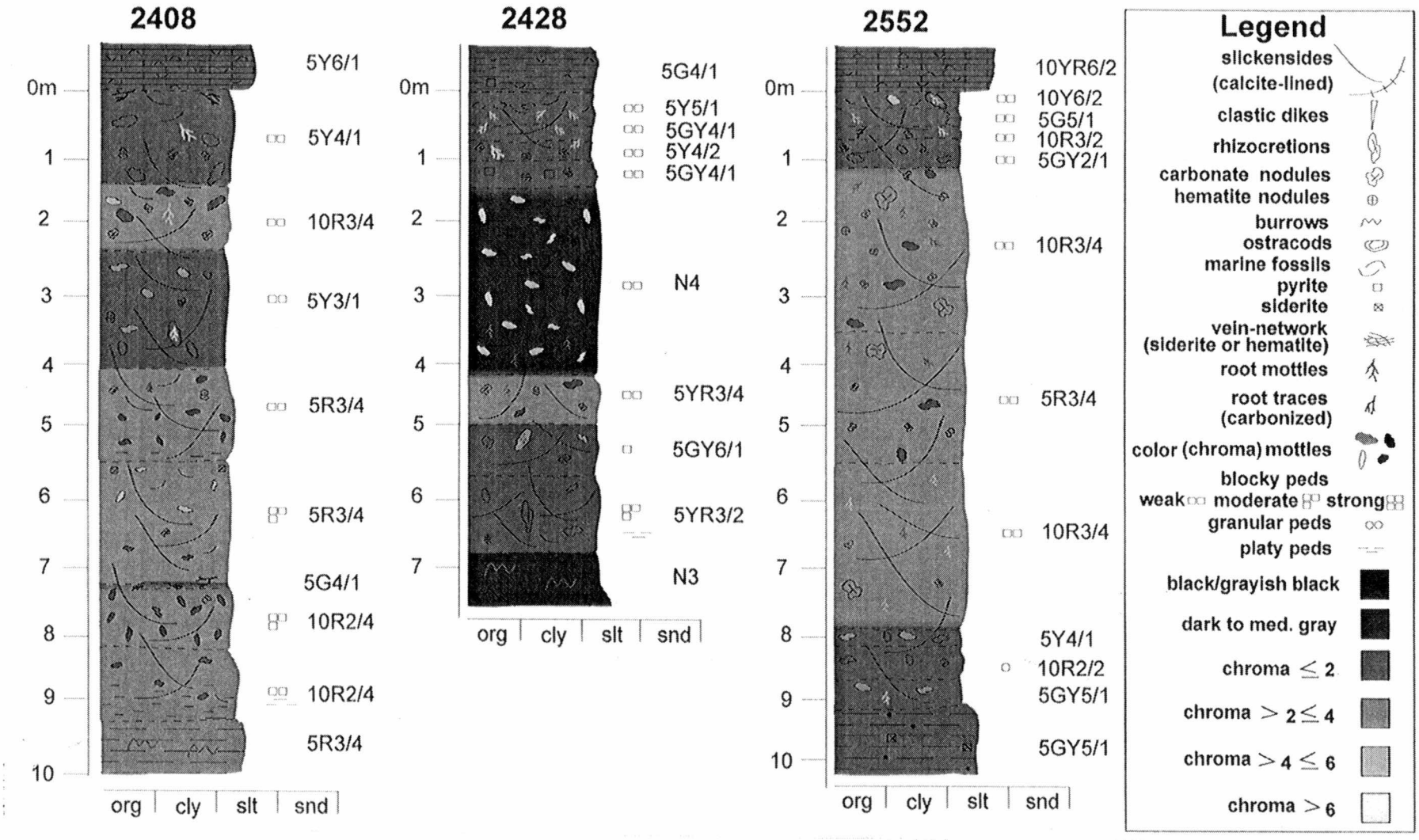


Figure 4.4- Schematic profiles of the sub-Ames paleosol complex at sites interpreted to have been well-drained.

broad components based on matrix chroma: low-chroma (≤ 2) units and high-chroma (> 2) units. Note, however, that in this study "low-chroma units" include the "Harlem coal underclay" and "strongly calcareous, low-chroma mudstones", both of which are categorized separately in Joeckel (1995). In the following two sections, the macromorphology of low- and high-chroma units is described and the geochemistry of the profiles presented.

Low-chroma (≤ 2) Units

Mudstone of olive gray and greenish gray dominate the low-chroma component of the paleosol, but a few low-chroma units have dark gray, red and rarely red purple hues. The dark gray units typically preserve crumb soil structure, horizontal, carbonized root traces, and small, irregular- to dish-shaped slickensides. The more prevalent, greenish, low-chroma units preserve weak to moderate blocky soil structure (Fig. 4.5A).Pores between blocky peds in the lower part of the thick low-chroma portion of profile 2402 are filled with illuvial clay (argillans) (Fig. 4.5B).

Faint, fine and medium, greenish gray (5GY6/1) mottles are common in many of the low-chroma units. Typically these mottles follow interpedal pores and vertical to sub-vertical root channels. Many of the low-chroma units in the profiles overlain by medium, dusky red (10R3/4) (Fig. 4.5C) or pale yellowish orange (10YR6/6) mottles. The yellowish mottles are goethite-rich (confirmed by XRD), and they and the red ones follow vertical and sub-vertical root channels or interpedal pores. Patchy, irregularly-distributed, and medium to coarse, reddish (10R and rarely 5RP) mottles are common in low-chroma units that bound high-chroma units (e.g., 2432).

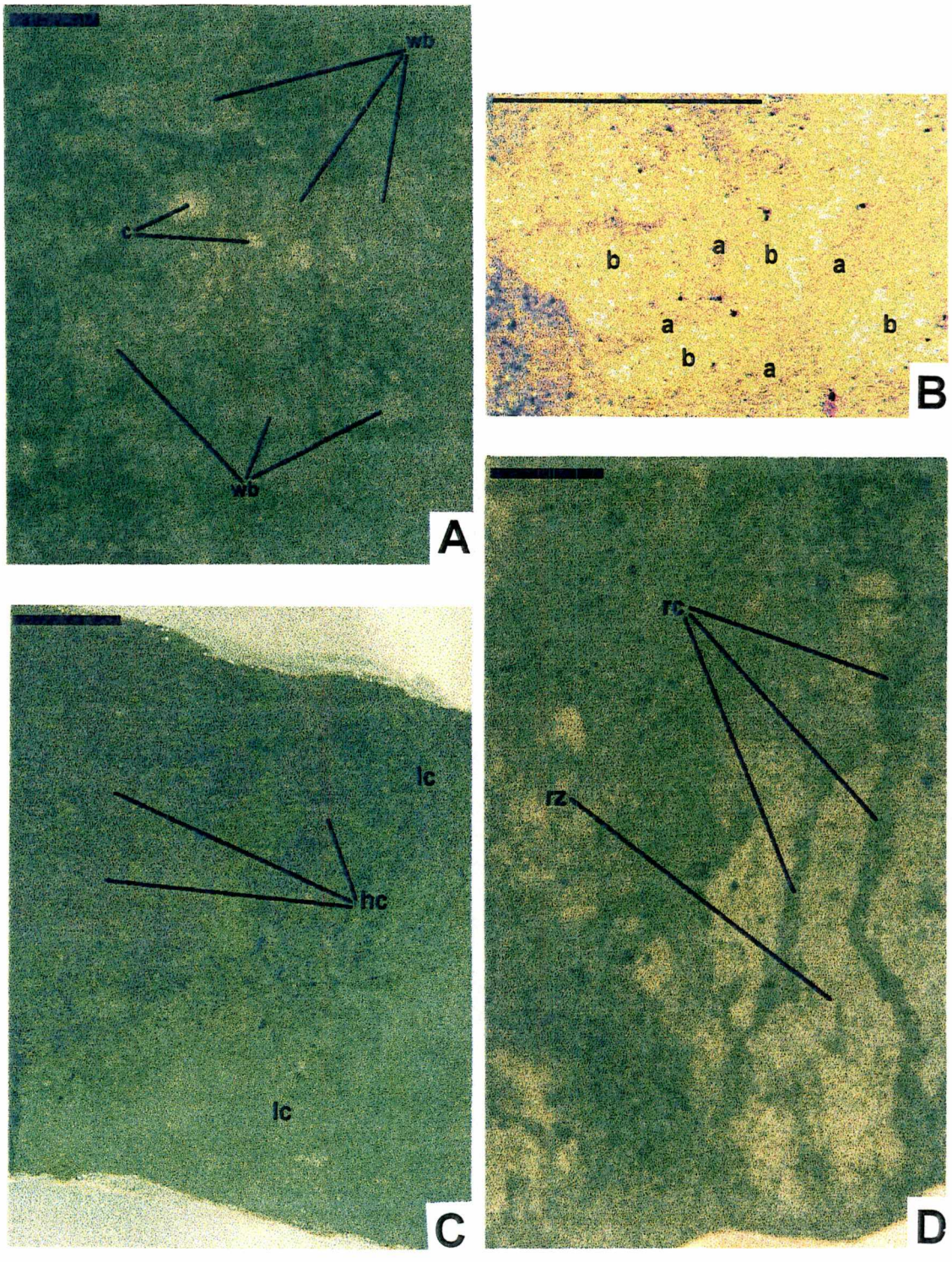


Figure 4.5 - Morphological features in low-chroma units (a=argillan, b= blocky ped, c=carbonate nodule, hc=high-chroma mottle, lc=low-chroma matrix, rc=root channel, rz=rhizocretion, wb=weak, blocky peds). Scale bars are 1cm in length.

marine limestone and fossiliferous shale (2408, 2552, & 2428) contain prominent, fine

Slickensides with polished and grooved surfaces cutting the entire width of core are common in these low-chroma units and clearly mark intersection of the drill core with large arcuate slickensides so common to the paleosol complex in outcrop (c.f., Joeckel 1995). A few of these large slickensides are blanketed by a thin (> 2mm) sheet of calcite. Carbonized root traces are also present on some of them (e.g., core 2432).

Spherical to tuberous, carbonate nodules (1 to 10 mm in diameter) with sharp margins are rare to common in most of the low-chroma units, and commonly form small clusters. Masses of smaller nodules comprise some larger (20 to 60 mm in diameter) nodules, present in a few units, which can have elongated forms, vertically oriented, in a fashion common to rhizocretions (Fig. 4.5D).

Pyrite and siderite are present in some of the low-chroma units. Pyrite is most prevalent in the uppermost units of core 2402 where it is preserved as fine, disseminated framboidal grains, as fine-grained patches commonly in association with carbonized roots, and as vein fillings. Siderite is present in the two lowermost units of core 2405, where it forms disseminated spherulites and fills a massive net of fine veins. Abundant siderite spherulites are also present in a red (10R) low-chroma unit in core 2432.

High-chroma (> 2) Units

The high-chroma units are similar to the low-chroma units in many aspects; color is the most obvious departure. The reddish matrix colors (10R and 5R hues) that characterize the high-chroma units are a striking reflection of the abundance of ferric iron in the form of hematite (confirmed by XRD).

Less striking differences include soil structure, slickensides, and root traces. Blocky soil structure is characteristic of the high-chroma horizon and is typically better developed (moderate to strong, versus weak to moderate) (Fig. 4.6A) than in the low-chroma units. Large slickensides similar to those of the low-chroma units are present (Fig. 4.6A). Absent from the high-chroma units are thin sheets of calcite and carbonized root traces on slickenside surfaces, and carbonized root traces similar to those underlying coal at the top of some profiles.

Siderite and pyrite are noticeably absent in the high-chroma units, except in the basal unit of profile in core 2405, in which spherulitic siderite is common. Although not noted in the low-chroma units, small hematite glaebules (Fig.4.6B), 1 to 5 mm in diameter, range from rare to common in the high-chroma units. Carbonate nodules are similar in character and distribution to those in the low-chroma units, including the elongate vertical masses (rhizocretion) (Fig. 4.6C). Carbonate nodules are abundant in the uppermost high-chroma unit of profile in core 2552.

Color mottles are present in all of the high-chroma units. Greenish gray, low-chroma mottles (5GY6/1 or 5G5/1) are present in varying abundance in all of the high-chroma units (Fig. 4.6A,4.6B,4.6C). Patchy, medium and large, irregularly-shaped, low-chroma mottles are present in all but the lowermost units in cores 2402 and 2552. Mottles of similar color, ranging from fine to medium, are common and follow interpedal pores and vertical root channels (Fig. 4.6D). Many of the high-chroma units also contain fine, vermicular, goethite-rich mottles (Fig. 4.6D), which appear to follow roots and interpedal pores, but were also observed in the interiorsof some blocky peds.

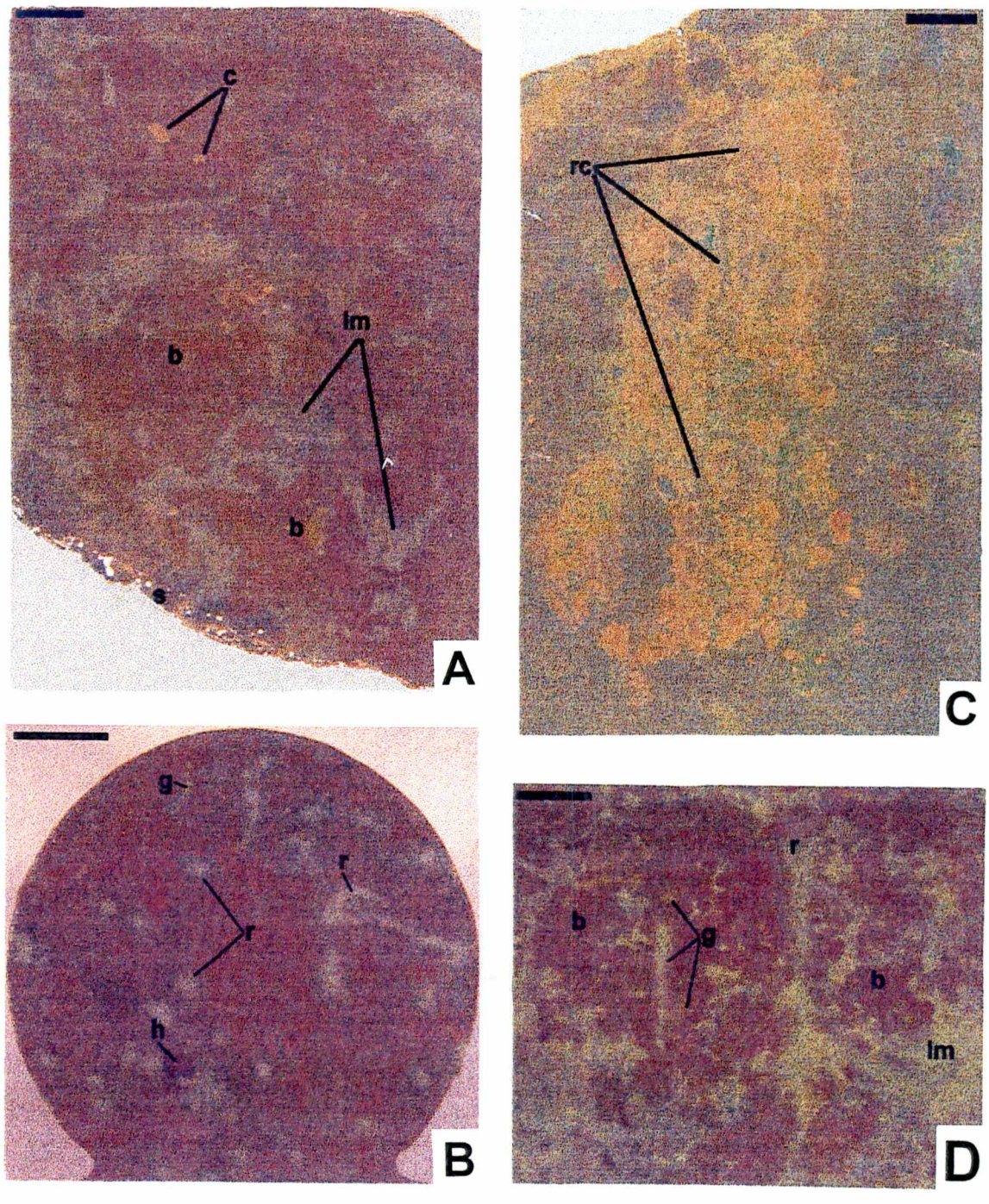


Figure 4.6 - Morphological features of high-chroma units (b=blocky ped, c=carbonate nodule, g=goethitic mottle, h=hematite glaebule, lm=low-chroma mottle, r=root mottles, rc=root channel, s=slickenside). Scale bars are 1 cm long.

Cumulative Thickness and Superjacent Strata

Examination of descriptions of superjacent strata in 48 drill-core records revealed that the paleosol complex is directly overlain by either coal, limestone, or shale. "Shale" includes both fossiliferous and non-fossiliferous shale and siltstone. Lithologic descriptions of the interval correlative to the sub-Ames paleosol complex were of sufficient quality in forty-three of the drill-core records to permit calculation of the cumulative thickness of low-chroma units in profiles as a percentage of the total profile thickness (%LCU).

Low chroma-units comprise the upper part of the paleosol complex all 48 cores utilized in this study. On average, low-chroma units comprised 46% ± 29% of the total thickness of an individual profile. Profiles were grouped into categories based on lithology of the overlying strata; profiles overlain by limestone (POL), shale (POS), or coal (POC). Mean %LCU was calculated for each category (Table 4.1). The Students t-test indicate that the means are statistically different at the 95% confidence- level, although the standard deviations indicate there is considerable overlap between profiles overlain by shale and those overlain by marine limestone or coal. Not surprisingly, however, POC are clearly distinct from those overlain by marine limestone. Based on these data there appears to be a crude gradient in terms of %LCU in which POL have the lowest values, POC have the highest values, and POS have the intermediate values.

Of the six examined in detail, low-chroma units dominate the POC, comprising 67% of profile thickness in core 2402, 72% in core 2405, and 82% in core 2432. The profile in core 2405 is compound, consisting of both upper and lower sub-profiles,

Table 4.1. Comparison of %LCU relative to lithology of overlying strata.

Type	Mean (%LCU)	standard deviation	number
All profiles	47	29	44
Profiles overlain by limestone (POL)	22	15	15
Profiles overlain by shale (POS)	50	25	17
Profiles overlain by coal (POC)	73	19	12

separated by limestone containing ostracodes and/or molluscan fragments. The limestone is similar to those commonly referred to as "freshwater" and is directly overlain and underlain by calcareous mudstone containing a similar fauna. Lacking evidence of pedogenic modification, the limestone and associated calcareous mudstones were not included in calculation of the percent of low-chroma horizons for core 2405.

Low-chroma units dominate the POS in core 2428 (90%), but are markedly less prevalent in POL in cores 2408 and 2552 (37% and 26%, respectiely). Low-chroma units are particularly significant in profile in core 2408. In this profile, two, thin (10 and 15 cm), low-chroma units with faint granular structure and fine, vermicular, horizontal mottles after roots appear to be the remnants of A horizons separating thick high-chroma B horizons. This arrangement indicates that the profile is composite and suggests stacking and partial welding of two relatively thin profiles in the base of the much thicker paleosol complex. Indeed, given the great thickness (9.18m ± 3.08, n=48) characteristic of the paleosol complex, welding of stacked profiles was probably an integral aspect of its formation.

SPATIAL VARIATIONS

The spatial distribution of profile characteristics relative to the lithology of strata overlying the paleosol complex are critical for assessing the influence of the soil land-scape on subsequent deposition. To this end, five stratigraphic cross-sections are presented (Figs. 4.7, 4.8, 4.9, 4.10,4.11). These demonstrate variations in the character of the paleosol complex relative to the super- and subjacent strata. The datum used in construction of the stratigraphic sections is the top of the sub-Ames paleosol complex,

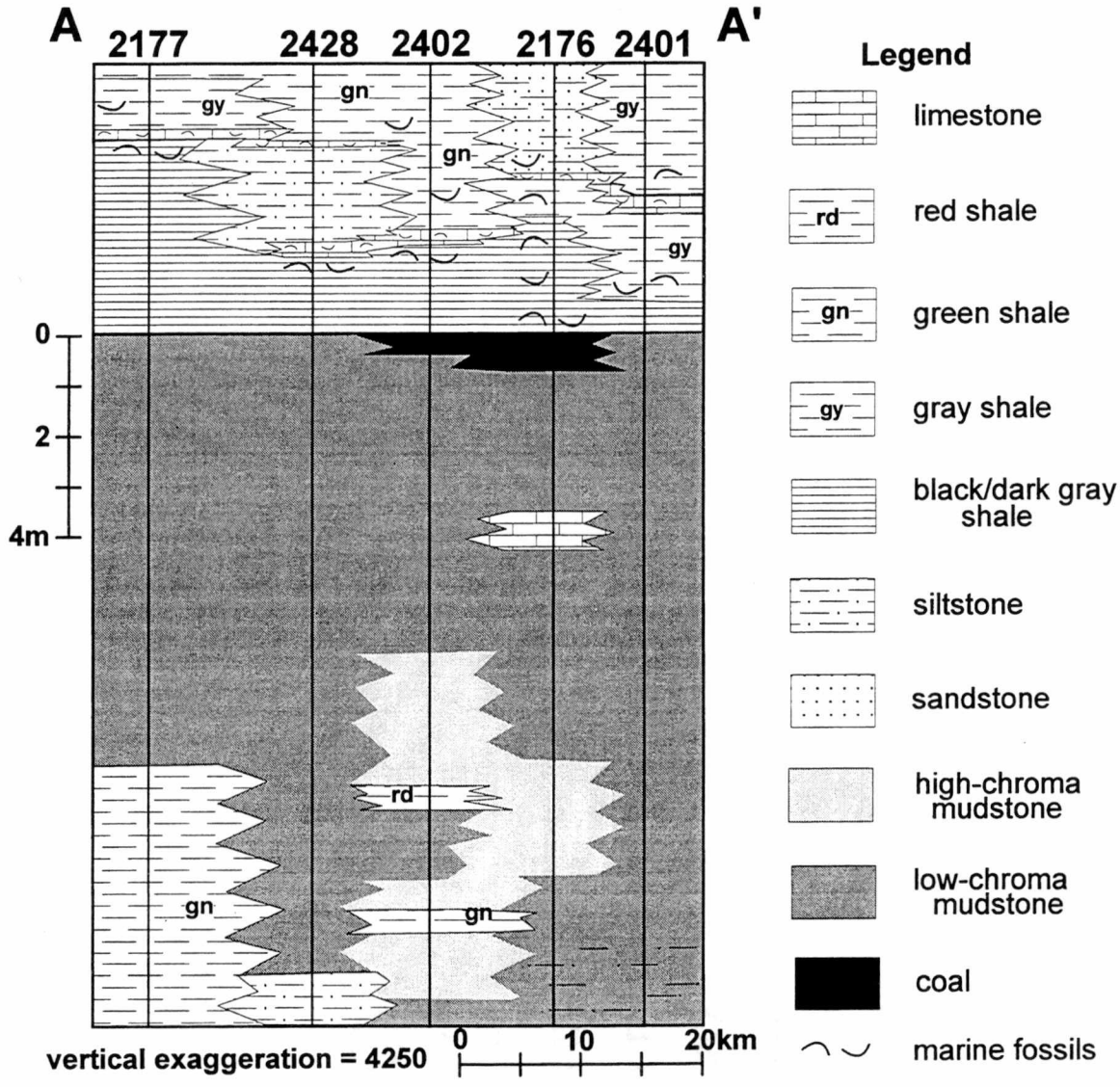


Figure 4.7 - Stratigraphic cross-section A-A'. See Figure 4.1 for location of section lines.

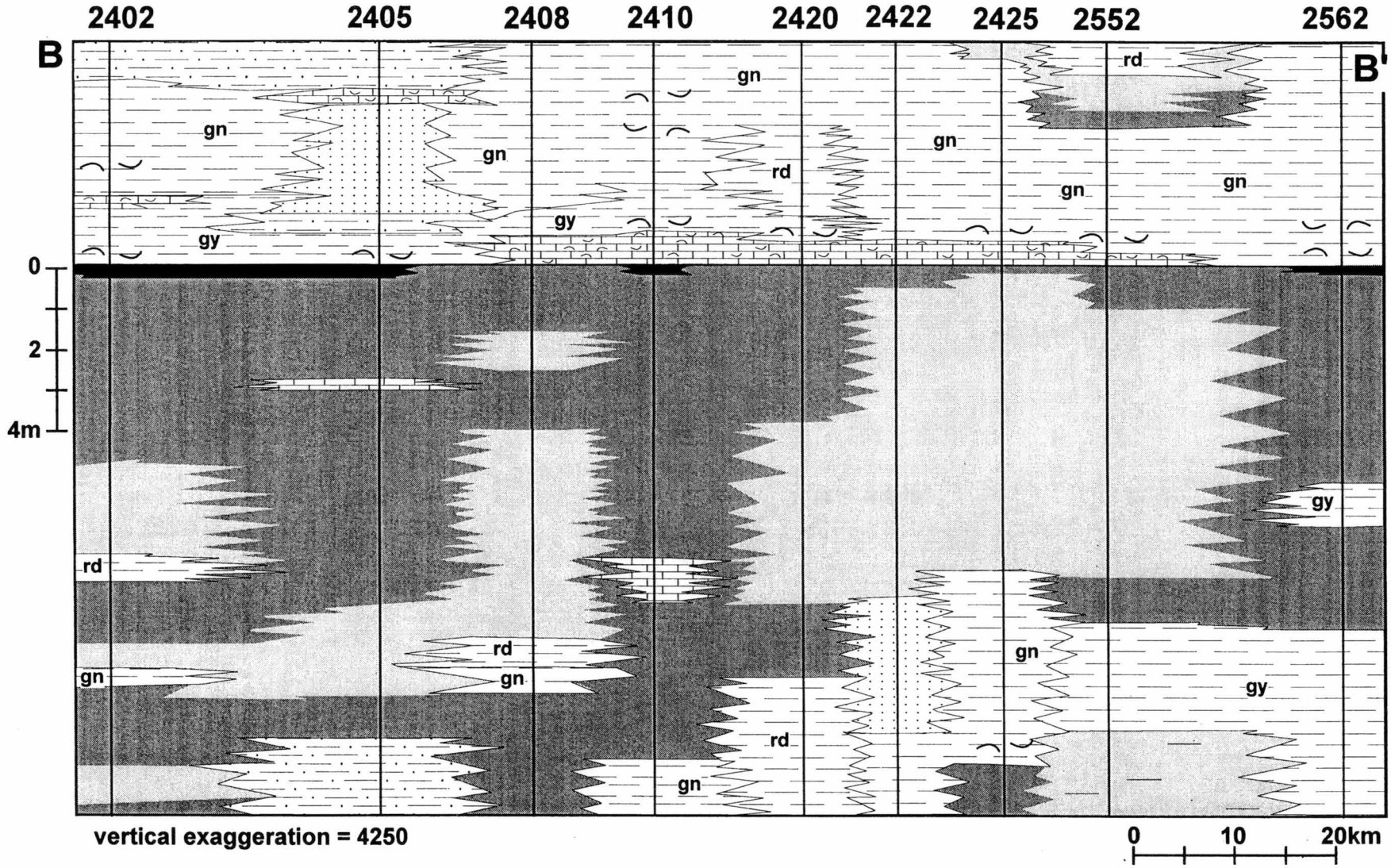


Figure 4.8 - Stratigraphic cross-section B-B'. See Figure 4.1 for location of sections and Figure 4.7 for lithologic symbols.

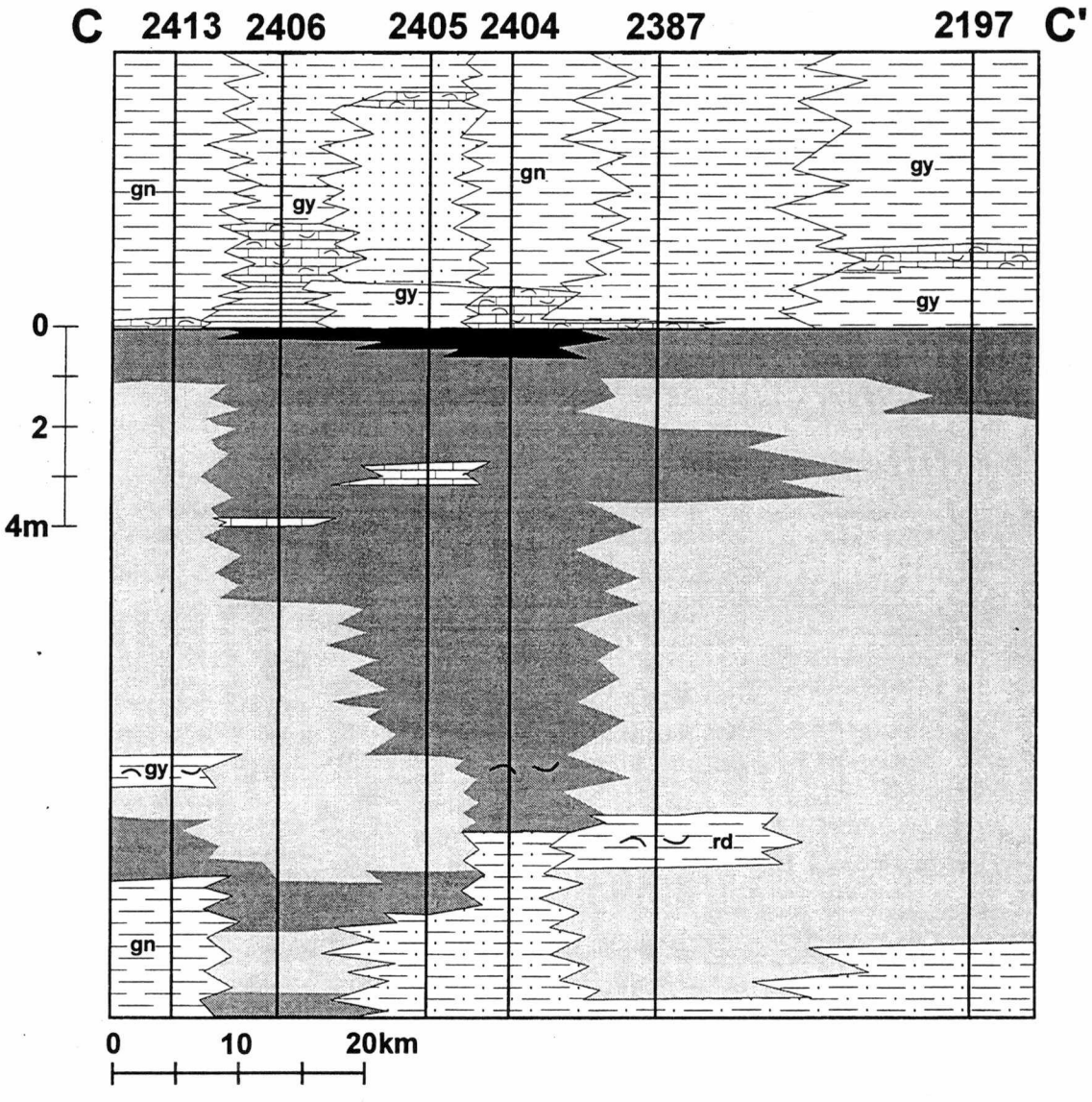


Figure 4.9 - Stratigraphic cross-section C-C'. See Figure 4.1 for location of sections and Figure 4.7 for lithologic symbols.

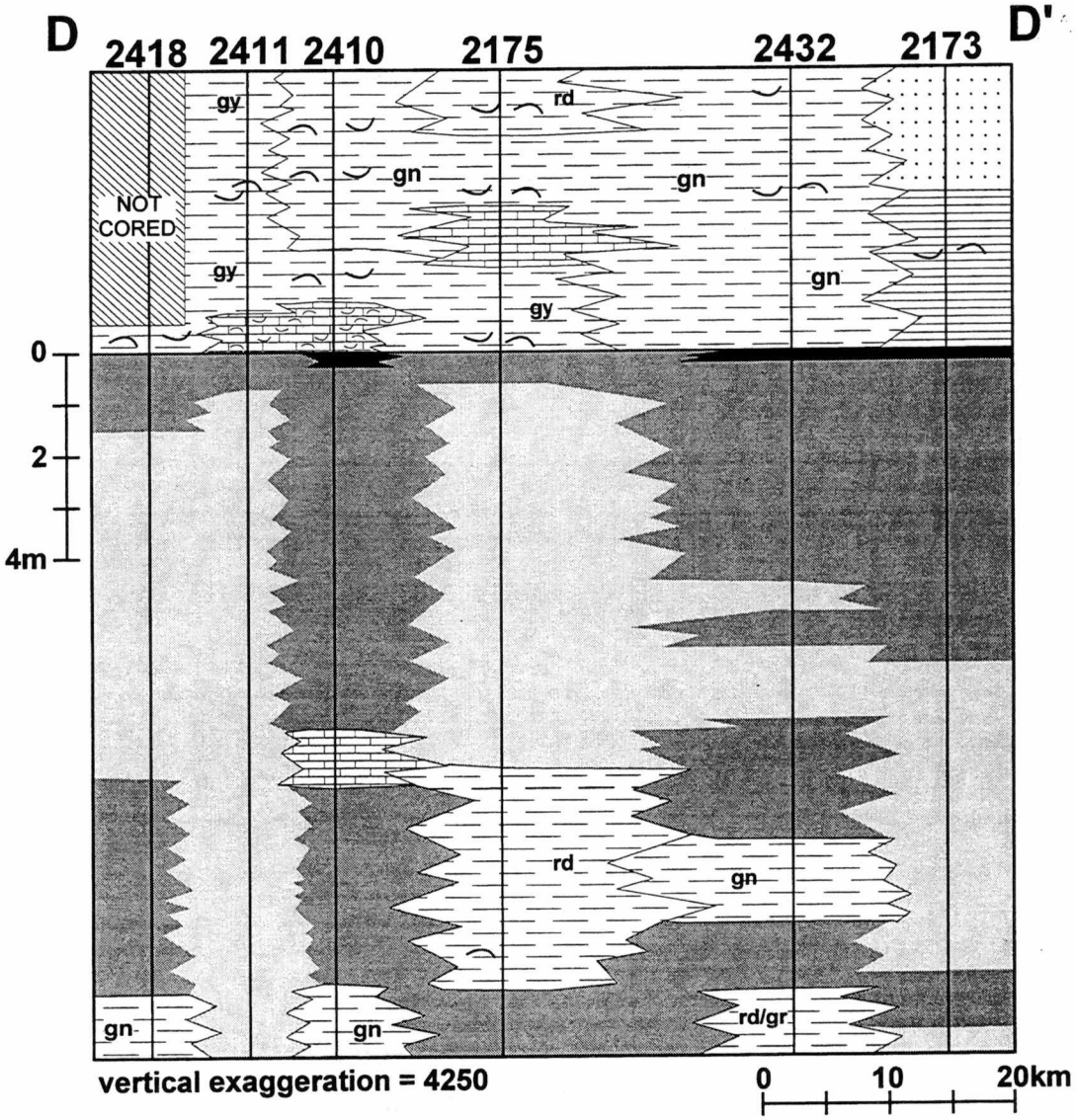


Figure 4.10 - Stratigraphic cross-section D-D'. See Figure 4.1 for location of sections and Figure 4.7 for lithologic symbols.

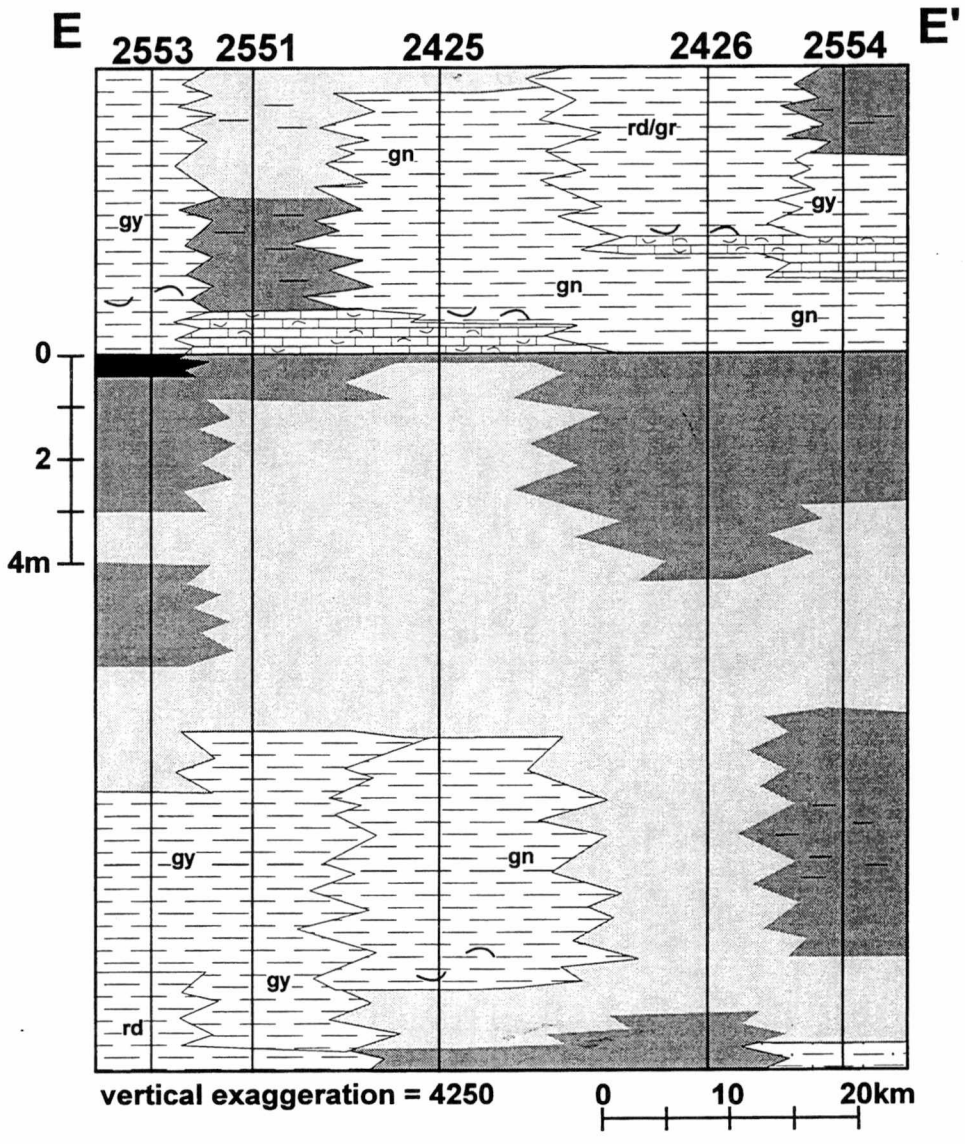


Figure 4.11 - Stratigraphic cross-section E-E'. See Figure 4.1 for location of sections and Figure 4.7 for lithologic symbols.

which correlates to the top of the Harlem coal, where it is present; this is equivalent to correlating the landscape surface that existed just prior to the "Ames transgression".

To examine lateral variability, a map was constructed of the cumulative thickness of high-chroma units (%HCU; where %HCU=100% - %LCU) (Fig. 4.12). As discussed later, areas where profiles contain large cumulative thicknesses of high-chroma units are thought to have been paleotopographic highs. Therefore, contour values of %HCU correspond to higher topographic areas of the paleolandscape. Data defining bodies of the Harlem coal are superimposed on the cumulative thickness contours to further the interpretive value of the map.

INTERPRETATIONS AND DISCUSSION

The Paleosol Complex

Significance of color--. The most striking profile feature of the sub-Ames paleosol complex is a strongly contrasting mix of green-gray low-chroma (≤ 2) units and reddish high-chroma (> 2) units. In modern soils, green-gray and yellowish-brown to reddish colors record reducing and oxidizing conditions (i.e., the redox potential), respectively (Birkeland 1984, Singleton 1991, Schwertmann 1993, Vepraskas 1992). Color patterns in the sub-Ames paleosol complex are assumed to record the redox potentials that either: 1) existed in the paleosol while it was in the pedogenic realm, or 2) developed shortly after a given part of the paleosol passed out of the pedogenic realm (roughly 2 to 3 m below the soil surface). The 10R hues characteristic of high-chroma units in the paleosol complex most liekly developed by transformation of ferrihydrite and/or goethite to hematite (XRD confirmed) after pedogenesis ceased (c.f. Blodgett 1993). The sub-Ames

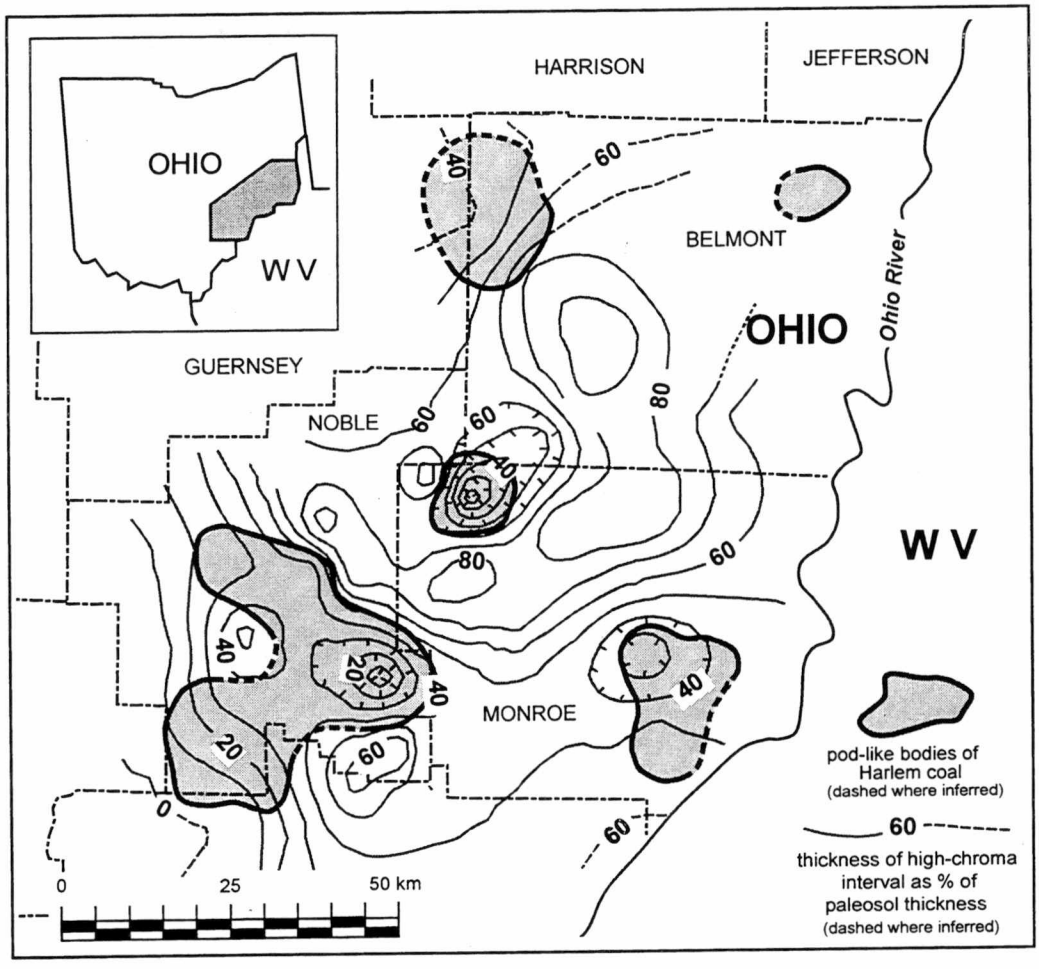


Figure 4.12 - Contour map of percentage of profile thickness composed of **high-chroma units (%HCU)**. Contours are superimposed onto map of the distribution of bodies of the Harlem coal. Interpretations from paleosol complex suggest areas dominated by high-chroma units correspond to well-drained and topographically higher settings.

complex contains a variety of juxtaposed yellow, brown, and red mottles which elsewhere have been cited as evidence to exclude burial diagenesis as the cause of matrix reddening (PiPujol and Buurman 1994).

Diagenesis of the sub-Ames paleosol complex during burial to 3 km or less (c.f. Beaumont et al. 1987) had no effect on the green-gray, low-chroma versus reddish, high-chroma color patterns. Burial diagenetic environments are commonly reducing, but hematite reduction is very sluggish, the mineral persists in paleosols into the greenschist metamorphic facies (Retallack 1990). In addition, low-chroma units in the paleosol complex contain a variety of high-chroma mottles, which would have been destroyed if burial reduction had transformed reddish, high-chroma units into green-gray, low-chroma units.

Diagenetic transformation of green-gray low-chroma units to reddish high-chroma units is also unlikely. Given the fine-grained nature of the parent material suggested by shale units associated with the paleosol complex in cores 2402, 2408, and 2562 (Fig. 4.7), it is doubtful that fine-grained, easily-altered, iron-bearing silicates would have survived pedogenesis. It is unlikely that exotic, oxygenated fluids were introduced into the paleosol after it left the pedogenic realm. The high initial bulk density of vertic paleosols suggests limited transmissivity, even at shallow depths of burial (Chapter 3; Caudill et al. in press). Although hues in the high-chroma units may have been slightly reddened, burial diagenesis did not change green-gray, low-chroma units into reddish, high-chroma units, or vice-versa.

The great thickness of the paleosol complex and its composite and compound nature reveal that it was constructed by progressive amalgamation of thinner soils. The color mottling (particularly prevalent in the high-chroma units) reflects the distribution of redox potentials in these thinner precursor soils, and formed in response to: 1) fluctuations in redox potentials brought on by seasonal wetting and drying, 2) root decay, and 3) pedogenic conditions superimposed during welding to the aggrading paleosol complex.

Soil structure, slickensides, carbonate nodules--. Unweathered, polished slabs of low-chroma units reveal faint to moderate soil structure. Granular structure was observed in low-chroma units at the very top of POC. These units correspond to portions of A horizons that escaped erosive destruction. In other low-chroma units in POC weak to moderate, blocky, soil structure is common (Figs. 4.5A,4.5C). In one example, argillans surround blocky peds in thin-section. Soils formed in saturated, poorly drained settings typically show poor structural development, and argillans are characteristic of well-drained settings (Retallack 1990, Birkeland 1984).

Large slickensides and pedogenic carbonate nodules are present in these thick low-chroma intervals. Slickensides are produced by alternate wetting and drying due to strongly seasonal precipitation (c.f. Ahmad 1983), and pedogenic carbonate nodules are commonly interpreted to record relatively dry climates and well-drained landscape positions (c.f. Retallack 1990). Therefore, it appears that upper parts of the POC were once well-drained and oxidizing, though they possess greenish gray low-chroma colors now. Therefore, the interval of contiguous low-chroma units comprising the upper part of

the paleosol complex indicate that a saturation/ reduction event occurred after the blocky peds, argillans, carbonate nodules, and slickensides had formed. As is discussed in a later section, this event entailed a new set of superimposed pedogenic conditions.

Geochemistry--. The geochemistry of the six profiles representative of (3) POC, (2) POL, and (1) POS provides clues to some of the processes that effected the paleosol complex. To evaluate these processes three molar ratios were calculated (see Methods section). The implications of these ratios are considered below.

Clayeyness can be evaluated by the ratio of SiO_2/Al_2O_3, which decreases as clayeyness increases. Clayeyness increases with depth (over a range of approximately 0.5-5.0m) in the profiles examined in detail, although the trend is somewhat erratic (Fig. 4.13). Argillans preserved near the low/high-chroma boundary in profile in core 2402 indicate that this trend was not simply inherited from parent material. Indeed, increased clayeyness with depth and the presence of argillans suggests that clay illuviation was an active process (c.f. Birkeland 1984) at some point during formation of the paleosol complex . Seasonal shrinkage and swelling, such as produced large slickensides in the paleosol complex, tends to quickly destroy any argillans that form (c.f., Nettleton et al. 1969) and foster soil mixing to the extend that textural differentiation is precluded (c.f. Ahmad 1983). Therefore, clay enrichment and argillan formation must post-date slickenside formation and suggests cessation, or at least dramatic reduction, of expansion and contraction of the soil body.

Clay illuviation would affect molar ratios utilizing Al_2O_3 , such as the base loss and calcification ratios, and these ratios were not calculated for the paleosol complex.

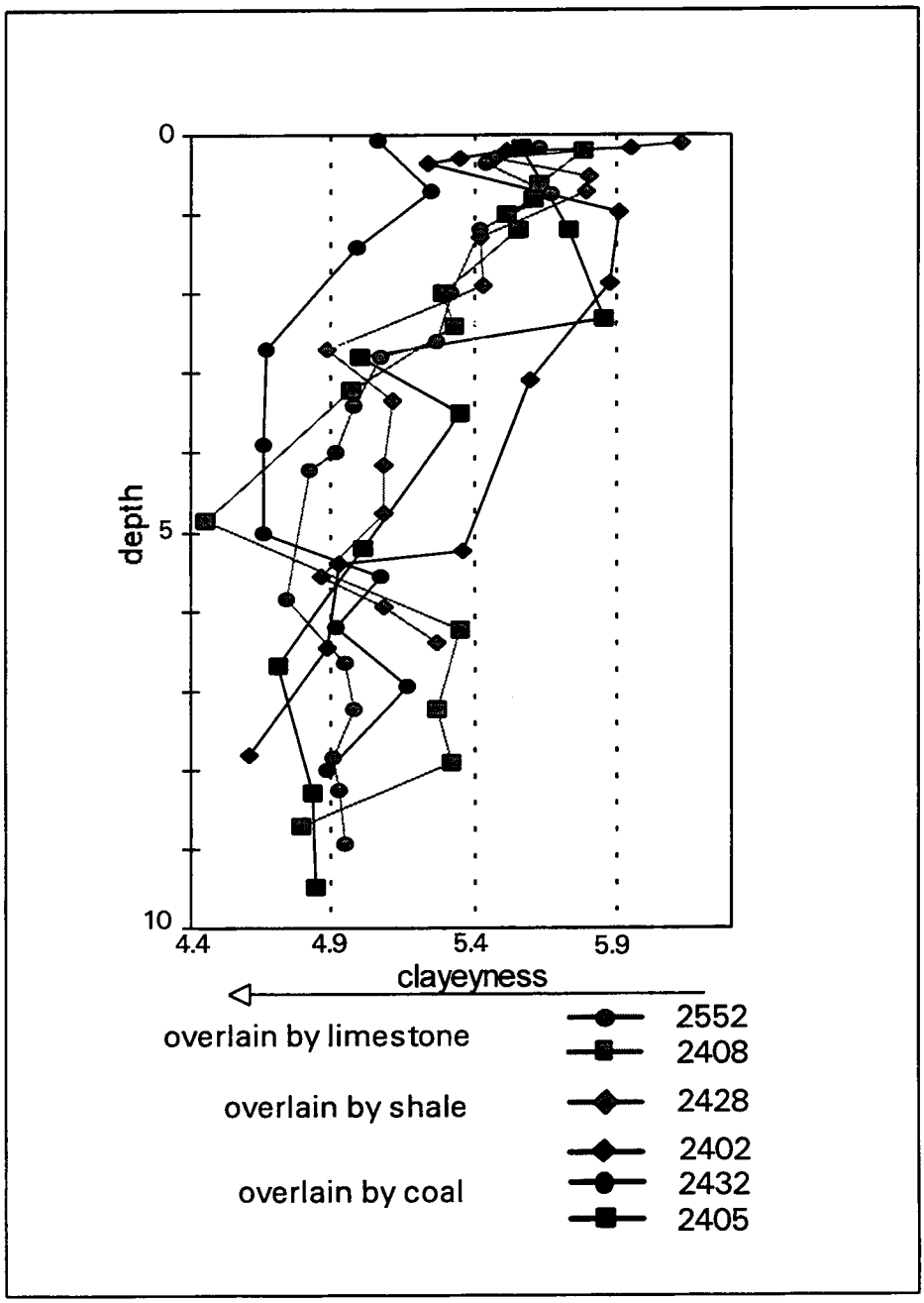


Figure 4.13 - Plot of the clayeyness ratio. Note general increase of clayeyness depth over the range from approximately 0.5-5.0 m.

Calcification (generally calculated by $CaO+MgO/Al_2O_3$) can be assessed in a very general way, however, by direct comparison of calcium concentrations. Based on this approach, a thick interval of contiguous low-chroma interval in the upper part of POC appears to be the most calcified component of the paleosol complex and has calcium concentrations ranging to 25%. POL and POS appear less calcified with calcium concentrations ranging to 12%. This trend may be related to drainage conditions and topographic position of the soil sites. In dry climates, soils forming on well-drained, typically elevated, areas of the landscape are more leached of bases than those forming in depressions, which tend to be alkaline or saline (Birkeland 1984). With this in mind, it is not surprising that the POC (presumably formed in topographic lows) show significantly greater concentrations of calcium.

Leaching can be evaluated by the ratio of Ba/Sr, which increases as leaching increases. The ratio is smaller in calcareous rocks and soils, which are high in Sr by virtue of their mineralogy (c.f., Vinogradov 1959). The potential effect of mineralogy can be ruled out, however, in the uppermost units of the profiles. These units are uncalcified, as indicated by concentrations of calcium ranging from 0.5 to 0.8%.

The tops of POC appear to be more leached than those of POL and POS (Fig. 4.14). This is the opposite of the relationship expected based on the topographic setting, because, in dry climates, higher sites (i.e., POL and POS) tend to be more highly leached than lower sites (POC) (Birkeland 1984). The greater leaching indicated for the lower sites may be explained by; 1) leaching of Sr in POC by organic acids derived from the overlying peat , and/or 2) the introduction of Sr or marine allochem grains containing Sr

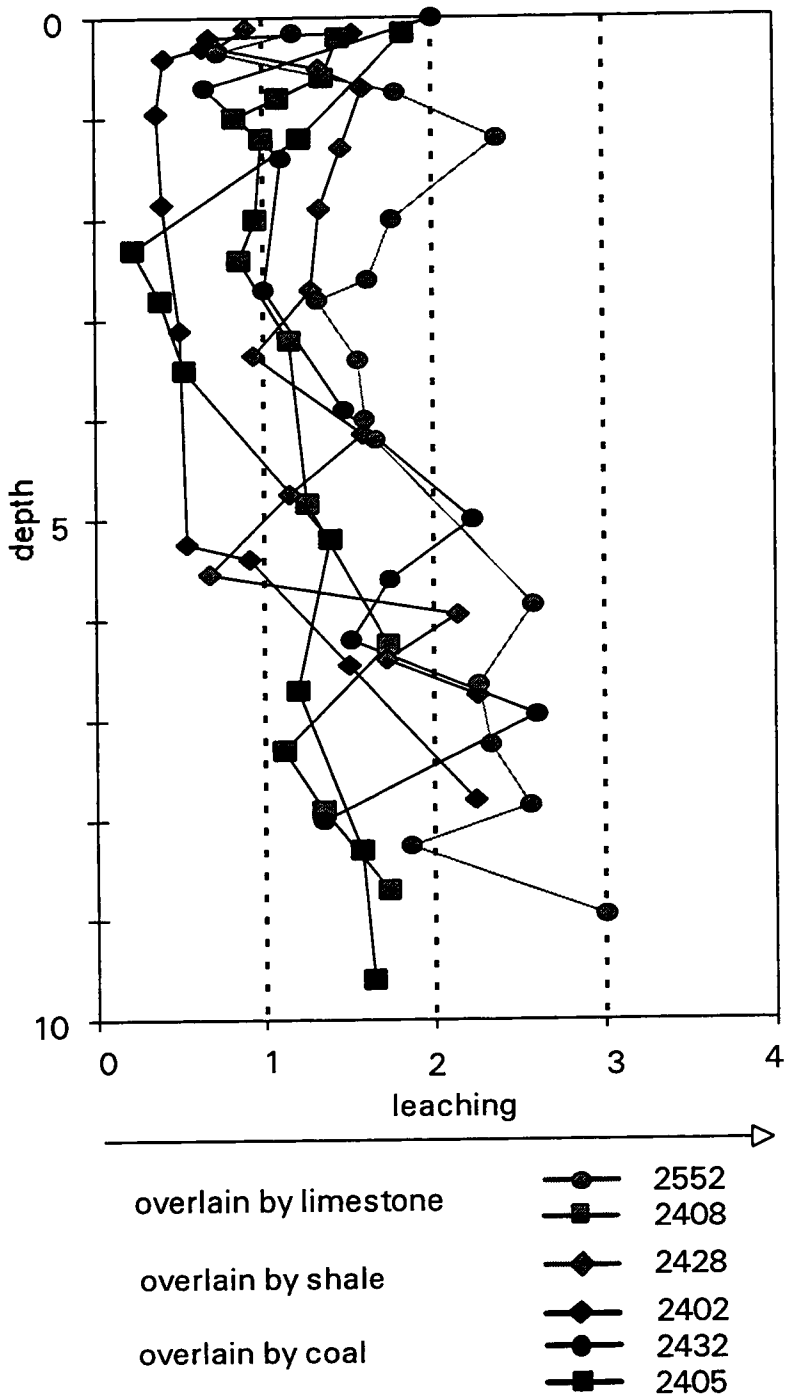


Figure 4.14 - Plot of the leaching ratio suggests that the uppermost units of profiles overlain by coals are slightly more leached than uppermost units in profiles overlain by marine limestone and shale.

(Driese et al. 1992) into the tops of POL and POS during marine inundation (i.e., marine hydromorphism). Both processes would have been imposed on the soil as it passed from the pedogenic realm into the very shallow burial realm and thus may not reflect the intensity of leaching chracteristics of the higher soil-forming sites versus lower sites.

The ratio Ca/Sr provides additional support for marine hydromorphism at well-drained soil forming sites. Matrices of the uppermost parts of the profiles have very low calcium contents (0.8-0.3%) and thus are clearly not calcareous. Therefore, most Sr probably resides in interlayer sites of 2:1 clay minerals, where it has displaced calcium, or adsorbed to the surfaces of clays. Saturation of the upper part of the profiles with marine fluids would make more Sr available to replace Ca, resulting in a lower value for Ca/Sr. Table 4.2 compares ratios for the uppermost sampled units of profiles overlain by marine limestone or shale to those of the uppermost units of the POC. Values are distinctively lower for profiles overlain by marine limestone or shale and support "marine hydromorphism" at well-drained soil forming sites.

Weathering can be evaluated by the ratio of SiO_2/Fe_2O_3, which decreases as leaching increases. The weathering ratio suggests that the uppermost units of the profiles in cores 2402 and 2432 (POC), and 2428 (POS) are distinctly less weathered than the underlying parts of these profiles (Fig. 4.15). These units are directly overlain by orangic rich strata and their elevated weathering ratios (intensity of weathering is inversely proportional weathering ratio) may reflect the removal of iron by metallo-organic chelation driven by organic acids draining from overlying deposits (i.e., coal and carbonaceous shale) (c.f. Birkeland 1984).

Table 4.2. Ca/Sr for uppermost profile units sampled, relative to lithology of the overlying strata

Core #	Depth (m)	Ca/Sr	Lithology of overlying unit
2402	0.13	41	coal
2405	0.16	47	coal
2432	0.06	52	coal
2408	0.18	29	limestone (marine)
	0.58	31	
2428	0.08	32	shale (marine)
	0.29	11	
2552	0.15	20	limestone (marine)
	0.36	9	

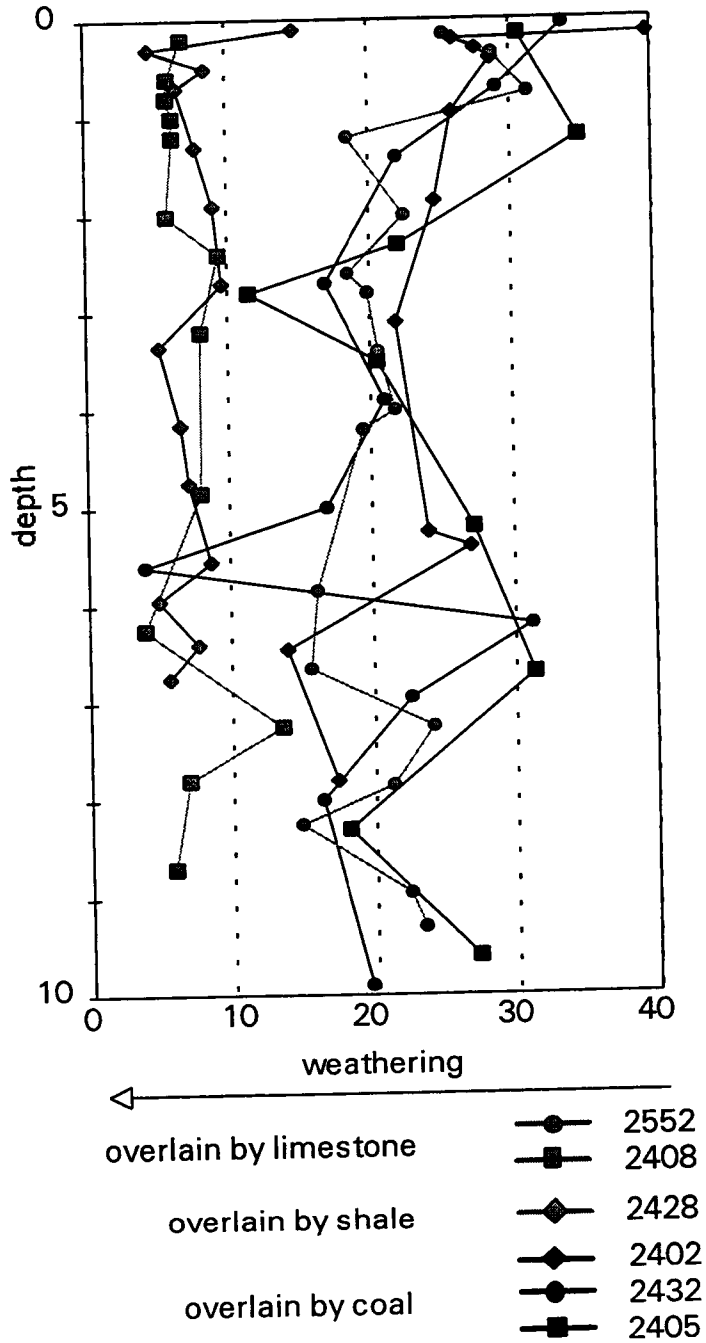


Figure 4.15 - The weathering ratio suggests the tops of profiles 2402, 2428, and 2432 are less weathered than other parts of the profiles and separates profiles 2408 and 2428 from remaining profiles.

The weathering ratio plot suggests that profiles in cores 2408 and 2428 are distinctly more weathered than the other profiles. Both of these profiles overlie shale containing horizonal burrow mottles suggestive of a marine affinity. The reddish high-chroma color of the borrowed shale beneath profile in core 2408 indicates a significant amount of iron-oxide. The weathering ratios displayed by these profiles may reflect the influence of iron-oxide enriched parent material, thus hindering easy comparison to the other profiles.

Paleoclimate

The macromorphology of the paleosol complex supports the paleoclimate interpretations proposed by Joeckel (1995), wherein precipitation was moderate (500-1000 mm/yr, and probably >750 mm/yr) and markedly seasonal. Note, however, that a moderate level of precipitation (e.g., 750 mm/yr) does not necessarily indicate that the overall climate can be characterized in terms of its wetness or dryness, as moderate. The relative aridity of a climate depends on evapo-transpiration, as well as on rainfall. As an example, annual precipitation of 630 mm/yr in northwestern Europe produces a humid climate, but in tropical lowland settings results in semiarid conditions (Akin 1990). Heckel (Fig. 8, 1995) placed Ohio well within the tropics during the deposition of the fluvio-deltaic Conemaugh Group. Therefore, despite a moderate level of precipitation, the climate as a whole is best described as semiarid (c.f., Fig. 2, Cecil 1990).

Perched Water Table and the Harlem coal

If the matrix color of soil units records redox potentials during or very shortly following pedogenesis, then the casual and routine invocation of a broad, ubiquitous and

uniformly rising regional water table to explain the initiation of coals swamps is inadequate for the origin of the "Harlem coal swamp". At sites where the regional water table rose progressively upward through the paleosol to intersect the surface and facilitate coal swamp development, the entire soil profile would have become saturated and the matrix reduced. Initiation of the "Harlem coal swamp" in this manner would thus preclude the existence of reddish, high-chroma units in POC. Yet, of the 12 cores with POC only three (2420, 2410, 2562) lack reddish high-chroma units (Fig. 4.8).

At the culmination of major Late Pennsylvanian regressions, the paleoshoreline stood in southern Kansas and Oklahoma (Heckel 1995). Joeckel (1994) correlated the sub-Ames paleosol complex to a thinner vertic paleosol in the Midcontinent. I have mapped the paleosol complex in southeastern Ohio and Joeckel (1995) correlated over much of the Conemaugh outcrop belt. Taken together, these observations suggest that the paleosol complex is essentially continuous over the whole Appalachian basin. The sub-Ames paleosol complex formed on the very broad, low-lying alluvial plain that developed, for the most part, atop the marine deposits that were exposed when the Appalachian basin was drained during the pre-Ames regression. The regional water table was low during this time, due to both lower base level and lack of a nearby moisture source (Heckel 1995).

In this study, subtle topographic differences in broad flood basin areas, far from presumably incised fluvial systems (c.f. Heckel 1995), produced significantly different pedogenic responses under a relatively dry climate. These responses are demonstrated in study the study area by differences in the character of the POC, versus those of POL,

versus those of POS. The greater degree of calcification in upper portions of POC and the higher %LCU (71%) in POC together suggest formation in more poorly drained, and thus presumably topographically lower sites, than those POL. Calcification in POC may be due, in part, to interruption of pedogenesis in low areas by deposition of "freshwater" limestones in seasonal wetlands like those described in Wright and Platt (1995). This is generally compatible with Cecil's (1990) climate change model, which defines such limestones as the basinal response to short-wet/long-dry climatic seasonality. Lesser degrees of calcification and lower %LCU (22%) collectively suggest POL and POS formed at well-drained sites. These would be the Vertisols of Cecil's model, which he suggests are the upland equivalent of lacustrine limestones.

The map in Figure 4.12 shows the preferential development of the Harlem coal in areas where the paleosol complex is distinguished by smaller %HCU (i.e., greater %LCU). Not surprisingly then, the Harlem coal appears to have formed by initiation of planar, topogenous swamps in topographic lows (c.f., Cecil et al. 1985, Cecil 1990). Note, however, that the distribution of the coal suggests that the Harlem coal formed in numerous (and probably contemporaneous), small, isolated swamps spread along the margin of areas characterized by soils with higher %HCU. Because of the presence of reddish high-chroma units in most POC, we infer that the water table(s) that fed these coals swamps were locally developed zones of saturation perched at the top of the paleosol complex in poorly drained topographic lows. Clay enrichment and calcification of the matrix (noted earlier) contributed to restricted subsoil permeability and facilitated perching.

A variation of this process may have been active in profile in core 2408. This profile contains a thick (1.7 m) low-chroma unit at 2.3 to 4.0 m depth and separated from the 1.3 m, low-chroma unit at the top of the profile, by a 1.0 m, high-chroma unit (Fig. 4.4). The base of the thick low-chroma unit lies within the clay-enriched interval at 2.4 to 4.85 m depth (Fig. 4.13). This profile is overlain by limestone, and such profiles are thought to have formed at well-drained sites. Thus, the low-chroma unit comprising the interval 2.4 to 4.85m in depth may represent formation of a perched zone that failed to grow to intersection with the soil surface due to its development on a well-drained, and perhaps, elevated portion of the landscape. A similar occurrence may be recorded by profile in core 2428, but here, at a slightly less elevated site, the saturated zone grew upward far enough be overlapped later by the saturated and reduced zone produced in the top of the profile by marine hydromorphism.

There are three POC comprised entirely of low-chroma units. One of these profiles is composite (core 2410; Fig. 4.8), containing a thin "freshwater" limestone). The portion of the profile below the limestones probably records saturation and reduction associated with the establishment of a seasonal wetland similar to those described in Wright and Platt (1995). Perching of a localized water table atop the limestone led to saturation and reduction in the upper part of the profile and eventually to initiation of the coal swamp. The profiles lacking a "freshwater" limestone (cores 2404, 2562; Fig. 4.8, 4.9) may have formed in the same fashion, but pedogenesis eventually assimilated the lake sediments.

Ames Marine Unit

In addition to the influence topography exerted on the formation of the Harlem coal, it also controlled deposition of some lithofacies of the Ames marine unit. The stratigraphic cross-sections illustrate significant lateral lithologic variation in the Ames marine unit (Figs. 4.7,4.8,4.9,4.10,4.11), particularly the patchy and discontinuous nature of the marine limestone. The data in this study suggest that marine limestone units are markedly less continuous than indicated by the broader-scale study of Al-Qayim (1983).

The laterally discontinuous nature of the marine limestone lithofacies, at least in part, appears to record shoal-like carbonate deposition localized on topographic highs of the sub-Ames landscape. This characteristic emerges from analysis of the percentage of total profile thickness comprised of low-chroma units relative to the lithology of strata immediately overlying the profiles. Low-chroma units comprise 22% of profile thickness in POL. As noted earlier, we equate profiles dominated by high-chroma units to well-drained settings. In the stratigraphic cross-sections, profiles in cores 2408, 2413, 2197, 2551, and 2425 illustrate the association of limestone units with topographic highs. In the profile in core 2405 carbonate accumulation appears to have been localized at a **depositional** high consisting of thick sandstone, perhaps a bar deposit (distributary mouth bar?). In profiles in cores 2404 and 2410 (Figs. 4.8,4.9), however, marine limestone directly overlies the Harlem coal. This may reflect facies variations such that one limestone lithofacies was deposited in association with localized coal swamps and another lithofacies at topographically higher sites. In a study of the Ames marine unit, Sarg (1979) attributed deposition of a limestone lithofacies atop the Harlem coal to

highs by either compaction of fine-grained sediment surrounding the peat, or to subaerial erosion of this sediment as the Ames sea moved eastward. Alternatively, some Harlem coal swamps, or portions of them, could have evolved slightly domed morphologies in the later phases of their growth and thus have localized deposition of a limestone lithofacies similar to that associated with topographic highs on the sub-Ames soilscape.

STIMULI

One of the primary goals of this study was to assess the stimulus for development of the perched, local water tables that initiated formation of the "Harlem" coal swamp. Cecil's (1990) model suggests that coals such as the Harlem formed largely in response to a climatic change from long-dry/short-wet to long-wet/short-dry seasonality. Tandon and Gibling (1994) suggested a similar change in climate to explain the association of Late Pennsylvanian coals and calcic Vertisols in the Sydney Basin of Nova Scotia. Heckel's (1995) work implies that a similar climatic change may have accompanyied the Ames transgression. Joeckel (1995) described the primary impetus for development of the Harlem coal as "the perching of water tables at the onset of the Ames transgression, rather than greatly increased rainfall." In his scenario, perched water tables developed in response to base level rise with the approach of the Ames transgression. Joeckel, however, considered that higher rainfall or a decrease in the seasonality of rainfall (or both) may have accompanied the Ames transgression, and elaborated that the data available at the time of his study would not support testing of a paleoclimatic change hypothesis.

In this study, the formation of local perched zones of saturation in topographic lows are described and have provided micro-morphological and geochemical evidence that indicates paleoclimate change was, indeed, the primary impetus for localized formation of the Harlem coal swamps. Argillans and clay-enriched units in the paleosol complex record increased infiltration of water into the paleosol complex. This infiltration culminated in formation of perched zones of saturation and reduction of the upper parts of POC. The onset of increased infiltration followed an extensive period of soil formation under a relatively dry climate of long-dry/short-wet seasonality. This climate produced abundant vertic features (slickensides) and accounts for the particularly calcareous nature of the contiguous low-chroma mudstones that comprise the tops of POCs. The onset of increased infiltration began as the Ames transgression approached the Appalachian region, making available a large surface-supply of moisture (Heckel 1994).

The regional climate responded to this new and nearby source of moisture by a transition to long-wet/short dry seasonality, and perhaps, an increase in mean annual precipitation. As a result, the soil was saturated to greater depths seasonally. As the new climate began to assert its influence on pedogenesis, the onset of the annual rainy season, characterized by abrupt, high intensity monsoonal-like rainfall, would have delivered vast amounts of water deep into the soil via deep cracks and other macropores. This process led to formation of argillans, clay-enriched zones, and fostered upward growth of perched zones of saturation. The longer annual period of continuous saturation, imposed by the new long-wet/short-dry seasonality, reduced the frequency with which the soil was wetted and dried. This reduced the intensity of churning in the soil body, facilitating

preservation of argillans and clay-enriched units.

Chhiata series soils, which developed on Pleistocene, terrace-like landforms near the confluence of the Brahmaputra and Meghna Rivers with the Ganges River in Bangladesh experienced a similar change in precipitation seasonality (Brammer and Brinkman 1977). These are surface-water gley soils that currently lie in a tropical monsoonal climate with mean annual rainfall and evapo-transpiration of 1,900 and 1,100 mm, respectively. Based on the presence of slickensides and carbonate nodules at depth, the Chhiata soils appear to have begun as Vertisols during the Pleistocene, when the regional climate was markedly drier than at present, but with well-expressed seasonal difference in rainfall still existing. Following this phase of pedogenesis, clay illuviation took place during the Holocene when wet seasons became more pronounced than during earlier Vertisol formation, but still less extreme than at present. In the final, and wettest, phase of development, these soils have underwent extensive ferrolysis in the latest stage of their formation and now contain extensive and well-developed albic horizons (Brinkman 1977).

Early in the second phase of formation of the sub-Ames paleosol complex, argillans and clay-enriched units formed. This occurred immediately prior to, and during, the early growth phase of the perched water table. As the perched zones grew upwards, clay translocation ceased in newly effected parts of the of the paleosol complex. Except for the formation of extensive albic horizons, the sub-Ames paleosol complex may have been similar to the Chhiata soils. The climate change that produced surface water gleying and formation of the zones of saturation in the sub-Ames paleosol complex appears to

have stopped short of achieving a level of annual precipitation equivalent to that which produced extensive albic horizons in the Chhiata soils.

Birkeland (1984) noted that little translocation of clay takes place in soils high in $CaCO_3$, due to clay flocculation. Furthermore, in soils of high clay content, rapid translocation takes place along deep cracks produced by seasonal drying. This latter process overcame the negative influence that the calcareous nature of the sub-Ames paleosol complex may have had on clay translocation.

The scenario described above provides strong support for the correspondence of Conemaugh coals to cyclic changes in precipitation seasonality, as initially proposed by Cecil (1990). No evidence was found that rising base level associated with the Ames transgression directly effected formation of the Harlem coal. Given the color patterns in the paleosols complex, a broad, uniform rise in the regional water table, in tandem with base level, appears to have left little record in the paleosol complex. The "Ames transgression" did provide the local source of moisture that fostered the climate change described above, and so indirectly contributed to formation of the perched zones of saturation and the Harlem coal.

PRE-AMES PALEOLANDSCAPE AND ITS GENESIS

Further scrutiny of the spatial variation of the paleosol complex and the units overlying it provides additional insight into the genesis of the pre-Ames landscape and how it influenced subsequent deposition. The map in Figure 4.12 is at least a crude reflection of the landscape shortly before arrival of the Ames transgression. Pedogenesis of the sub-Ames paleosol was controlled largely by topography. We have recognized

three broad catenary components; 1) thick, vertic paleosols overlain by shale (POC) dominated by high-chroma units, and formed in low, but well-drained areas (e.g., 2197, 2426, 2554, Figs. 4.9,4.11), 2) thinner, vertic paleosol overlain by marine limestone (POL), dominated by high chroma units, overlying sandstones and laterally associated fine-grain strata, and formed in higher topographic positions (e.g., 2420, 2422, 2552, Fig. 4.8), and 3) vertic paleosols dominated by low-chroma units, overlain by the Harlem coal (POC), and formed in poorly drained topographic lows (e.g., 2405, 2410, 2402, 2562, Figs. 4.7,4.8).

On the map (Fig. 4.12), contours of % high-chroma units outline a hook-shaped topographic high in the center of the study area. Critical insight into the origin of this topographic feature is provided by stratigraphic section B-B' (Fig. 4.8). Here, in core 2422 a thin sandstone underlies the paleosol and is flanked by red and green shale in profiles in cores 2410, 2420, 2425, 2552, and 2562. These strata appear to comprise a fluvial channel tract or, perhaps, a stranded marginal marine bar complex preserved as a component of the vast new landscape that developed as seas began to withdraw from the Appalachian basin during the pre-Ames regression. In broad, low areas adjacent to this feature soils formed on flood basin deposits or exposed clastic lagoons/shallow shelf sediments. The latter interpretation is favored due to the presence of marine fossils in the green shale underlying the profile in core 2425. Most of soil formation in the study area took place when the seas stood far enough westward from the Appalachian basin that they could not serve as a significant moisture source for the climate of the region. The climate was dry with long-dry/short wet seasonality during this period of time, and soil-forming

sites were predominantly well-drained due to the low regional water table. As the Ames transgression brought a moisture source into the area and regional climate responded with a change to long-wet/short/dry seasonality, a new soilscape was produced. Many low areas immediately adjacent to the topographically high feature created by the relict bar complex became poorly drained, and were favored sites of peat formation and preservation, perhaps due to ponding of runoff from the topographic high. Slightly higher areas removed from the flanks of the topographic high remained well-drained and ultimately produced thick profiles dominated by high-chroma units. Still other areas removed from the flanks of the topographic high were low enough that they became less well drained. The upper parts of soils at these sites became gleyed, but any peats that may have accumulated were not preserved.

CONCLUSIONS

Subtle topographic difference on the landscape on which the sub-Ames paleosol formed; 1) strongly influenced pedogenesis, 2) controlled formation of the Harlem coal, and 3) influenced deposition of the Ames marine unit. Equally significant, the Harlem coal of the study area formed in isolated topographic lows on this landscape in response to the establishment of saturated zones in the top of the paleosol complex. Growth of these perched zones was initiated by the onset of long-wet/short-dry seasonality in precipitation. Development of these perched water tables was facilitated by formation of clay-enriched subsoil intervals. In the study area, the topography of the landscape reflected the presence of an abandoned fluvial channel tract or perhaps a marginal marine bar complex stranded on the broad, newly exposed surface produced by withdrawal of the pre-Ames sea from

the Appalachian basin.

In addition to the interpretations recounted above, this study bears on several broad procedural and interpretive themes in the study of paleosols. 1) Evaluation of regional-scale features such as paleolandscape, catenary relationships, etc. is best conducted using large data bases (i.e., core or substantial outcrop coverage). 2) Paleosol-based paleoclimate and paleolandscape studies should include consideration of sub- and superjacent strata in order to get the "complete" picture. 3) Paleosol color, in spite of all the negative "press", does survive burial diagenesis in some, and perhaps many, situations and can provide sensitive data on soil drainage and redox conditions. 4) Molecular ratios must be interpreted with great care, because the applicability of a given ratio depends on the array of processes that have effected the paleosol. 5) The depositional histories of stratigraphic intervals containing paleosols should include thorough appraisals of the potential roles of paleo-landscape/soilscape.

CHAPTER 5

GENERAL CONCLUSIONS AND SUGGESTIONS FOR FURTHER RESEARCH

GENERAL CONCLUSIONS

A) Paleoprecipitation can be estimated for paleosols using depth to pedogenic carbonate, provided that;

1) a complete, untruncated (or nearly so), profile was preserved,

2) physical compaction can be accounted for, and

3) paleoatmospheric pCO_2 is known.

4) Depth to pedogenic carbonate in vertic paleosols is best measured in areas between pseudo-anticlines, where translocation of carbonate along slickensides was primarily horizontal.

Late Mississippian mean annual paleoprecipitation in east-central Tennessee is estimated at 648 mm. The paleoclimate can be described qualitatively as semi-arid.

B) Vertic claystone paleosols do not experience significant physical compaction, even with appreciable burial depth, because of their high initial (i.e., pre-burial) bulk densities.

1) Burial compaction equations/curves for argillaceous sediment, sand/sandstone, and generic paleosols do not provide reliable compaction estimates for vertic paleosols.

2) A "vertic-calibrated" compaction equation/curve yields estimates that compare well with compaction values obtained from clastic dikes preserved in Proterozoic, Ordovician, Mississippian, and Pennsylvanian vertic paleosols of known burial depth.

3) The "vertic-calibrated" compaction equation/curve can be used to estimate compaction in vertic paleosols of known burial history, but lacking well-preserved clastic dikes.

4) Improved estimates of burial compaction translate to improved predictions of paleoprecipitation using depth to pedogenic carbonate.

5) High initial (pre-burial) bulk densities for vertic paleosols suggests low transmissivity, and thus vertic paleosols;

a) may have operated as closed systems during diagenesis, and

b) may have constrained the movement of fluids (burial fluids, hydrocarbons?) through the stratigraphic sequence.

C) Variations in the pre-Ames paleolandscape/soilscape influenced:

a) soil drainage setting, which in turn affected soil color, development of peat swamps/mires, and

b) deposition of marine sediment during the subsequent "Ames" transgression.

1) Gross color patterns in thick, widely distributed paleosols provide clues to regional and local paleohydrology.

a) High-chroma units in the sub-Ames paleosol contradict a broad, ubiquitous, uniform rise of the regional water during the "Ames" transgression and support formation of local perched zones of saturation as the impetus for coal swamps.

2) Soil morphology and the molar ratio that assesses clayeyness (SiO_2/Al_2O_3), support a change to a more humid climate with a longer wet season as the underlying stimulus for coal swamp development.

SUGGESTIONS FOR FURTHER RESEARCH

A) Extend study of Pennington (Mississippian) vertic paleosols into Kentucky:

1) look for regional differences in morphology as might be attributed to proximity to shoreline, catenary relationships, parent material, etc.,

2) evaluate exposures for suitability of use in paleoprecipitation estimates (additional estimates needed to qualify estimate presented here),

3) evaluate paleosols in lower Pennington in Tennessee. Columnar peds, noted in reconnaissance, suggest saline setting and may reflect a more arid climate than that indicated by paleosols higher in the section.

B) Expand study of physical compaction of vertic paleosols:

1) further define burial compaction curve, particularly for depths of 5 to 10 km,

a) conduct literature search to identify vertic paleosols with well-preserved clastic dikes.

C) Initiate new research to examine earliest stages of physical and chemical diagenesis in coastal Holocene and Pleistocene vertic soils, to assess whether they functioned as closed systems and how they may have influenced or been influenced by coastal hydrology during sea-level fluctuations.

1) Focus on shallow, buried soils in drill core from Texas coastal plain and compare to present-day surface soils; clay mineralogy, clay packing arrangement, and bulk densities.

2) Expand on study above, by incorporating physical model similar to the type Ethridge and Schumm have used to study the effects of base-level changes in fluvial-deltaic-shelf systems. In this model, however, simulate Vertisols intercalated in a sequence of coastal sediments.

a) Use tracers to determine how sea-level rise effects coastal hydrology (i.e., does entire sequence become saturated or is groundwater channeled along more permeable conduits?).

b) When sea level falls, do Vertisols influence the way in which coastal drainage system adjusts. For example, assuming Vertisols are intercalated with sediments that comprise the shelf, do they effect development of cross-shelf channels or other processes.

D) Expand study of sub-Ames (Pennsylvanian) paleosol complex to provide further evidence of a climate change associated with "Ames" transgression.

1) Correlate paleosol complex in core and outcrop, throughout the basin in search of a paleotopographic high that escaped inundation during the transgression. At

such a site the paleosol should preserve evidence of increased precipitation unobscured by overprinting from coal swamps or "marine hydromorphism".

REFERENCES

Ahmad, N., 1983, Vertisols, *in* Wilding L.P., Smeck, N.E. and Hall G.F. (eds.), Pedogenesis and Soil Taxonomy, II. The Soil Orders: Developments in Soil Science 11B: New York, Elsevier, p. 91-123.

Akin, W.E., 1990, Global patterns: climate, vegetation, and soils: University of Oklahoma Press, 370p.

Allen, J.R.L., 1985, Principles of Physical Sedimentology: London, George Allen and Unwin, 272p.

Al-Qayim, B.A., 1983, Facies analysis and depostional environment of the Ames marine member (Virgilian) of the Conemaugh Group (Pennsylvanian) in the Appalachian Basin [unpublished Ph.D. dissertation]: Univeristy of Pittsburgh, Pittsburgh, Pennsylvania, 306p.

Aslan, A., Kraus, M., and Autin, W.J., 1993, Interpretation of alluvial paleosols in aggradational landscapes: International Union of Quaternary Research/ International Society of Soil Science, Paleopedology Newsletter, no. 9, p.20-21.

Baker, P.A. and Kastner, M., 1981, Constraints on the formation of sedimentary dolomite: Science, v. 213, p. 214-216.

Baldwin, B., 1971, Ways of deciphering compacted sediments: Journal of Sedimentary Petrology, v. 41, p.293-301.

Baldwin, B. and Butler, C.O., 1985, Compaction Curves: American Association of Petroleum Geologists Bulletin, v. 69, p. 622-626.

Beaumont, C., Quinlan, G.M., and Hamilton, J., 1987, The Alleghanian Orogeny and its relationship to the evolution of the Eastern Interior, North America, *in* Beaumont, C. and Tankard, A.J. (eds.), Sedimentary Basins and Basin-Forming Mechanisms: Memoirs of Canadian Society Petroleum Geologists, v. 12, p. 425-445.

Bergenback, R.F., Horne, J.C., and Inden, R.F., 1972, Depositional environment of Mississippian carbonate rocks at Monteagle, Tennessee: Tennessee Division of Geology, Report of Investigations no. 33, p. 14-18.

Berndt, R.D. and Coughlan. R.J., 1977, The nature of changes in bulk density with water in a cracking clay: Australian Journal of Soil Research, v. 15, p. 27-37.

Berner, R.A., 1993, Paleozoic Atmospheric CO_2: Importance of Solar Radiation and Plant Evolution: Science, v. 261, p. 68-70.

Birkeland, P.W., 1984, Soils and Geomorphology: New York, Oxford University Press, 372p.

Blodgett, R.H., 1985, Paleovertisols as indicators of climate[abst.]: American Association of Petroleum Geologist Bulletin, v. 69, p. 239.

Blodgett, R.H., Crabaugh, J.P., and McBride, E.F., 1993, The color of red beds - A geologic perspective, *in* Bigham, J.M. and Ciolkosz, E.J. (eds.), Soil color: Soil Science Society of America Special Publication 31, p. 127-159.

Blokhuis, W.A., 1989, Vertisols of the Semi-Arid Tropics, *in* Burford, J.R. and Sahrawat, K.L. (eds.), Management of Vertisols for Improved Agricultural Production: Patancheru, India, Proceedings of International Board of Soil Research and Management Inaugural Workshop, International Crops Research Institute for Semi-Arid Tropics (ICRISAT), p. 37-43.

Blokhuis, W.A., Kooistra, M.J. and Wilding. L.P., 1990, Micromorphology of Cracking Clays (Vertisols), *in* Douglas, L.A. (ed.), Soil Micromorphology - a Basic and Applied Science: New York, Elsevier, p. 123-148.

Brammer, H., and Brinkman, R., 1977, Surface-water gley soils in Bangladesh: Environment, landforms, and soil morphology: Geoderma, v. 17, p. 91-109.

Brinkman, R., 1977, Surface-water gley soils in Bangladesh: Genesis: Geoderma, v. 17, p. 111-144.

Brewer, R., 1976, Fabric and Mineral Analysis of Soils: New York, R. E. Krieger Publishing, 482p.

Buol, S.W., Hole, F.D., and McCracken, R.J., 1989, Soil Genesis and Classification: Ames, Iowa, Iowa State University Press, 446p.

Caudill, M.R. and Driese, S.G., 1994, Paleo-precipitation estimate from a full-profile, Early Carboniferous paleo-Vertisol; Pennington Formation, central Tennessee [abst.]: Geological Society of America, Abstracts with Program, v. 26, no. 4, p. 7.

Caudill, M.R. and Driese, S.G., 1995, The origin of some Late Pennsylvanian Coals - a pedologic perspective; Glenshaw Formation, Conemaugh Group (Missourian), Appalachian basin: Geological Society of America, Abstracts With Programs, v. 27, no.2, p. 42.

Caudill, M.R., Driese, S.G., and Mora, C.I., 1996, Preservation of a paleo-Vertisols and an estimate of Late-Mississippian paleo-precipitation: Journal of Sedimentary Research, v. A66, p. 58-70.

Caudill, M.R., Driese, S.G., and Mora, C.I., in press, Compaction of vertic palaeosols: implications for burial diagenesis and palaeo-precipitation estimates: Sedimentology.

Caudill, M.R., Driese, S.G., Mora, C.I., and Fastovsky, D.E., 1992a, Influence of paleotopography and superimposed pedogenic conditions on an Upper Pennsylvanian paleosol complex; Round Knob shale (Pittsburgh Reds), eastern Ohio [abst.]: Geological Society of America, Abstracts with Program, v. 24, p. 229.

Caudill, M.R., Mora, C.I., Tobin, K.J., and Driese, S.G., 1992b, Preliminary interpretations of paleosols associated with Late Mississippian marginal marine deposits, Pennington Formation, Monterey, Tennessee, *in* Driese, S.G., Mora, C.I., and Walker, K.R. (eds.), Paleosols, paleoweathering surfaces, and sequence boundaries: University of Tennessee Studies in Geology, no. 21, p. 57-78.

Cecil, C.B., 1990, Paleoclimate controls on stratigraphic repetition of chemical and siliciclastic rocks: Geology, v. 18,p. 533-536.

Cecil, C.B., Stanton, R.W., Neuzil, S.G., Dulong, F.T., Ruppert, L.F., and Pierce, B.S., 1985, Paleoclimate controls on late Paleozoic sedimentation and peat formation in the central Appalachian basin (U.S.A.): International Journal of Coal Geology, v. 5, p. 195-230.

Condit, D., 1912, Conemaugh Formation in Ohio: Ohio Geological Survey (Fourth Series), Bulletin 17, 363p.

Crawford, T.J., 1985, Upper Mississippian and Lower Pennsylvanian series in the southern Appalachians: United States Geological Survey, Open File Report 85-577, p. 9-10.

DeLong, R.M., 1969, Bedrock geology of the Carrollton Quadrangle, Carroll County, Ohio: Ohio Department of Natural Resources, Division of Geological Survey, Report of Investigations No. 71.

Donaldson, A.C., Renton, J.J., and Presley, M.W.,1985, Pennsylvanian deposystems and paleoclimates of the Appalachians: International Journal of Coal Geology, v. 5, p. 167-193.

Driese, S.G., Capelle, D.G., Glumac, B., Srinivasan, K., Stefaniak, A., Paleokarst Study Group, and Stapor, F.W., 1994, Pre-Pennsylvanian paleokarst at the top of the Upper Pennington Formation, central Tennessee [abst.]: Geological Society of America, Abstracts With Programs, v. 26, no. 4, p. 11.

Driese, S.G. and Foreman, J.L., 1992, Paleopedology and paleoclimatic implications of Late Ordovician vertic paleosols, Juniata Formation, southern Appalachians: Journal of Sedimentary Petrology, v. 62, p. 71-83.

Driese, S.G., and Mora, C.L., 1993, Physico-chemical environment of pedogenic carbonate formation in Devonian vertic palaeosols, central Appalachians, U.S.A.: Sedimentology, v. 40, p. 199-216.

Driese, S.G., Mora, C.I., Cotter, E., amd Foreman, J.L., 1992, Paleopedology and stable isotope chemistry of Late Silurian vertic paleosols, Bloomsburg Formation, central Pennsylvania: Journalof Sedimentary Petrology, v. 62, p. 825-841.

Dudal, R., 1989, Vertisols of Subhumid and Humid Zones, *in* Burford, J.R. and Sahrawat, K.L. (eds.), Management of Vertisols for Improved Agricultural Production: Patancheru, India, Proceedings of International Board of Soil Research and Management Inaugural Workshop, International Crops Research Institute for Semi-Arid Tropics (ICRISAT), p. 55-59.

Eswaran, H., Kimble, J. and Cook, T., 1989, Properties, Genesis, and Classification of Vertisols, *in* Hirekerur, L.R., Pal, D.K., Sehgal, J.L., and Deshpande, S.B. (eds.), Classification Management and Use Potential of Swell-Shrink Soils: Transactions of International Workshop on Swell-Shrink Soils,: Rotterdam, A.A. Balkema, p. 1-22.

Feakes, C.R., and Retallack, G.J., 1988, Recognition and chemical characterization of fossil soils developed on alluvium; A Late Ordovician example: Geological Society of America, Special Paper 216, p. 35-48.

Ferm, J.C, Milici, R.C., and Eason, J.E., 1972, Carboniferous depositional environments in the Cumberland Plateau of southern Tennessee and northern Alabama: Tennessee Division of Geology, Report of Investigations no. 33, p. 1-22.

Ferm, J.C., 1974, Carboniferous environmental models in the eastern United States and their significanc, *in* Briggs, G. (ed.), Carboniferous of the southeastern United States: Geological Society of America Special Paper 148, p. 45-95.

Fox, W.E., 1964, A study of bulk density and water in a swelling soil: Soil Science, v. 98, p. 307-316.

Freytet, P. and Plaziat, J.C., 1982, Continental Carbonate Sedimentation and Pedogenesis - Late Cretaceous and Early Tertiary of Southern France: Contributions to Sedimentology 12, 213p.

Goudie, A., 1973, Duricrusts in Tropical and Subtropical Landscapes: Oxford, Clarendon Press, 174p.

Harris, A.G., 1979, Conodont color alteration, an organo-mineral metamorphic index, and its application to Appalachian basin geology, *in* Scholle, P.A. and Schluger, P.R. (eds.), Aspects of Diagenesis: Special Pulication of Society of Economic Paleontologists and Mineralogist, no. 26, p. 3-16.

Heckel, P.H., 1995, Glacial-eustatic base-level-climatic model for late Middle to Late Pennsylvanian coal-bed formation in the Appalachian Basin: Journal of Sedimentary Research, v. B65, p. 348-356.

Hutton, J.T. and Dixon, J.C., 1981, The chemistry and mineralogy of some South Australian calcretes and associated soft carbonates and their dolomitisation: Journal of Geological Society of Australia, v. 28, p. 71-79.

Jenny, H.J. and Leonard, C.D., 1935, Functional relationships between soil properties and rainfall: Soil Science, v. 38, p. 363-381.

Joeckel, R.M., 1994, Virgilian (Upper Pennsylvanian) paleosols in the Upper Lawrence Formation (Douglas Group) and in the Snyderville Shale Member (Oread Formation, Shawnee Group) on the northern midcontinent, U.S.A.: pedologic contrasts in a cyclothem sequence: Journal of Sedimentary Research, v. A64, p. 853-866..

Joeckel, R.M., 1995, Paleosols below the Ames marine unit (Upper Pennsylvanian, Conemaugh Group) in the Appalachian Basin, U.S.A.: variability on an ancient depositional landscpe: Journal of Sedimentary Research, v. A65, p. 393-407.

Lynn, W. and Williams, D., 1992, The making of a Vertisol: Soil Survey Horizons, v. 33, no. 2, p. 45-50.

Mack, G.H., James, W.C., and Monger, H.C., 1993, Classification of paleosols: Geological Society of America Bulletin, v. 105, p. 129-136.

Merrill, G.K., 1986, Lithostratigraphy and lithogenesis of Conemaugh (Carboniferous) depositional systems near Huntington, West Virginia: Southeastern Geology, v. 26, no. 3, p. 155-171.

Milici, R.C., 1974, Stratigraphy and depositional environments of Upper Mississippian and Lower Pennsylvanian rocks in the southern Cumberland Plateau of Tennessee, *in* Briggs, G. (ed.), Carboniferous of the southeastern United States: Geological Society of America Special Paper 148, p. 115-133.

Milici, R.C., Briggs, G., Knox, L.M., Sitterly, P.D. and Statler, A.T., 1979, The Mississippian and Pennsylvanian (Carboniferous) Systems in the United States - Tennessee: United States Geological Survey Professional Paper 1110-G, 38p.

Milnes, A.R. and Hutton, J.T., 1983, Calcretes in Australia, *in* Soils: An Australian viewpoint: London, Melbourne/Academic Press, p. 119-162.

Mora, C.I., and Driese, S.G., 1993, A steep, mid- to late Paleozoic decline in atmospheric CO_2: evidence from the soil carbonate CO_2 paleobarometer: Chemical Geology, v. 107, p. 217-219.

Mora, C.I., Driese, S.G., and Colarusso, L.A., 1996, Middle to Late Paleozoic atmospheric CO_2 levels from soil carbonate and organic matter: Science, v. 271, p. 1105-1107.

Mora, C.I., Fastovsky, D.E., and Driese, S.G., 1993, Geochemistry and stable isotopes of paleosols: University of Tennessee Studies in Geology no. 23, 66p.

Mora, C.I., Sheldon, B.T., Elliott, W.C., and Driese, S.G.,(in review), An oxygen isotope study of illitization and diagenesis in Appalachian Paleozoic vertic paleosols: Journal of Sedimentary Research.

Muchez, Ph. and Viaene, W., 1987, Dolocretes from the Lower Carboniferous of the Capine-Brabat Basin, Belgium: Pedologie, v. 37. p. 187-202.

Muller, M.J., 1982, Selected climatic data for a global set of standard stations for vegetation science: Tasks for Vegetation Science, v. 5, The Hague, Dr. W. Junk Publishers, 306p.

Nettleton, W.D., Flach, K.W., Brasher, B.R., 1969, Argillic horizons without clay skins: Soil Science of America Proceedings, v. 33, p. 121-125.

Olhoeft, G.R. and Johnson, G.R., 1989, Densities of Rocks and Minerals, *in* Carmichael, R.S. (ed.), Practical Handbook of Physical Properties of Rocks and Minerals: Boca Raton, CRC Press, 552p.

Paton, T.R., 1974, Origin and terminology for gilgai in Australia: Geoderma, v. 11, p. 221-242.

Phillips, S.E. and Milnes, A.R., 1983, The Pleistocene terrestrial carbonate mantle on the southeastern margin of the St. Vincent Basin, South Australia: Australian Journal of Science, v. 35, p. 463-481.

PiPujol, M.D. and Buurman, P., 1994, The distinction between groud-water gley and surface-water gley phenomena in Tertiary paleosols of the Ebro basin, NE Spain: Palaeogeography, Palaeoclimatology, Palaeoecology, v. 110, 103-113.

Retallack, G.J, 1983, Late Eocene and Oligocene paleosols from the Badlands National Park, South Dakota: Geological Society of America, Special Paper 193, 82p.

Retallack, G.J, 1986, Reappraisal of a 2200Ma-old paleosol near Waterval Onder, South Africa: Precambrian Research, 32, p.195-232.

Retallack, G.J., 1988, Field recognition of paleosols, *in* Reinhardt, J. and Sigleo, W.R. (eds.), Paleosols and Weathering Through Geologic Time: Geological Society of America, Special Paper 216, p. 1-20.

Retallack, G.J., 1990, Soils of the Past: Boston, UnwinHyman, 520p.

Retallack, G.J., 1991a, Untangling the effects of burial alteration and ancient soil formation: Annual Reviews of Earth and Planetary Science, v. 19, p. 183-206.

Retallack, G.J.,1991b, Miocene paleosols and ape habitats of Pakistan and Kenya: New York, Oxford University Press, 346p.

Retallack, G.J., 1993, Late Ordovician Paleosols of the Juniata Formation near Potters Mills, Pennsylvania, *in* Driese, S.G. (ed.), Paleosols, Paleoweathering and Paleoatmospheric CO_2; Paleozoic Paleosols of Central Pennsylvania: University of Tennessee, Studies in Geology, no. 22, p. 33-49.

Retallack, G.J., 1994a, The Environmental Factor Approach to the Interpretation of Paleosols, *in* Amundson, R., Harden, J., and Singer, M. (eds.), Factors of Soil Formation: A Fiftieth Annniversary Retrospective: Soil Science Society of America Special Publication 33, p. 31-64.

Retallack, G.J., 1994b, A pedotype approach to latest Cretaceous and earliest Tertiary paleosols in eastern Montana: Geological Society of America Bulletin, v.106, p. 1377-1397.

Retallack, G.J. and Mindszenty, A., 1994, Well preserved late Precambrian paleosols from northwest Scotland: Journal of Sedimentary Research, v. A64, p. 264-281.

Rieke, H.H. and Chilingarian, G.V., 1974, Compaction of Argillaceous Sediments: Amsterdam, The Netherlands, Elsevier, 424p.

Robertson, E.C., 1967, Laboratory consolidation of carbonate sediments, *in* Richards, A.F. (ed.), Marine Geotechnique: Urbana, Illinois, University of Illinois Press.

Sarg, J.F., 1979, Sedimentology of the Ames Limestone (Conemaugh Group) in the Pittsburgh (Pennsylvania) area--evidence for Virgilian eustatic rise in sea level, *in* Geldsetzer, H.H.J., Nassichuk, W.W., Belt, E.S., and Macqueen, R.W., (eds.), Ninth International Congress on Carboniferous Stratigraphy adn Geology, v. 3, p. 554-560.

Schwertmann, U., 1993, Relations between iron oxides, soil colorm and soil formation, *in* Bigham, J.M. and Ciolkosz, E.J. (eds.), Soil color: Soil Science Society of America Special Publication 31, p. 127-159.

Sclater, J.G. and Christie, P.A.F., 1980, Continental stretching: an explanation of the post-mid-Cretaceous subsidence of the central North Sea basin: Journal of Geophysical Research, v. 85, p. 3711-3739.

Scotese, C.R., Bambach, R.K., Barton, C., Van Der Voo, R., and Ziegler, A.M., 1979, Paleozoic base maps: Journal of Geology, v. 87, p. 217-277.

Searl, A., 1988, Pedogenic dolomites from the Oolite Group (Lower Carboniferous) of South Wales: Geological Journal, v. 23, p. 157-169.

Sedimentation Seminar, 1981, Mississippian and Pennsylvanian section at Interstate 75 south of Jellico, Campbell County, Tennessee: Tennessee Division of Geology Report of Investigations 38, 37p.

Sheldon, B.T., 1995, An Oxygen Isotope Study of Illitization and Diagenesis in Appalachian Vertic Paleosol: University of Tennesse-Knoxville, unpublished M.Sc. thesis, 163p.

Singleton, P.L., 1991, Water Tables and Soil Colour as an Indicator of Staturation in Some Soils of the Waikato, New Zealand: Soil Physics and Hydrology, v. 29, p. 467-481.

Smith, G.A., 1994, Climatic influences on continental deposition during late-stage filling of an extensional basin, southeastern Arizona: Geological Society of America Bulletin, v. 106, p. 1212-1228.

Soil Survey Staff, 1990, Keys to Soil Taxonomy, fourth edition: Soil Management Support Services technical monograph no. 6, Blacksburg, Virginia, 422 p.

Stace, H.T.C., Hubble, G.D., Brewer, R., Northcote, K.H., Sleeman, J.R., Mulcahy, M.J., and Hallsworth, E.G., 1968, A Handbook of Australian Soils: Glenside, South Australia, Rellim Technical Publications, 435p.

Tandon, S.K. and Gibling, M.R., 1994, Calcrete and coal in late Carboniferous cyclothems of Nova Scotia, Canada: Climate and sea-level changes linked: Geology, v. 22, p.755-758.

Trask, P.D., 1931, Compaction of sediments: American Association of Petroleum Geologists Bulletin, v. 15, p. 271-276.

Vepraskas, M.J., 1992, Redoximorphic Features for Identifying Aquic Conditions: North Carolina Agricultural Research Service, Technical Bulletin 301, 31p.

Vinogradov, A.P., 1959, The geochemistry of rare and dispersed chemical elements in soils: New York, Consultants Bureau.

Watts, N.L., 1980, Quaternary pedogenic calcretes from the Kalahari (southern Africa): mineralogy, genesis and diagenesis: Sedimentology, v. 27, p. 661-686.

Weaver, C.E., 1989, Clays, Muds, and Shales: Developments in Sedimentology 44: New York, Elsevier, 819 p.

Wilding, L.P., Williams, D., Miller, W., Cook, T., and Eswaran, H., 1990, Close interval spatial variability of Vertisols: a case study in Texas, *in* Kimble, J.M. (ed.), Characterization, Classification, and Utilization of Cold Aridisols and Vertisols: Proceedings of the Sixth International Soil Correlation Meeting, Lincoln, Nebraska, United States Department of Agriculture, Soil Conservation Service, p. 232-247.

Williams, D., Thompson, C.M., and Jacobs, J.L., 1977, Soil Survey of Cameron County, Texas: United States Department of Agriculture Soil Conservation Service, 92 p.

Winston, R.B., 1990, Implications of paleobotany of Pennsylvanian-age coal of the central Appalachian basin for climate and coal-bed development: Geological Society of America Bulletin, v. 102, p. 1720-1726.

Wright, V.P., 1990, A micromorphological classification of fossil and recent calcic and petrocalcic microstructures, *in* Douglas, D.A. (ed.), Soil Micromorphology: A Basic and Applied Science: Developments in Soil Science Volume 19, Amsterdam, Elsevier, p. 401-407.

Wright, V.P. and Platt, N.H., 1995, Seasonal wetlands carbonate sequences and dynamic catenas: a re-appraisal of palustrine limestones: Sedimentary Geology , v. 99, p. 65-71.

Wright, V.P. and Robinson, D., 1988, Early Carboniferous floodplain deposits from South Wales: a case study of the controls on paleosol development: Journal of the Geological Society of London, v. 145, p. 847-857.

Wright, V.P. and Tucker, M.E., 1991, Calcretes: An Introduction, *in* Wright, P.V. and Tucker, M.E. (eds.), Calcretes: Oxford, Blackwell Scientific Publications, p. 1-22.

APPENDICES

APPENDIX A

MACROMORPHOLOGICAL DESCRIPTIONS OF PALEOSOLS

NOTE

1. Paleosols profile units (i.e., horizons) are given in descending order as is the practice for describing profiles of modern soils.

2. Paleosols are referred to using the following code:

(drill core)(paleosol)
2432 RK

refers to drill core 2432, and RK refers to the sub-Ames paleosol. Other paleosol symbols include;

BC = sub-Brush Creek paleosol, and
PV = sub-Portersville paleosol.

Drill core numbers are the core record file numbers of the Ohio Geological Survey.

3. Profiles are described according to the approach of Retallack (1988); (see next page). Colors refer to moistened state.

Suggested Format for Description of Paleosols

+0 cm, ... (description of sediment overlying paleosol, using format below) ..... contact to

-0 cm, ... (description of topmost horizon of paleosol, using format below) ..... contact to

-(depth to top of horizon) cm; horizon designation (Table 1); rock type (e.g., claystone, siltstone); fresh Munsell color of whole horizon and of special features; weathered Munsell color; nature of root traces (Fig. 1), soil structure (Fig. 9), or other features (Tables 4, 7); reaction with dilute acid (Table 2); mineralogy and microfabric (to be considerably amplified following laboratory work); nature of contact (Table 3) to

-(depth to top of horizon) cm, horizon designation .....

Note: Examples of this kind of description are given in Retallack (1983b). Usually they are published as a sentence fragments connected by colons and semicolons, but I find it best in the field to write longhand paragraphs on each horizon, discussing field interpretations and subsequent efforts to test them.

Terminology for Description of Various Features of Paleosols

SIZE, ABUNDANCE, AND CONTRAST OF MOTTLES IN PALEOSOLS

Category	Class	Features
Contrast	Faint	Indistinct mottles or glaebules visible only on close examination: both mottles and matrix have closely related hues and chromas
	Distinct	Mottles are readily seen, with hue, value, and chroma different from that of surrounding matrix
	Prominent	Mottles are obvious and form one of the outstanding features of the horizon; their hue, value, and chroma differing from that of the matrix by as much as several Munsell color units
Abundance	Few	Mottles occupy less than 2% of the exposed surface
	Common	Mottles occupy about 2 to 20% of the exposed surface
	Many	Mottles occupy more than 20% of the exposed surface. This class can be subdivided according to whether (a) the mottles are set in a definite matrix, or (b) the sample is almost equally two or more kinds of mottle
Size	Fine	Mottles less than 5 mm diameter in greatest visible dimension
	Medium	Mottles between 5 and 15 mm in greatest dimension
	Coarse	Mottles greater than 15 mm in greatest dimension

SCALE OF ACID REACTION TO APPROXIMATE CARBONATE CONTENT OF PALEOSOLS

Carbonate Content	Reaction with Dilute Acid
Noncalcareous	Acid unreactive; often forms an inert bead
Very weakly calcareous	Little movement within the acid drop, which could be flotation of dust particles as much as bubbles
Calcareous	Numerous bubbles, but not coalescing to form a froth
Strongly calcareous	Bubbles forming a white froth, but drop of acid not doming upward
Very strongly calcareous	Drop vigorously frothing and doming upward

SHARPNESS AND LATERAL CONTINUITY OF PALEOSOL HORIZON BOUNDARIES

Category	Class	Features
Sharpness	Abrupt	Transition from one horizon to another completed within 1 in (2cm)
	Clear	Transition completed within 1-2.5 in (2-5 cm)
	Gradual	Transition spread over 2.5-5 in (5-15 cm)
	Diffuse	One horizon grading into another over more than 5 in (15 cm)
Lateral Continuity	Smooth	Horizon boundary forms an even plane
	Wavy	Horizon boundary undulates, with pockets wider than deep
	Irregular	Horizon boundary undulates, with pockets deeper than wide
	Broken	Parts of the adjacent horizon are disconnected, e.g., by deep and laterally persistent clastic dikes in Vertisols

PALEOSOL: 2432RK

Location: Monroe Cty, OH; Green Twp.; SW1/4, NE1/4, NE1/4, SEC. 1; Antioch 71/2' quad; UTM COORD. zone 17, X=497,091E Y= 4,394,000N

UNIT	THK.(m)	DPTH(m)	DESCRIPTIONS
1	0.92	0.92	mudstone; N2, gray black; weak, granular; abundant large, black, carbonized plant fossils; very weakly calcareous; clear.
2	1.01	1.93	mudstone; 5Y3/1, dark, olive-gray; weak, medium, blocky; few, large, ; few, fine, sub-vertical, carbonized root traces, some are present on slickenside planes; few, medium, irregularly-shaped, 5YR3/2, grayish brown, mottles with diffuse margins; common carbonate nodules, 1-5mm diameter; calcareous; gradual.
3	0.81	2.74	mudstone; 5Y4/1, olive gray: weak, medium blocky; common, large, slickensides with very thin calcite fill and few, carbonized root traces on slickenside surfaces ; few, large, vertical, 5Y2/1, olive black, mottles with sharp margins (appear to be cracks or root channels); common carbonate nodules,1-5mm diameter; calcareous; gradual.
4	1.51	4.25	mudstone; 5G4/1, dark, greenisk gray; weak, medium, blocky; common, large, slickensides; few, large, vertical, 10R3/2, very dark reddish brown mottles with sharp margins (filled cracks?); common,small to large (1 to 30mm) carbonate nodules, some large ones have vertical habit and contain clay-filled root channels; calcareous; gradual.
5	1.12	5.37	mudstone; 5GY5/1; greenish gray; weak, medium, blocky; many, large slickensides some are calcite-filled and some with few, fine, carbonized root traces on surfaces; many, large, irregularly-shaped, 10R3/4, dark, reddish brown, sub-vertical mottles some contain fine and medium, 5GY6/1, greenish gray, vermicular mottles (roots); few, carbonate nodules 1 to 5mm diameter; weakly calcareous, gradual.

PALEOSOL: 2432RK (cont'd)

UNIT	THK.(m)	DPTH(m)	DESCRIPTIONS
6	0.68	6.05	mudstone; 10R3/4, dark reddish brown; coarse, moderate, blocky; common, large, slickensides some with metallic (Mn?) coating on surfaces; common, fine, 5GY5/1, greenish gray, vermicular, mottles (root channels and interpedal pores); few, medium, irregular, 5GY5/1, greenish gray mottles with diffuse margins; few, carbonate nodules 1 to 3mm diameter; weakly calcareous; gradual.
7	0.54	6.59	mudstone; 10R3/2, very dark reddish brown; few, large, slickensides; few, large, irregular 5GY5/1, greenish gray mottles with diffuse margins, common, fine and medium, vertical 5Y5/6 light, olive brown mottles (after roots?), and many, medium, irregular 5Y5/6 mottles with diffuse margins; abundant spherulitic siderite; weakly calcareous; gradual.
8	1.78	8.37	mudstone; 10R3/4,dark reddish brown; weak, coarse, blocky; common, large, slickensides; many, large, irregular, 5GY5/1,greenish gray mottles with diffuse margins; common carbonate nodules 5 to 10mm diameter and few stacked carbonate nodules 30 to 50mm diameter (rhizocretions); weakly calcareous; gradual.
9	1.95	10.32	mudstone; 5GY5/1; greenish gray; weak, medium, blocky; common, large slickensides; many, tuberous, stacked carbonate nodules 20 to 30mm diameter (rhizocretions); non-calcareous; clear.
10	1.00	11.32	mudstone; 5RP3/2, dusky red purple; weak, medium, blocky; few, large slickensides; common, large, irregular, 5GY4/1 dark greenish gray mottles with diffuse margins, and common, fine and medium, vertical, 10YR6/6 dark yellowish orange mottles that surround fine, vertical, 5G6/1 greenish gray mottles (root traces); common, carbonate nodules 1 to 5mm diameter; weakly calcareous; clear.

PALEOSOL: 2432RK (cont'd)

UNIT	THK.(m)	DPTH(m)	DESCRIPTIONS
11	1.52	12.84	shale, very silty; 5GY5/1, greenish gray; many, large, contorted veins filled with carbonate (give brecciated appearence, especially in lower 0.15m); weakly calcareous; abrupt.
12	0.15	12.99	shale; N3, dark gray; common, finely disseminated organics; non-calcareous; sharp.

PALEOSOL: 2402RK

Location: Noble Cty, OH; Jackson Twp.; SW1/4, SW1/4, SE1/4, SEC. 4; Caldwell South 71/2' quad; UTM COORD. zone 17, X=453,716E Y= 4,389,823N

UNIT	THK.(m)	DPTH(m)	DESCRIPTIONS
1	0.26	0.26	mudstone; N3, dark gray; weak, fine, granular; few, small, slickensides; common, fine and medium, black, carbonized, horizontal root traces; calcareous; clear.
2	0.23	0.49	mudstone; 5Y4/1, olive gray; weak, medium, blocky; rare, large, slickensides; rare, fine, dessiminated, coaly organics; few, small patches of fine pyrite grains; few, small (<1mm)carbonatenodules; calcareous; gradual.
3	0.77	1.26	mudstone; same as above, except contains few, small (<1mm) siderite(?) nodules.
4	0.84	2.10	mudstone; 5Y4/1, olive gray; weak, medium, blocky; few, large, slickensides; few, vertical, carbonized, root traces; few, small patches of fine pyrite grains, associated with carbonized root traces; few, carbonate nodules, 0.5 to 3mm diameter; calcareous; gradual.
5	1.95	4.05	mudstone; 5Y4/1, olive gray; weak, medium, blocky; few, large, slickensides; few, small patches of fine pyrite grains, and few, medium, vertical, vein-like features (root channels?) with common, fine grains of pyrite; calcareous; gradual.
6	0.88	4.93	mudstone; 5Y4/1, olive gray; weak, medium, blocky; common, large, slickensides; rare, small patches of fine pyrite grains; few, carbonate nodules 0.1 to 1.0mm diameter; calcaroeus; gradual.
7	0.78	5.71	mudstone; 10R2/4, very dark reddish brown; moderate, medium, blocky; common, large, slickensides; many, large, 5GY5/1, greenish gray, mottles, some are vertical; few, medium, 5RP4/2, grayish red purple mottles; common; carbonate nodules, 0.2 to 1.0mm diameter; calcareous; gradual.

PALEOSOL: 2402RK (cont'd)

UNIT	THK.(m)	DPTH(m)	DESCRIPTIONS
8	1.66	7.37	mudstone; 10R3/4, dark reddish brown; moderate, medium, blocky; common, large, slickensides; common, medium, sub-vertical, vermicular, 5GY6/1, greenish gray mottles (after roots or cutans); few, fine, irregular, 10YR6/6, dark yellowish orange mottles; few, carbonate nodules, 0.2 to 0.5mm diameter; calcareous; gradual.
9	0.69	8.06	shale; 5RP2/2, very dusky red purple; common, coarse, patchy, horizontal, 5G6/1, greenish gray mottles (may follow horizontal burrows); few, brachiopod fossils, *Lingula and Mesolobus*; calcareous; abrupt.

PALEOSOL: 2405RK

Location: Noble Cty, OH; Stock Twp.; NW1/4, NE1/4, SE1/4, SEC. 13; Stafford 71/2' quad; UTM COORD. zone 17, X=469,396E Y= 4,395,343N

UNIT	THK.(m)	DPTH(m)	DESCRIPTIONS
1	0.48	0.48	mudstone; 5Y3/1, dark olive gray; weak, medium, granular; common, medium, horizontal, carbonized root traces; non-calcareous; contact gradual.
2	1.40	1.88	mudstone; 5GY4/1, dark greenish gray; weak medium blocky; few, large slickensides; common, carbonate nodules 1 to 20mm diameter; weakly calcareous; gradual.
3	0.57	2.45	mudstone; 5Y4/1, olive gray; very, hard, and dense (carbonate cemented); few ostracodes; strongly calcareous; gradual.
4	0.46	2.91	limestone; very argillaceous;10Y5/2, light grayish olive; common, ostracodes; many ganules of carbonate and mudstone; clear.
5	0.78	3.69	mudstone; same as in unit 3.
6	3.59	7.28	mudstone; 5GY3/2, grayish olive green; common, large slickensides some with thin sheets of calcite on surface; few carbonate nodules 1 to 15mm diameter; calcareous; gradual.
7	1.41	8.69	mudtone; 5GY3/2, grayish olive green; few, large slickensides; few, large, vertical, 10R2/2, very dusky red mottles with diffuse margins; few large, vertical, 5Y5/1, olive gray mottles following root channels; few, carbonate nodules 5 to 10mm diameter; weakly calcareous; gradual.
8	1.70	10.39	mudstone; 5R4/3, grayish red; moderate, medium, blocky; common, large slickensides, surfaces have strongly metallic, polished appearance; few, large, vertical, 10YR6/6, dark yellowish orange mottles filling interpedal pores; few, medium, irregular, N5, medium gray mottles; few, medium, 5GY5/1, greenish gray

PALEOSOL: 2405RK (cont'd)

UNIT	THK.(m)	DPTH(m)	DESCRIPTIONS
8 (cont'd)			mottles after root channels; few, carbonate nodules 5 to 10mm diameter; weakly calcareous; gradual.
9	1.65	12.04	mudstone; 5Y4/1, olive gray; strong, medium blocky; few, large slickensides; common, medium, 5R4/3, grayish red mottles filling interpedal pores; non-calcareous; gradual.
10	0.20	12.24	mudstone; 5G6/1, greenish gray; weak, medium, blocky; few, large slickensides; few, medium, irregular 10YR6/6, dark yellowish orange mottles; fine vein-like network of siderite(?); non-calcareous; clear.
11	0.43	12.67	mudstone; 5Y5/6, light olive brown; few, medium 5G6/1, geenish gray mottles with diffuse margins; few, medium, vermicular 5Y3/2 olive gray mottles after roots (?); common, spherulitic siderite; non-calcareous; gradual.
12	1.30	13.90	shale; silty with thin, discontinuous laminae of fine-grained sandstone; 5GY5/1, greenish gray; common, spherulitic siderite; non-calcareous; gradual.

PALEOSOL: 2408RK

Location: Monroe Cty, OH; Seneca Twp.; NW1/4, SE1/4, NW1/4, SEC. 19; Summerfield 71/2' quad; UTM COORD. zone 17, X=473,410E Y= 4,404,210N

UNIT	THK.(m)	DPTH(m)	DESCRIPTIONS
1	1.43	1.43	mudstone; 5Y4/1, olive gray; weak, medium blocky; few, large slickensides and few, small slickensides; distinct, common, fine and medium, 5Y5/6 light olive brown mottles, some sub-vertical, vermicular (after roots), also common, distinct, fine-medium, patchy, 5RP2/2, very dusky red purple mottles with diffuse margins; common, carbonate nodules (1-5mm diameter); non-calcareous at top to calcareous in lower half; irregular, gradual.
2	0.88	2.31	mudstone; 10R3/4, dark reddish brown; moderate blocky; few, large slickensides and few, small slickensides; common, distinct, fine-medium, N3, medium dark gray mottles, and common, fine, 5R3/6, dark red, sub-vertical, vermicular mottles (after roots), and few, distinct, fine-medium, circular, 5Y5/6, light olive brown mottles with diffuse margins; common, carbonate nodules (1-10mm), smaller ones more abundant; calcareous; clear.
3	1.77	4.08	mudstone; 5Y3/1, dark olive gray; weak blocky; common, large, slickensides; many, distinct, medium-course, sub-vertical, 10R3/3, dark reddish mottles surrounding few, distinct, fine, vermicular, 5Y2/1, olive black mottles (after roots); few, carbonate nodules (1-15mm), some septarian, all sub-spherical with sharp margins; weakly calcareous; gradual.
4	1.41	5.49	mudstone; 5R3/4, dusky red; moderate blocky; few, large slickensides and few, small slickensides; common, distinct, fine, some vermicular, 5GY6/1, greenish gray mottles, and few, distinct, medium, 5G4/1, dark greenish gray, mottles with diffuse margins, and few, distinct, fine 5Y5/6, light olive brown mottles; few, sub-spherical carbonate nodules (1-5mm) in upper part; slightly calcareous at top to non-calcareous downward; clear.

PALEOSOL: 2408RK (cont'd)

UNIT	THK.(m)	DPTH(m)	DESCRIPTIONS
5	0.14	5.63	mudstone; 5G2/1, greenish black; fine, granular; few, large slickensides; common, faint, medium, 5Y5/1, olive gray mottles in upper part, and few, distinct, course, 5R2/6, very dusky red mottles, and few, distinct, fine, 5Y5/6, light olive brown mottles (goethite-rich) surrounding fine peds; very slightly calcareous; clear.
6	1.58	7.21	mudstone; 5R3/4, dusky red; few, large slickensides and few, small slickensides; moderate blocky; common, distinct, fine, 5Y5/6, light olive brown mottles surrounding peds, and common, distinct, fine-medium, 5G6/1, greenish gray, sub-vertical, vermicular mottles after roots and surrounding some peds; few, carbonate nodules (1-5mm); weakly calcareous; clear.
7	0.09	7.30	mudstone; 5G4/1, dark greenish gray; weak granular; common, faint, fine, subhorizontal, vermicular, 5GY6/1 mottles after roots; rare, carbonate nodules (1-5mm); weakly calcareous; clear.
8	0.90	8.23	mudstone; 10R2/4, very dusky reddish brown; few, large slickensides; moderate blocky; many, distinct, medium, sub-vertical, 5Y2/1, olive black mottles with diffuse margins, some contain faint, fine, vermicular, 5Y5/1, medium olive gray mottles after roots; rare carbonate nodules (1-5mm); calcareous; gradual.
9	1.09	9.32	mudstone; 10R2/4, very dusky reddish brown; weak blocky to moderate platy; few, large slickensides and in lower part common small slickensides; common, distinct, fine, 5Y5/6, light olive brown (goethite-rich) mottles, and few, distinct, fine-medium, 5Y6/1, light olive gray mottles surrounding peds; weakly calcareous; gradual.
10	0.77	10.09	shale; 5R3/4, dusky red; fissile; common, 5Y4/1, olive gray, horizontal mottles after burrows; non-calcareous; contact gradational.

PALEOSOL: 2428RK

Location: Noble Cty, OH; Sharon Twp.; SE1/4, NW1/4, SE1/4, SEC. 24; Caldwell South 71/2' quad; UTM COORD. zone 17, X=449,351E Y= 4,394,229N

UNIT	THK.(m)	DPTH(m)	DESCRIPTIONS
1	0.42	0.42	mudstone; 5Y5/1, medium olive gray; weak blocky; few, large slickensides and few small slickensides (in upper part); thin zone with many, distinct, medium, 5RP2/2, very dusky red mottles surrounded by 5Y5/6, light olive brown mottles (define fine blocky peds), also common, distinct, fine, sub-vertical, vermicular, 5Y5/6, light olive brown mottles after roots (in lower half); non-calcareous; clear.
2	0.24	0.66	mudstone; 5GY4/1, dark, greenish gray; weak blocky; few, large slickensides; few, distinct, fine, 5Y5/6, light olive brown, sub-vertical mottles after roots; very slightly calcareous; clear.
3	0.35	1.01	mudstone; 5Y4/2, medium olive gray; weak blocky; common, distinct, fine, vermicular, 5Y5/6, light olive brown, sub-vertical mottles after roots; common, carbonate nodules (0.5-5mm); calcareous; gradual.
4	0.39	1.40	mudstone; 5GY4/1, dark, greenish gray; weak blocky; few, carbonate nodules (2-7mm); very fine-grain, disseminated pyrite common; calcareous; gradual.
5	2.85	4.25	mudstone; N4, medium dark gray; few, large slickensides and few, small slickensides; weak blocky; many, distinct, fine and medium, 10R2/, dark reddish brown, mottles with sharp margins the surround peds and follow root traces; few, sub-spherical, carbonate nodules (5-15mm), calcareous; gradual.
6	0.75	5.00	mudstone; 5Y3/4, moderate brown; few large slickensides; weak blocky; common, distinct, fine, 5Y6/1, medium olive gray mottles, some are sub-vertical and branching, after roots; common, tuberous, carbonate nodules (2-10mm); non-calcareous; gradual.

PALEOSOL: 2428RK (cont'd)

UNIT	THK.(m)	DPTH(m)	DESCRIPTIONS
7	0.69	5.69	mudstone; 5GY6/1, greenish gray; few large slickensides; very weak blocky; common, distinct, medium-coarse, 10R3/4, dark reddish brown, sub-vertical mottles with diffuse margins, some contain, few, distinct, fine vermicular, 5Y5/1, medium olive gray mottles after roots; few, large, irregular-shaped, carbonate nodules (15-40mm); non-calcareous; gradual.
8	1.08	6.77	mudstone; 5YR3/2, grayish brown; common, large slickensides with metallic shine on surface; moderate blocky to platy near base; common, distinct, fine-medium, 10R2/4, reddish brown mottles; rare, elongate, vertical, carbonate nodules (rhizocretions); weakly calcareous; clear.
9	0.64	7.41	shale; N3, dark gray; fissile; common, faint, fine-medium, horizontal, 5GY5/1 medium greenish gray mottles after burrows; calcareous; clear.

PALEOSOL: 2552RK

Location: Belmont Cty, OH; Goshen Twp.; SW1/4, NE1/4, NE1/4, SEC. 6; Bethesda 71/2' quad; UTM COORD. zone 17, X=499,200E Y= 4,431,200N

UNIT	THK.(m)	DPTH(m)	DESCRIPTIONS
1	0.22	0.22	mudstone; 10Y6/2, pale olive; weak blocky; rare large and small slickensides; common, distinct, fine-medium, N3, dark gray mottles after roots, and common, distinct, coarse, 5Y5/6, light olive gray mottles after roots surrounded by 5RP4/2, grayish red purple mottles with diffuse margins; very weakly calcareous; clear.
2	0.29	0.51	mudstone; 5G5/1, medium greenish black; weak blocky; few, large slickensides; few, distinct, fine, sub-vertical, vermicular 5Y2/1 mottles after roots, and few, distinct, fine, sub-vertical, vermicular 5Y5/6 mottles after roots; non-calcareous; clear.
3	0.22	0.73	mudstone; 10R3/4, dusky red; few, large slickensides; weak blocky; few, distinct, fine, sub-vertical, vermicular, 5GY6/1, greenish gray mottles, and few, distinct, fine, sub-vertical, vermicular 5Y5/6 mottles, both after roots; few, small (1-5mm) carbonate nodules; very weakly calcareous; gradual.
4	0.39	1.12	mudstone; 5GY4/1, dark greenish gray; few, large slickensides; weak blocky; many, faint, medium, 5GY6/1, greenish gray mottles with diffuse margins; few, carbonate nodules (1-5mm); slightly calcareous, clear.
5	2.45	3.56	mudstone; 10R3/4, dark reddish brown; few large slickensides; weak blocky; common, distinct, fine-medium, sub-vertical, 5G6/1, greenish black mottles after roots, and few, distinct, coarse, 5G6/1, greenish black, patchy mottles; many, small (1-5mm) carbonate nodules, and few, large (10-20mm) carbonate nodules, and few , large (30-50mm) carbonate nodules with slickensides margins; weakly calcareous; gradual, diffuse.

PALEOSOL: 2422PV

Location: Belmont Cty, OH; Wayne Twp.; NW1/4, NW1/4, NW1/4, SEC. 29; Hunter 71/2' quad; UTM COORD. zone 17, X=449,351E Y= 4,394,229N

UNIT	THK.(m)	DPTH(m)	DESCRIPTIONS
1	0.12	0.12	mudstone; N3, dark gray; weak crumb; few small slickensides; common, fine, carbonized roots; common, very fine-grain, disseminated organic matter; few, thin, coaly laminations; non-calcareous; clear.
2	0.67	0.79	mudstone; 5Y6/1, light olive gray; weak granular; few, prominent, branching, horizontal, carbonized roots; few, small patches of fine-grain pyrite; very weakly calcareous; clear.
3	0.84	1.63	mudstone; 5Y4/1, olive gray; weak blocky; common, large slickensides; common to many, small to large (1-50mm), carbonate nodules, large ones are tuberous, complex, and septarian; few, small patches of fine-grained pyrite; calcareous; gradual.
4	0.66	2.29	mudstone; 5GY5/1, greenish gray; weak blocky; common, large slickensides, some with thin coating of carbonate; common to many, small to large (1-50mm), carbonate nodules, large ones are tuberous, complex, and septarian; few, small patches of fine-grained pyrite; calcareous; clear.
5	0.32	2.61	mudstone; 10R3/4, dark reddish brown; moderate blocky; common, large slickensides; few, distinct, 5GY5/1, greenish gray, vertical mottles after roots; common, medium (5-15mm) carbonate nodules, some with stacked vertical form (rhizocretions) and clay-filled root channels; calcareous; clear.
6	0.20	2.81	sandstone; medium-grain; argillaceous; 5GY5/1, greenish gray; 5cm layer at top very argillaceous; few, vertical, root channels filled with clay; calcareous; abrupt.

PALEOSOL: 2422PV (cont'd)

UNIT	THK.(m)	DPTH(m)	DESCRIPTIONS
7	0.31	3.12	mudstone; 5GY5/1, greenish gray; weak blocky; few, large slickensides; few, prominent, medium, irregular-shaped, 10R3/4, dark reddish brown mottles with indistinct margins; few, vertical cracks (30-50mm long and <2mm wide), filled with silt and very fine-grain sand; weakly calcareous; gradual.
8	0.32	2.43	mudstone; 10R3/4, dark red brown; weak blocky; few large slickensides; few, prominent, fine, 5GY5/1, greenish gray, vertical mottles after roots, some preserve organic matter; common, distinct, fine, 5Y4/1, olive gray mottles surrounding peds; very weakly calcareous; gradual.
9	0.43	2.86	mudstone; 10R3/4, dark red brown; medium platy; few, prominent, medium, irregular-shaped mottles surrounding peds; few, vertical root channels filled with red clay, disrupt general fabric; non-calcareous; gradual.
10	0.53	3.39	shale; 5R3/4, dusky red; fissile; non-calcareous; gradual.

PALEOSOL: 2552BC

Location: Belmont Cty, OH; Goshen Twp.; SW1/4, NE1/4, NE1/4, SEC. 6; Bethesda 71/2' quad; UTM COORD. zone 17, X=499,200E Y= 4,431,200N

UNIT	THK.(m)	DPTH(m)	DESCRIPTIONS
1	0.36	0.36	mudstone; 5GY4/1, dark greenish gray; weak granular; rare, large slickensides; few, carbonized, sub-horizontal root traces; non-calcareous; gradual.
2	1.81	2.17	mudstone; 5GY4/1, dark greenish gray; weak blocky; common, large slickensides; common, tuberous, small to medium (1-15mm) carbonate nodules; rare, vertical, cracks; calcareous; gradual.
3	0.55	2.72	mudstone; 5Y5/1, olive gray; strong blocky; common, large slickensides; common, 5Y3/1, dark olive gray mottles surrounding some peds; few, medium, sub-vertical, carbonized roots near base of unit; calcareous; clear.
4	0.25	2.97	mudstone; carbonaceous; 5Y2/1, olive black; weak blocky; few, small slickensides; few, faint, fine, 5Y4/1, olive gray mottles surrounding some peds; scattered fine-grain organic matter; weakly calcareous; gradual.
5	0.58	3.55	mudstone; 5Y4/1, olive gray; weak blocky; few, large slickensides; weakly calcareous; clear.
6	1.10	4.65	shale; 5GY5/1, greenish gray; sandy; few, 5Y2/1, olive black ,vertical, mottles after root channels filled with clay; common, large patches of net-like veins of carbonate; variably brecciated in lower part with ptygmatically folded cracks.

PALEOSOL: 2552RK (cont'd)

UNIT	THK.(m)	DPTH(m)	DESCRIPTIONS
6	2.00	5.56	mudstone; 5R3/4, dusky red; few large slickensides; weak blocky; common, distinct, medium-coarse, sub-vertical, 5Y6/1, light olive gray mottles with diffuse margins (roots?); few, large (20-50mm), sub-spherical, septarian carbonate nodules, and few zones with common, small (1-5mm) carbonate nodules; isolated, sub-vertical vein filled with carbonate; weakly calcareous; diffuse.
7	2.3	7.86	mudstone; 10R3/4, dark reddish brown; common, large slickensides; weak blocky; common, distinct, fine, sub-vertical, branching, vermicular 5Y5/6, light olive brown mottles, and few, distinct, fine, vermicular, 5GY5/1, greenish gray mottles, both after roots and surrounding peds; few, small (1-5mm) and few medium (5-10mm) carbonate nodules, also rare, sub-vertical vein filled with carbonate; non-calcareous; gradual.
8	0.28	8.14	mudstone; 5Y4/1, olive gray; few large slickensides; common, faint, fine, 5GY6/1, greenish gray mottles with diffuse margins, and many, prominent, coarse, 10R3/4, dark reddish brown with diffuse margins; non-calcareous; clear.
9	0.54	8.68	mudstone; 10R2/2, very dusky red; weak granular; few large slickensides; few, distinct, fine, 5GY6/1 greenish gray mottles surrounding fine peds; few, small (1-5mm) carbonate nodules; weakly calcareous; clear.
10	0.49	9.17	mudstone; 5GY5/1, medium greenish gray; few, large slickensides; common, distinct, sun-vertical, 10R3/4, dark reddish brown mottles after roots; non-calcareous; gradual.
11	1.0	10.17	shale, silty; 5GY5/1, medium greenish gray; scattered zones of spherulitic siderite; non-calcareous; gradual.

APPENDIX B

GEOCHEMICAL DATA

RK2402

smpl #	depth in core		depth from top of psol		weight percent and ppm (ppm in italics)								
	(feet)	(meters)	(meters)	Na2O	MgO	Al2O3	SiO2	K2O	CaO	MnO	Fe2O3	Ba	Sr
R1	238.40	73.24	0.13	1.39	1.89	18.18	63.67	2.90	0.55	*290*	4.26	*500*	*210*
RA	238.55	73.28	0.17	1.05	4.58	13.09	42.51	2.32	13.57	0.13	4.34	*400*	*380*
RB	238.90	73.39	0.28	0.79	5.13	11.77	37.06	2.00	17.32	0.14	3.57	*410*	*410*
R2	239.20	73.48	0.37	0.62	3.45	10.22	31.54	1.39	25.29	0.19	2.92	*250*	*380*
R3	241.00	74.04	0.93	0.98	6.08	9.96	34.63	1.68	19.26	0.15	3.55	*280*	**490*
R4	244.00	74.96	1.85	1.04	5.99	9.96	34.63	1.68	17.30	0.16	3.99	*310*	**490*
R5	248.00	76.19	3.08	0.99	6.09	11.04	36.40	1.99	16.68	0.18	4.43	*380*	**490*
R6	255.00	78.34	5.23	1.01	5.10	12.78	40.31	2.26	14.19	0.18	4.47	*360*	**420*
R7	255.50	78.49	5.38	0.82	2.77	16.23	47.10	2.21	10.54	0.10	4.65	*430*	*300*
R8	259.00	79.56	6.45	0.92	1.73	20.12	57.85	2.57	0.63	*290*	11.07	*440*	*190*
R9	263.30	80.89	7.78	0.83	1.56	20.87	56.62	3.47	1.15	*280*	8.68	*650*	*180*

molecular ratios

depth (m)	$\frac{SiO_2}{Al_2O_3}$	$\frac{SiO_2}{Fe_2O_3}$	$\frac{Ba}{Sr}$	$\frac{Al_2O_3}{CaO+MgO+Na_2O+K_2O}$	$\frac{Fe_2O_3+MnO}{Al_2O_3}$	$\frac{CaO+MgO}{Al_2O_3}$
0.13	5.94	39.72	1.53	1.62	0.15	0.32
0.17	5.51	26.03	0.68	0.32	0.23	2.77
0.28	5.35	27.62	0.64	0.25	0.22	3.78
0.37	5.24	28.70	0.41	0.18	0.22	5.35
0.93	5.90	25.92	0.37	0.19	0.26	5.06
1.85	5.90	23.07	0.40	0.21	0.27	4.36
3.08	5.60	21.83	0.50	0.22	0.29	4.14
5.23	5.36	23.97	0.54	0.30	0.25	3.03
5.38	4.93	26.92	0.91	0.54	0.19	1.61
6.45	4.88	13.90	1.50	2.05	0.35	0.27
7.78	4.61	17.34	2.24	1.87	0.27	0.29

RK2405

smpl #	depth in core		depth from top of psol		weight percent and ppm (ppm in italics)								
	(feet)	(meters)	(meters)	Na2O	MgO	Al2O3	SiO2	K2O	CaO	MnO	Fe2O3	Ba	Sr
R1	121.60	37.36	0.16	1.40	1.87	18.50	60.64	3.10	0.81	*370*	5.27	*760*	*270*
R2	125.00	38.40	1.20	1.03	2.07	15.02	50.72	2.61	8.39	*610*	3.87	*600*	*310*
R3	128.55	39.49	2.29	2.21	1.45	5.50	18.99	1.03	36.60	0.14	2.29	*140*	*400*
R4	130.20	40.00	2.80	2.29	9.38	7.51	22.13	1.57	20.30	0.25	5.13	*300*	*490*
R5	132.40	40.67	3.47	0.94	6.28	11.98	37.71	2.46	13.54	0.15	4.89	*370*	**450*
R6A	138.00	42.39	5.19	0.89	4.74	13.59	43.02	2.82	11.43	0.13	4.54	*460*	*380*
R6B	142.80	43.87	6.67	0.98	2.62	16.70	49.27	3.44	7.87	0.10	4.82	*660*	*300*
R7	148.10	45.50	8.30	0.89	1.40	21.86	60.70	3.22	1.22	*150*	5.15	*700*	*370*
R8	152.40	46.82	9.62	0.89	1.38	20.89	59.45	2.99	0.27	*190*	8.70	*660*	*370*
R9	156.00	47.92	10.72	0.79	1.40	21.19	60.47	3.08	0.26	*120*	5.90	*690*	*270*
R11	157.90	48.51	11.31	0.74	1.38	19.88	60.02	2.76	0.13	*410*	11.01	*540*	*170*
R12	160.00	49.15	11.95	0.90	1.34	16.69	65.13	2.11	1.80	0.11	6.61	*490*	*140*

molecular ratios

depth (m)	SiO_2 / Al_2O_3	SiO_2 / Fe_2O_3	Ba / Sr	Al_2O_3 / $CaO+MgO+Na_2O+K_2O$	Fe_2O_3+MnO / Al_2O_3	$CaO+Mg($ / Al_2O_3
0.16	5.56	30.59	1.83	1.56	0.19	0.33
1.20	5.73	34.81	1.22	0.60	0.17	1.36
2.29	5.86	22.00	0.22	0.07	0.31	12.76
2.80	5.00	11.47	0.39	0.11	0.50	8.07
3.47	5.35	20.51	0.52	0.27	0.28	3.38
5.19	5.01	27.19	1.39	0.64	0.19	1.25
6.67	4.71	31.34	1.20	2.04	0.15	0.26
8.30	4.83	18.17	1.57	2.40	0.27	0.19
9.62	4.84	27.24	1.64	2.46	0.18	0.19
10.72	5.13	14.50	2.10	2.50	0.36	0.19
11.31	6.11	24.13	2.19	1.60	0.27	0.40

RK2408

smpl #	depth in core (feet)	(meters)	depth from top of psol (meters)	Na2O	MgO	Al2O3	SiO2	K2O	CaO	MnO	Fe2O3	Ba	Sr
R2A	290.82	89.34	0.18	1.20	1.90	18.72	63.75	2.92	0.47	*300*	7.24	*570*	*250*
R2B	292.12	89.74	0.58	1.09	1.93	18.60	61.67	2.76	0.50	*320*	8.41	*520*	*250*
R3	292.79	89.95	0.79	0.97	2.12	15.98	52.75	2.29	8.42	*560*	7.31	*490*	*290*
R3A	293.45	90.15	0.99	0.82	2.19	14.49	47.09	2.07	11.91	*600*	6.24	*360*	*280*
R3B	294.12	90.35	1.19	1.01	2.18	17.30	56.60	2.52	5.46	*430*	7.41	*410*	*270*
R4	296.75	91.16	2.00	0.94	2.12	17.68	55.06	2.52	5.30	*410*	8.21	*410*	*280*
R5	298.07	91.57	2.41	0.88	2.05	17.06	53.60	2.36	8.31	*510*	4.85	*410*	*300*
R6	300.71	92.38	3.22	1.14	1.95	19.35	56.64	2.19	3.73	*380*	6.38	*190*	*280*
R7	305.99	94.00	4.84	1.01	1.67	22.65	59.37	1.88	1.08	*190*	7.55	*470*	*240*
R8	310.61	95.42	6.26	0.98	1.54	18.80	59.24	3.02	0.34	*610*	12.70	*570*	*210*
R9	313.91	96.43	7.27	0.87	1.72	18.45	57.20	2.83	5.53	*460*	3.64	*500*	*280*
R10	315.89	97.04	7.88	1.01	1.66	19.08	59.85	3.18	2.94	*360*	7.36	*560*	*260*
R11	318.53	97.85	8.69	0.74	1.31	20.83	58.80	2.97	0.34	*420*	9.45	*630*	*230*
R12	321.17	98.66	9.50	0.95	1.58	21.11	58.84	3.14	0.32	*240*	9.33	*570*	*250*

RK2408

molecular ratios

depth (m)	SiO_2 / Al_2O_3	SiO_2 / Fe_2O_3	Ba / Sr	Al_2O_3 / $CaO+MgO+Na_2O+K_2O$	Fe_2O_3+MnO / Al_2O_3	CaO+MgO / Al_2O_3
0.18	5.78	6.88	1.45	1.74	0.25	0.30
0.58	5.63	5.88	1.35	1.76	0.29	0.31
0.79	5.60	5.81	1.09	0.65	0.30	1.29
0.99	5.52	6.18	0.83	0.47	0.28	1.88
1.19	5.55	6.21	0.99	0.87	0.28	0.89
2.00	5.29	5.73	0.95	0.92	0.30	0.85
2.41	5.33	9.36	0.86	0.70	0.19	1.19
3.22	4.97	8.06	1.15	1.21	0.21	0.60
4.84	4.45	7.97	1.25	2.29	0.21	0.27
6.26	5.35	3.94	1.73	2.00	0.44	0.24
7.27	5.26	13.48	1.11	0.98	0.13	0.78
7.88	5.32	6.89	1.35	1.30	0.25	0.50
8.69	4.79	5.86	1.73	2.49	0.29	0.19

RK2428

smpl #	depth in core		depth from top of psol			weight percent		and ppm (ppm in italics)					
	(feet)	(meters)	(meters)	Na2O	MgO	Al2O3	SiO2	K2O	CaO	MnO	Fe2O3	Ba	Sr
R2	233.18	71.63	0.08	1.15	1.30	18.54	66.91	3.33	0.34	*250*	3.35	*240*	*170*
R3	233.84	71.84	0.29	1.12	1.78	19.14	61.71	2.74	0.29	*300*	11.17	*450*	*600*
R3A	234.50	72.04	0.49	1.35	2.17	18.97	64.86	2.60	1.08	*250*	5.94	*410*	*200*
R4	235.16	72.24	0.69	1.32	2.05	18.78	64.13	3.00	0.64	*340*	7.67	*510*	*200*
R5	237.14	72.85	1.30	1.18	2.27	18.08	57.72	2.66	4.87	*450*	6.16	*490*	*220*
R6	239.12	73.46	1.91	1.04	2.16	18.13	58.02	2.98	5.62	*500*	5.35	*520*	*250*
R7	241.76	74.27	2.72	1.13	1.93	20.27	58.28	2.85	4.67	*390*	5.61	*470*	*230*
R8	243.74	74.88	3.33	0.97	1.98	18.08	54.47	2.58	5.83	*580*	9.34	*350*	*240*
R9	246.38	75.69	4.14	1.01	1.65	20.36	60.95	2.67	1.68	*280*	8.23	*480*	*200*
R10	248.36	76.30	4.75	0.91	1.70	16.50	49.41	2.08	11.29	*510*	6.14	*400*	*220*
R11	251.00	77.11	5.56	0.92	1.57	21.90	62.81	3.20	0.35	*230*	6.73	*180*	*170*
R12	252.32	77.51	5.96	1.10	1.62	20.42	61.14	3.26	3.26	*300*	11.04	*560*	*170*
R13	253.64	77.92	6.37	0.92	1.39	20.55	63.80	3.34	0.30	*170*	7.12	*530*	*200*
R14	254.83	78.28	6.73	1.25	2.06	18.08	63.10	3.53	0.49	*310*	8.52	*620*	*180*

RK2428

molecular ratios

depth (m)	SiO_2 / Al_2O_3	SiO_2 / Fe_2O_3	Ba / Sr	Al_2O_3 / $CaO+MgO+Na_2O+K_2O$	Fe_2O_3+MnO / Al_2O_3	CaO+MgO / Al_2O_3
0.08	6.13	14.73	0.90	1.97	0.12	0.21
0.29	5.47	4.56	0.72	1.94	0.38	0.26
0.49	5.81	8.49	1.33	1.52	0.20	0.39
0.69	5.80	6.51	1.59	1.59	0.26	0.34
1.30	5.42	7.80	1.46	0.93	0.22	0.81
1.91	5.43	9.01	1.33	0.88	0.19	0.86
2.72	4.88	9.61	1.28	1.11	0.18	0.66
3.33	5.12	5.14	0.94	0.90	0.34	0.86
4.14	5.08	6.58	1.58	1.73	0.26	0.35
4.75	5.09	7.14	1.15	0.58	0.24	1.51
5.56	4.87	8.65	0.68	2.29	0.20	0.21
5.96	5.08	4.92	2.14	1.33	0.35	0.49
6.37	5.27	7.68	1.72	2.23	0.22	0.20
6.73	5.93	5.64	2.26	1.51	0.30	0.34

RK2432

smpl #	depth in core (feet)	(meters)	depth from top of psol (meters)	Na2O	MgO	Al2O3	SiO2	K2O	CaO	MnO	Fe2O3	Ba	Sr
					weight percent			and ppm (ppm in italics)					
R1	564.55	173.43	0.06	1.04	1.87	20.00	59.59	3.10	0.72	*210*	4.69	*680*	*210*
R2	566.70	174.09	0.72	0.70	2.42	14.07	43.50	1.84	14.70	*510*	3.98	*310*	*300*
R3	568.80	174.74	1.37	0.73	2.40	15.29	44.89	1.99	12.87	*630*	5.43	*380*	*220*
R4	573.20	176.09	2.72	0.77	2.48	17.00	46.78	2.07	10.88	0.10	7.37	*380*	*240*
R5	577.10	177.29	3.92	0.09	1.68	21.61	59.35	2.80	0.39	*200*	7.52	*460*	*200*
R6	580.65	178.38	5.01	0.93	1.33	21.03	57.76	3.44	0.31	*180*	9.14	*610*	*170*
R7	582.50	178.94	5.57	0.96	2.44	14.00	41.82	2.30	2.59	0.42	28.06	*500*	*150*
R8	584.50	179.56	6.19	0.64	1.52	17.46	50.54	2.91	8.40	*460*	4.30	*500*	*210*
R9	586.90	180.30	6.93	0.77	1.85	19.91	60.55	3.44	0.58	0.10	7.11	*670*	*160*
R10	590.50	181.40	8.03	0.90	1.64	17.49	50.33	3.66	5.57	*800*	8.21	*620*	*290*
R11	596.65	183.29	9.92	0.93	1.71	17.38	57.50	2.06	3.22	0.20	7.79	*130*	*210*

molecular ratios

depth (m)	SiO_2/Al_2O_3	SiO_2/Fe_2O_3	Ba/Sr	$Al_2O_3/(CaO+MgO+Na_2O+K_2O)$	$(Fe_2O_3+MnO)/Al_2O_3$	$(CaO+MgO)/Al_2O_3$
0.06	5.06	33.77	2.01	1.80	0.15	0.30
0.72	5.25	29.06	0.66	0.39	0.19	2.34
1.37	4.99	21.99	1.11	0.47	0.23	1.93
2.72	4.67	16.88	1.00	0.58	0.29	1.53
3.92	4.66	20.99	1.47	2.65	0.22	0.23
5.01	4.66	16.81	2.23	2.29	0.28	0.19
5.57	5.07	3.96	1.74	0.94	1.34	0.78
6.19	4.91	31.23	1.51	0.75	0.16	1.09
6.93	5.16	22.64	2.60	1.86	0.24	0.29
8.03	4.89	16.31	1.35	0.89	0.31	0.82
9.92	5.62	19.64	3.89	1.25	0.31	0.59

RK2552

smpl #	depth in core		depth from top of psol			weight percent		and ppm (ppm in italics)					
	(feet)	(meters)	(meters)	Na2O	MgO	Al2O3	SiO2	K2O	CaO	MnO	Fe2O3	Ba	Sr
R1A	341.81	105.00	0.15	1.13	1.55	19.05	63.14	3.26	0.35	*380*	6.61	*500.00*	*270.00*
R2	342.47	105.21	0.36	1.17	1.67	19.09	61.20	2.75	0.23	*260*	5.65	*460.00*	*400.00*
R3	343.77	105.61	0.76	0.78	1.75	16.70	55.76	2.82	5.44	*660*	4.74	*480.00*	*170.00*
R4	345.11	106.02	1.17	0.92	1.75	17.66	56.39	2.92	3.50	*520*	8.10	*580.00*	*160.00*
R5	347.75	106.83	1.98	0.96	1.82	17.85	55.94	2.91	4.53	*500*	6.61	*460.00*	*170.00*
R6	349.73	107.44	2.59	0.82	1.82	17.22	53.38	2.56	5.75	*630*	7.68	*480.00*	*190.00*
R7	350.39	107.64	2.79	0.91	1.74	17.63	52.68	2.44	6.76	*550*	7.05	*420.00*	*200.00*
R8	352.37	108.25	3.40	0.81	1.78	18.54	54.37	2.35	5.44	*430*	7.03	*450.00*	*180.00*
R9	354.35	108.86	4.01	0.98	1.64	19.81	57.37	2.37	3.76	*350*	7.02	*420.00*	*170.00*
R10	355.01	109.06	4.21	0.95	1.49	20.72	58.88	2.33	1.77	*370*	8.03	*400.00*	*160.00*
R11	360.29	110.68	5.83	0.89	1.36	21.15	59.08	2.39	0.53	*340*	9.79	*570.00*	*140.00*
R12	362.93	111.49	6.64	0.95	1.40	20.61	60.25	2.91	0.39	*320*	10.26	*490.00*	*140.00*
R13	364.91	112.10	7.25	0.89	1.18	20.46	59.18	2.80	1.38	*300*	6.60	*540.00*	*150.00*
R14	366.89	112.71	7.86	0.82	1.24	20.77	60.59	2.79	0.65	*230*	7.49	*550.00*	*140.00*
R15	368.21	113.11	8.26	0.70	1.30	20.66	58.50	2.76	0.38	*310*	10.80	*500.00*	*170.00*
R16	370.49	113.81	8.96	1.02	1.48	20.58	61.40	3.51	0.34	*260*	7.11	*670.00*	*140.00*
R17	371.51	114.13	9.28	0.92	1.19	19.15	62.73	2.94	0.32	0.11	6.81	*700.00*	*130.00*

RK2552

molecular ratios

depth (m)	SiO_2 / Al_2O_3	SiO_2 / Fe_2O_3	Ba / Sr	Al_2O_3 / $CaO+MgO+Na_2O+K_2O$	Fe_2O_3+MnO / Al_2O_3	$CaO+MgO$ / Al_2O_3
0.15	5.63	25.38	1.17	1.92	0.23	0.24
0.36	5.44	28.79	0.73	2.00	0.19	0.24
0.76	5.67	31.27	1.79	0.90	0.19	0.86
1.17	5.42	18.50	2.38	1.14	0.30	0.61
1.98	5.32	22.49	1.76	1.02	0.24	0.72
2.59	5.26	18.48	1.62	0.90	0.29	0.87
2.79	5.07	19.87	1.32	0.85	0.26	0.95
3.40	4.98	20.57	1.56	1.01	0.25	0.78
4.01	4.92	21.74	1.60	1.31	0.23	0.55
4.21	4.83	19.49	1.66	1.87	0.25	0.34
5.83	4.74	16.05	2.58	2.50	0.30	0.21
6.64	4.94	15.54	2.26	2.30	0.32	0.21
7.25	4.98	24.19	2.34	2.05	0.21	0.27
7.86	4.90	21.29	2.57	2.39	0.23	0.21
8.26	4.93	14.77	1.87	2.54	0.34	0.19
8.96	4.95	22.43	3.00	2.09	0.22	0.21
9.28	5.32	23.42	3.35	2.31	0.24	0.19

Core #	Smple	Depth (m)	Ca/Sr
2402		0.13	41.0015
2405		0.16	47.3755
2432		0.06	52.3415
2408		0.18	29.3732
		0.58	31.3506
2428		0.08	31.9285
		0.29	11.3677
2552		0.15	20.2849
		0.36	9.0815

APPENDIX C

CORE LOCATIONS, COAL THICKNESS, AND CUMULATIVE THICKNESS OF LOW-CHROMA UNITS AS PERCENTAGE OF TOTAL PROFILE THICKNESS (%LC)

NOTE

1. For sample identification with respect to geographic location, paleosol, and profile unit (i.e., horizon) the following alpha-numeric code is used. For exmaple:

(location)	(paleosol)	(profile unit)
2432	RK	2

refers core 2432, RK refers to the sub-Ames paleosol, and 2 refers to unit 2 in the profile. Other paleosol symbols include;

BC = sub-Brush Creek paleosol, and
PV = sub-Portersville paleosol.

core no.	UTM coordinates x	y	coal*** thknss	%lc	lithology**
705	523646	4447570	0	*	o
706	520616	4444200	0	*	o
2071	500275	4420920	0	*	o
2072	506038	4429020	0	*	o
2073	484330	4417970	0	*	o
2074	511049	4427710	0	*	o
2173	498540	4385800	20	45	c
2174	489550	4391750	0	55	s
2175	488350	4407300	0	11	lm
2176	456560	4382780	45	82	c
2177	444710	4402100	0	98	s
2178	445110	4386150	0	*	lm
2179	475250	4399600	0	17	lm
2181	467200	4380800	0	36	s
2197	483200	4372010	0	42	s
2386	471120	4379790	0	52	s
2387	472100	4384080	0	24	lm
2388	474050	4383150	0	58	s
2401	455820	4377820	0	100	s
2402	453720	4389820	31	67	c
2403	456050	4396130	0	45	s
2404	470330	4391670	47	100	c
2405	469400	4395340	33	72	c
2406	463370	4402720	15	68	c
2407	467590	4402110	0	21	lm
2408	473410	4404210	0	37	lm
2409	479150	4403020	0	12	s
2410	479360	4410180	28	91	c
2411	475420	4412060	0	9	lm
2412	470000	4410000	0	41	s

average %lc relative to lithology of overlying strata

lmst	sh	coal	
11	55	45	
17	98	82	
24	36	67	
21	42	100	
37	52	72	
9	58	68	
12	100	91	
56	45	72	
8	12	38	
34	41	82	
3	44	61	
42	36	100	
13	11		
26	41		
15	90		
	49		
	46		
n=15	n=17	n=12	
21.87	50.35	73.17	mean %lc
14.75	25.19	19.45	s.d.

core no.	UTM coordinates x	y	coal*** thknss	%lc	lithology**
2413	464280	4407400	0	12	lm
2418	473720	4417590	0	44	s
2419	479840	4417610	0	36	s
2420	487020	4415700	0	56	lm
2421	498360	4407630	0	11	s
2422	490820	4420260	0	8	lm
2423	482030	4424110	0	34	lm
2425	494840	4426320	0	3	lm
2426	506430	4417490	0	41	s
2427	468530	4414320	0	42	lm
2428	449350	4394230	0	90	s
2429	457300	4403430	31	72	c
2430	509110	4400400	0	49	s
2431	503240	4493640	13	38	c
2432	497090	4394000	23	82	c
2551	486450	4432020	0	13	lm
2552	499200	4431200	0	26	lm
2553	480740	4437040	47	61	c
2554	511890	4412720	0	46	s
2559	487630	4438820	0	15	lm
2562	513307	4437920	26	100	c
2622	502788	4401760	0	*	o
				n=44	
				47	mean % lc
				28.63	s.d.

*** core descriptions not sufficient to permit calculation of %lc**

**** o=other, c=coal, s=shale, lm=limestone**

***** coal thickness in centimeters**

VITA

Michael R. Caudill was born in Louisa, Kentucky on March 17, 1953. He graduated from Fort Gay High School in Fort Gay, West Virginia in May of 1971. He entered Marshall University in the Fall of 1977 and graduate in May, 1982 (B.Sc. Geology). In September, 1983, he entered Ohio University. His thesis research focused on the sedimentology and provenance of Pennsylvanian-age strata in southeastern New Brunswick, Canada. In September, 1985, before completing his Master's degree, Michael was employed as a Project Geologist by the Ohio Geological Survey and conducted detailed field mapping in the Ohio coal fields. He remained at the Ohio Survey until the summer of 1991, during which time he completed his Master's degree in Geology in December 1989. He entered the Ph.D. program in the Fall of 1991.

APPENDICES

APPENDIX A

MACROMORPHOLOGICAL DESCRIPTIONS OF PALEOSOLS

NOTE

1. Paleosols profile units (i.e., horizons) are given in descending order as is the practice for describing profiles of modern soils.

2. Palesols are referred to using the following code:

(drill core)(paleosol)
2432 RK

refers drill core 2432, and RK refers to the sub-Ames paleosol. Other paleosol symbols include;

BC = sub-Brush Creek paleosol, and
PV = sub-Portersville paleosol.

Drill core numbers are the core record file numbers of the Ohio Geological Survey.

3. Profiles are described according to the approach of Retallack (1988); (see following pages). Colors refer to moistened state.

Suggested Format for Description of Paleosols

+0 cm, ... (description of sediment overlying paleosol, using format below) ..... contact to

-0 cm, ... (description of topmost horizon of paleosol, using format below) ..... contact to

-(depth to top of horizon) cm; horizon designation (Table 1); rock type (e.g., claystone, siltstone); fresh Munsell color of whole horizon and of special features; weathered Munsell color; nature of root traces (Fig. 1), soil structure (Fig. 9), or other features (Tables 4, 7); reaction with dilute acid (Table 2); mineralogy and microfabric (to be considerably amplified following laboratory work); nature of contact (Table 3) to

-(depth to top of horizon) cm, horizon designation .....

Note: Examples of this kind of description are given in Retallack (1983b). Usually they are published as a sentence fragments connected by colons and semicolons, but I find it best in the field to write longhand paragraphs on each horizon, discussing field interpretations and subsequent efforts to test them.

Terminology for Description of Various Features of Paleosols

SIZE, ABUNDANCE, AND CONTRAST OF MOTTLES IN PALEOSOLS

Category	Class	Features
Contrast	Faint	Indistinct mottles or glaebules visible only on close examination: both mottles and matrix have closely related hues and chromas
	Distinct	Mottles are readily seen, with hue, value, and chroma different from that of surrounding matrix
	Prominent	Mottles are obvious and form one of the outstanding features of the horizon; their hue, value, and chroma differing from that of the matrix by as much as several Munsell color units
Abundance	Few	Mottles occupy less than 2% of the exposed surface
	Common	Mottles occupy about 2 to 20% of the exposed surface
	Many	Mottles occupy more than 20% of the exposed surface. This class can be subdivided according to whether (a) the mottles are set in a definite matrix, or (b) the sample is almost equally two or more kinds of mottle
Size	Fine	Mottles less than 5 mm diameter in greatest visible dimension
	Medium	Mottles between 5 and 15 mm in greatest dimension
	Coarse	Mottles greater than 15 mm in greatest dimension

SCALE OF ACID REACTION TO APPROXIMATE CARBONATE CONTENT OF PALEOSOLS

Carbonate Content	Reaction with Dilute Acid
Noncalcareous	Acid unreactive; often forms an inert bead
Very weakly calcareous	Little movement within the acid drop, which could be flotation of dust particles as much as bubbles
Calcareous	Numerous bubbles, but not coalescing to form a froth
Strongly calcareous	Bubbles forming a white froth, but drop of acid not doming upward
Very strongly calcareous	Drop vigorously frothing and doming upward

SHARPNESS AND LATERAL CONTINUITY OF PALEOSOL HORIZON BOUNDARIES

Category	Class	Features
Sharpness	Abrupt	Transition from one horizon to another completed within 1 in (2cm)
	Clear	Transition completed within 1-2.5 in (2-5 cm)
	Gradual	Transition spread over 2.5-5 in (5-15 cm)
	Diffuse	One horizon grading into another over more than 5 in (15 cm)
Lateral Continuity	Smooth	Horizon boundary forms an even plane
	Wavy	Horizon boundary undulates, with pockets wider than deep
	Irregular	Horizon boundary undulates, with pockets deeper than wide
	Broken	Parts of the adjacent horizon are disconnected, e.g., by deep and laterally persistent clastic dikes in Vertisols

PALEOSOL: 2432RK

Location: Monroe Cty, OH; Green Twp.; SW1/4, NE1/4, NE1/4, SEC. 1; Antioch 71/2' quad; UTM COORD. zone 17, X=497,091E Y= 4,394,000N

UNIT	THK.(m)	DPTH(m)	DESCRIPTIONS
1	0.92	0.92	mudstone; N2, gray black; weak, granular; abundant large, black, carbonized plant fossils; very weakly calcareous; clear.
2	1.01	1.93	mudstone; 5Y3/1, dark, olive-gray; weak, medium, blocky; few, large, ; few, fine, sub-vertical, carbonized root traces, some are present on slickenside planes; few, medium, irregularly-shaped, 5YR3/2, grayish brown, mottles with diffuse margins; common carbonate nodules, 1-5mm diameter; calcareous; gradual.
3	0.81	2.74	mudstone; 5Y4/1, olive gray: weak, medium blocky; common, large, slickensides with very thin calcite fill and few, carbonized root traces on slickenside surfaces ; few, large, vertical, 5Y2/1, olive black, mottles with sharp margins (appear to be cracks or root channels); common carbonate nodules,1-5mm diameter; calcareous; gradual.
4	1.51	4.25	mudstone; 5G4/1, dark, greenisk gray; weak, medium, blocky; common, large, slickensides; few, large, vertical, 10R3/2, very dark reddish brown mottles with sharp margins (filled cracks?); common,small to large (1 to 30mm) carbonate nodules, some large ones have vertical habit and contain clay-filled root channels; calcareous; gradual.
5	1.12	5.37	mudstone; 5GY5/1; greenish gray; weak, medium, blocky; many, large slickensides some are calcite-filled and some with few, fine, carbonized root traces on surfaces; many, large, irregularly-shaped, 10R3/4, dark, reddish brown, sub-vertical mottles some contain fine and medium, 5GY6/1, greenish gray, vermicular mottles (roots); few, carbonate nodules 1 to 5mm diameter; weakly calcareous, gradual.

PALEOSOL: 2432RK (cont'd)

UNIT	THK.(m)	DPTH(m)	DESCRIPTIONS
6	0.68	6.05	mudstone; 10R3/4, dark reddish brown; coarse, moderate, blocky; common, large, slickensides some with metallic (Mn?) coating on surfaces; common, fine, 5GY5/1, greenish gray, vermicular, mottles (root channels and interpedal pores); few, medium, irregular, 5GY5/1, greenish gray mottles with diffuse margins; few, carbonate nodules 1 to 3mm diameter; weakly calcareous; gradual.
7	0.54	6.59	mudstone; 10R3/2, very dark reddish brown; few, large, slickensides; few, large, irregular 5GY5/1, greenish gray mottles with diffuse margins, common, fine and medium, vertical 5Y5/6 light, olive brown mottles (after roots?), and many, medium, irregular 5Y5/6 mottles with diffuse margins; abundant spherulitic siderite; weakly calcareous; gradual.
8	1.78	8.37	mudstone; 10R3/4,dark reddish brown; weak, coarse, blocky; common, large, slickensides; many, large, irregular, 5GY5/1,greenish gray mottles with diffuse margins; common carbonate nodules 5 to 10mm diameter and few stacked carbonate nodules 30 to 50mm diameter (rhizocretions); weakly calcareous; gradual.
9	1.95	10.32	mudstone; 5GY5/1; greenish gray; weak, medium, blocky; common, large slickensides; many, tuberous, stacked carbonate nodules 20 to 30mm diameter (rhizocretions); non-calcareous; clear.
10	1.00	11.32	mudstone; 5RP3/2, dusky red purple; weak, medium, blocky; few, large slickensides; common, large, irregular, 5GY4/1 dark greenish gray mottles with diffuse margins, and common, fine and medium, vertical, 10YR6/6 dark yellowish orange mottles that surround fine, vertical, 5G6/1 greenish gray mottles (root traces); common, carbonate nodules 1 to 5mm diameter; weakly calcareous; clear.

PALEOSOL: 2432RK (cont'd)

UNIT	THK.(m)	DPTH(m)	DESCRIPTIONS
11	1.52	12.84	shale, very silty; 5GY5/1, greenish gray; many, large, contorted veins filled with carbonate (give brecciated appearence, especially in lower 0.15m); weakly calcareous; abrupt.
12	0.15	12.99	shale; N3, dark gray; common, finely disseminated organics; non-calcareous; sharp.

PALEOSOL: 2402RK

Location: Noble Cty, OH; Jackson Twp.; SW1/4, SW1/4, SE1/4, SEC. 4; Caldwell South 71/2' quad; UTM COORD. zone 17, X=453,716E Y= 4,389,823N

UNIT	THK.(m)	DPTH(m)	DESCRIPTIONS
1	0.26	0.26	mudstone; N3, dark gray; weak, fine, granular; few, small, slickensides; common, fine and medium, black, carbonized, horizontal root traces; calcareous; clear.
2	0.23	0.49	mudstone; 5Y4/1, olive gray; weak, medium, blocky; rare, large, slickensides; rare, fine, dessiminated, coaly organics; few, small patches of fine pyrite grains; few, small (<1mm)carbonatenodules; calcareous; gradual.
3	0.77	1.26	mudstone; same as above, except contains few, small (<1mm) siderite(?) nodules.
4	0.84	2.10	mudstone; 5Y4/1, olive gray; weak, medium, blocky; few, large, slickensides; few, vertical, carbonized, root traces; few, small patches of fine pyrite grains, associated with carbonized root traces; few, carbonate nodules, 0.5 to 3mm diameter; calcareous; gradual.
5	1.95	4.05	mudstone; 5Y4/1, olive gray; weak, medium, blocky; few, large, slickensides; few, small patches of fine pyrite grains, and few, medium, vertical, vein-like features (root channels?) with common, fine grains of pyrite; calcareous; gradual.
6	0.88	4.93	mudstone; 5Y4/1, olive gray; weak, medium, blocky; common, large, slickensides; rare, small patches of fine pyrite grains; few, carbonate nodules 0.1 to 1.0mm diameter; calcaroeus; gradual.
7	0.78	5.71	mudstone; 10R2/4, very dark reddish brown; moderate, medium, blocky; common, large, slickensides; many, large, 5GY5/1, greenish gray, mottles, some are vertical; few, medium, 5RP4/2, grayish red purple mottles; common; carbonate nodules, 0.2 to 1.0mm diameter; calcareous; gradual.

PALEOSOL: 2402RK (cont'd)

UNIT	THK.(m)	DPTH(m)	DESCRIPTIONS
8	1.66	7.37	mudstone; 10R3/4, dark reddish brown; moderate, medium, blocky; common, large, slickensides; common, medium, sub-vertical, vermicular, 5GY6/1, greenish gray mottles (after roots or cutans); few, fine, irregular, 10YR6/6, dark yellowish orange mottles; few, carbonate nodules, 0.2 to 0.5mm diameter; calcareous; gradual.
9	0.69	8.06	shale; 5RP2/2, very dusky red purple; common, coarse, patchy, horizontal, 5G6/1, greenish gray mottles (may follow horizontal burrows); few, brachiopod fossils, *Lingula and Mesolobus*; calcareous; abrupt.

PALEOSOL: 2405RK

Location: Noble Cty, OH; Stock Twp.; NW1/4, NE1/4, SE1/4, SEC. 13; Stafford 71/2' quad; UTM COORD. zone 17, X=469,396E Y= 4,395,343N

UNIT	THK.(m)	DPTH(m)	DESCRIPTIONS
1	0.48	0.48	mudstone; 5Y3/1, dark olive gray; weak, medium, granular; common, medium, horizontal, carbonized root traces; non-calcareous; contact gradual.
2	1.40	1.88	mudstone; 5GY4/1, dark greenish gray; weak medium blocky; few, large slickensides; common, carbonate nodules 1 to 20mm; weakly calcareous; gradual.
3	0.57	2.45	mudstone; 5Y4/1, olive gray; very, hard, and dense (carbonate cemented); few ostracodes; strongly calcareous; gradual.
4	0.46	2.91	limestone; very argillaceous;10Y5/2, light grayish olive; common, ostracodes; many ganules of carbonate and mudstone; clear.
5	0.78	3.69	mudstone; same as in unit 3.
6	3.59	7.28	mudstone; 5GY3/2, grayish olive green; common, large slickensides some with thin sheets of calcite on surface; few carbonate nodules 1 to 15mm diameter; calcareous; gradual.
7	1.41	8.69	mudtone; 5GY3/2, grayish olive green; few, large slickensides; few, large, vertical, 10R2/2, very dusky red mottles with diffuse margins; few large, vertical, 5Y5/1, olive gray mottles following root channels; few, carbonate nodules 5 to 10mm diameter; weakly calcareous; gradual.
8	1.70	10.39	mudstone; 5R4/3, grayish red; moderate, medium, blocky; common, large slickensides, surfaces have strongly metallic, polished appearance; few, large, vertical, 10YR6/6, dark yellowish orange mottles filling interpedal pores; few, medium, irregular, N5, medium gray mottles; few, medium, 5GY5/1, greenish gray

PALEOSOL: 2405RK (cont'd)

UNIT	THK.(m)	DPTH(m)	DESCRIPTIONS
8 (cont'd)			mottles after root channels; few, carbonate nodules 5 to 10mm diameter; weakly calcareous; gradual.
9	1.65	12.04	mudstone; 5Y4/1, olive gray; strong, medium blocky; few, large slickensides; common, medium, 5R4/3, grayish red mottles filling interpedal pores; non-calcareous; gradual.
10	0.20	12.24	mudstone; 5G6/1, greenish gray; weak, medium, blocky; few, large slickensides; few, medium, irregular 10YR6/6, dark yellowish orange mottles; fine vein-like network of siderite(?); non-calcareous; clear.
11	0.43	12.67	mudstone; 5Y5/6, light olive brown; few, medium 5G6/1, geenish gray mottles with diffuse margins; few, medium, vermicular 5Y3/2 olive gray mottles after roots (?); common, spherulitic siderite; non-calcareous; gradual.
12	1.30	13.90	shale; silty with thin, discontinuous laminae of fine-grained sandstone; 5GY5/1, greenish gray; common, spherulitic siderite; non-calcareous; gradual.

PALEOSOL: 2408RK

Location: Monroe Cty, OH; Seneca Twp.; NW1/4, SE1/4, NW1/4, SEC. 19; Summerfield 71/2' quad; UTM COORD. zone 17, X=473,410E Y= 4,404,210N

UNIT	THK.(m)	DPTH(m)	DESCRIPTIONS
1	1.43	1.43	mudstone; 5Y4/1, olive gray; weak, medium blocky; few, large slickensides and few, small slickensides; distinct, common, fine and medium, 5Y5/6 light olive brown mottles, some sub-vertical, vermicular (after roots), also common, distinct, fine-medium, patchy, 5RP2/2, very dusky red purple mottles with diffuse margins; common, carbonate nodules (1-5mm); non-calcareous to calcareous downward; irregular, gradual.
2	0.88	2.31	mudstone; 10R3/4, dark reddish brown; moderate blocky; few, large slickensides and few, small slickensides; common, distinct, fine-medium, N3, medium dark gray mottles, and common, fine, 5R3/6, dark red, sub-vertical, vermicular mottles (after roots), and few, distinct, fine-medium, circular, 5Y5/6, light olive brown mottles with diffuse margins; common, carbonate nodules (1-10mm), smaller ones more abundant; calcareous; clear.
3	1.77	4.08	mudstone; 5Y3/1, dark olive gray; weak blocky; common, large, slickensides; many, distinct, medium-course, sub-vertical, 10R3/3, dark reddish mottles surrounding few, distinct, fine, vermicular, 5Y2/1, olive black mottles (after roots); few, carbonate nodules (1-15mm), some septarian, all sub-spherical with sharp margins; weakly calcareous; gradual.
4	1.41	5.49	mudstone; 5R3/4, dusky red; moderate blocky; few, large slickensides and few, small slickensides; common, distinct, fine, some vermicular, 5GY6/1, greenish gray mottles, and few, distinct, medium, 5G4/1, dark greenish gray, mottles with diffuse margins, and few, distinct, fine 5Y5/6, light olive brown mottles; few, sub-spherical carbonate nodules (1-5mm) in upper part; slightly calcareous to non-calcareous downward; clear.

PALEOSOL: 2408RK (cont'd)

UNIT	THK.(m)	DPTH(m)	DESCRIPTIONS
5 0.14	5.63		mudstone; 5G2/1, greenish black; fine, granular; few, large slickensides; common, faint, medium, 5Y5/1, olive gray mottles in upper part, and few, distinct, course, 5R2/6, very dusky red mottles, and few, distinct, fine, 5Y5/6, light olive brown mottles (geothite-rich) surrounding fine peds; very slightly calcareous; clear.
6	1.58	7.21	mudstone; 5R3/4, dusky red; few, large slickensides, few, small slickensides; moderate blocky; common, distinct, fine, 5Y5/6, light olive brown mottles surrounding peds, and common, distinct, fine-medium, 5G6/1, greenish gray, sub-vertical, vermicular mottles after roots and surrounding some peds; few, carbonate nodules (1-5mm); weakly calcareous; clear.
7	0.09	7.30	mudstone; 5G4/1, dark greenish gray; weak granular; common, faint, fine, subhorizontal, vermicular, 5GY6/1 mottles after roots; rare, carbonate nodules (1-5mm); weakly calcareous; clear.
8	0.90	8.23	mudstone; 10R2/4, very dusky reddish brown; few, large slickensides; moderate blocky; many, distinct, medium, sub-vertical, 5Y2/1, olive black mottles with diffuse margins, some contain faint, fine, vermicular, 5Y5/1, medium olive gray mottles after roots; rare carbonate nodules (1-5mm); calcareous; gradual.
9	1.09	9.32	mudstone; 10R2/4, very dusky reddish brown; weak blocky to moderate platy; few, large slickensides and in lower part common small slickensides; common, distinct, fine, 5Y5/6, light olive brown (goethite-rich) mottles, and few, distinct, fine-medium, 5Y6/1, light olive gray mottles surrounding peds; weakly calcareous; gradual.
10	0.77	10.09	shale; 5R3/4, dusky red; fissile; common, 5Y4/1, olive gray, horizontal mottles after burrows; non-calcareous; contact gradational.

PALEOSOL: 2428RK

Location: Noble Cty, OH; Sharon Twp.; SE1/4, NW1/4, SE1/4, SEC. 24; Caldwell South 71/2' quad; UTM COORD. zone 17, X=449,351E Y= 4,394,229N

UNIT	THK.(m)	DPTH(m)	DESCRIPTIONS
1	0.42	0.42	mudstone; 5Y5/1, medium olive gray; weak blocky; few, large slickensides and few small slickensides; thin zone with many, distinct, medium, 5RP2/2, very dusky red mottles surrounded by 5Y5/6, light olive brown mottles (define fine blocky peds), also common, distinct, fine, sub-vertical, vermicular, 5Y5/6, light olive brown mottles after roots (in lower half); non-calcareous; clear.
2	0.24	0.66	mudstone; 5GY4/1, dark, greenish gray; weak blocky; few, large slickensides; few, distinct, fine, 5Y5/6, light olive brown, sub-vertical mottles after roots; very slightly calcareous; clear.
3	0.35	1.01	mudstone; 5Y4/2, medium olive gray; weak blocky; common, distinct, fine, vermicular, 5Y5/6, light olive brown, sub-vertical mottles after roots; common, carbonate nodules (0.5-5mm); calcareous; gradual.
4	0.39	1.40	mudstone; 5GY4/1, dark, greenish gray; weak blocky; few, carbonate nodules (2-7mm); very fine-grain, disseminated pyrite common; calcareous; gradual.
5	2.85	4.25	mudstone; N4, medium dark gray; few, large slickensides and few, small slickensides; weak blocky; many, distinct, fine and medium, 10R2/, dark reddish brown, mottles with sharp margins the surround peds and follow root traces; few, sub-spherical, carbonate nodules (5-15mm), calcareous; gradual.
6	0.75	5.00	mudstone; 5Y3/4, moderate brown; few large slickensides; weak blocky; common, distinct, fine, 5Y6/1, medium olive gray mottles, some are sub-vertical and branching, after roots; common, tuberous, carbonate nodules (2-10mm); non-calcareous; gradual.

PALEOSOL: 2428RK (cont'd)

UNIT	THK.(m)	DPTH(m)	DESCRIPTIONS
7	0.69	5.69	mudstone; 5GY6/1, greenish gray; few large slickensides; very weak blocky; common, distinct, medium-coarse, 10R3/4, dark reddish brown, sub-vertical mottles with diffuse margins, some contain, few, distinct, fine vermicular, 5Y5/1, medium olive gray mottles after roots; few, large, irregular-shaped, carbonate nodules (15-40mm); non-calcareous; gradual.
8	1.08	6.77	mudstone; 5YR3/2, grayish brown; common, large slickensides with metallic shine on surface; moderate blocky to platy near base; common, distinct, fine-medium, 10R2/4, reddish brown mottles; rare, elongate, vertical, carbonate nodules (rhizocretions); weakly calcareous; clear.
9	0.64	7.41	shale; N3, dark gray; fissile; common, faint, fine-medium, horizontal, 5GY5/1 medium greenish gray mottles after burrows; calcareous; clear.

PALEOSOL: 2552RK

Location: Belmont Cty, OH; Goshen Twp.; SW1/4, NE1/4, NE1/4, SEC. 6; Bethesda 71/2' quad; UTM COORD. zone 17, X=499,200E Y= 4,431,200N

UNIT	THK.(m)	DPTH(m)	DESCRIPTIONS
1	0.22	0.22	mudstone; 10Y6/2, pale olive; weak blocky; rare large and small slickensides; common, distinct, fine-medium, N3, dark gray mottles after roots, and common, distinct, coarse, 5Y5/6, light olive gray mottles after roots surrounded by 5RP4/2, grayish red purple mottles with diffuse margins; very weakly calcareous; clear.
2	0.29	0.51	mudstone; 5G5/1, medium greenish black; weak blocky; few, large slickensides; few, distinct, fine, sub-vertical, vermicular 5Y2/1 mottles after roots, and few, distinct, fine, sub-vertical, vermicular 5Y5/6 mottles after roots; non-calcareous; clear.
3	0.22	0.73	mudstone; 10R3/4, dusky red; few, large slickensides; weak blocky; few, distinct, fine, sub-vertical, vermicular, 5GY6/1, greenish gray mottles, and few, distinct, fine, sub-vertical, vermicular 5Y5/6 mottles, both after roots; few, small (1-5mm) carbonate nodules; very weakly calcareous; gradual.
4	0.39	1.12	mudstone; 5GY4/1, dark greenish gray; few, large slickensides; weak blocky; many, faint, medium, 5GY6/1, greenish gray mottles with diffuse margins; few, carbonate nodules (1-5mm); slightly calcareous, clear.
5	2.45	3.56	mudstone; 10R3/4, dark reddish brown; few large slickensides; weak blocky; common, distinct, fine-medium, sub-vertical, 5G6/1, greenish black mottles after roots, and few, distinct, coarse, 5G6/1, greenish black, patchy mottles; many, small (1-5mm) carbonate nodules, and few, large (10-20mm) carbonate nodules, and few , large (30-50mm) carbonate nodules with slickensides margins; weakly calcareous; gradual, diffuse.

PALEOSOL: 2552RK (cont'd)

UNIT	THK.(m)	DPTH(m)	DESCRIPTIONS
6	2.00	5.56	mudstone; 5R3/4, dusky red; few large slickensides; weak blocky; common, distinct, medium-coarse, sub-vertical, 5Y6/1, light olive gray mottles with diffuse margins (roots?); few, large (20-50mm), sub-spherical, septarian carbonate nodules, and few zones with common, small (1-5mm) carbonate nodules; isolated, sub-vertical vein filled with carbonate; weakly calcareous; diffuse.
7	2.3	7.86	mudstone; 10R3/4, dark reddish brown; common, large slickensides; weak blocky; common, distinct, fine, sub-vertical, branching, vermicular 5Y5/6, light olive brown mottles, and few, distinct, fine, vermicular, 5GY5/1, greenish gray mottles, both after roots and surrounding peds; few, small (1-5mm) and few medium (5-10mm) carbonate nodules, also rare, sub-vertical vein filled with carbonate; non-calcareous; gradual.
8	0.28	8.14	mudstone; 5Y4/1, olive gray; few large slickensides; common, faint, fine, 5GY6/1, greenish gray mottles with diffuse margins, and many, prominent, coarse, 10R3/4, dark reddish brown with diffuse margins; non-calcareous; clear.
9	0.54	8.68	mudstone; 10R2/2, very dusky red; weak granular; few large slickensides; few, distinct, fine, 5GY6/1 greenish gray mottles surrounding fine peds; few, small (1-5mm) carbonate nodules; weakly calcareous; clear.
10	0.49	9.17	mudstone; 5GY5/1, medium greenish gray; few, large slickensides; common, distinct, sun-vertical, 10R3/4, dark reddish brown mottles after roots; non-calcareous; gradual.
11	1.0	10.17	shale, silty; 5GY5/1, medium greenish gray; scattered zones of spherulitic siderite; non-calcareous; gradual.

PALEOSOL: 2422PV

Location: Belmont Cty, OH; Wayne Twp.; NW1/4, NW1/4, NW1/4, SEC. 29; Hunter 71/2' quad; UTM COORD. zone 17, X=449,351E Y= 4,394,229N

UNIT	THK.(m)	DPTH(m)	DESCRIPTIONS
1	0.12	0.12	mudstone; N3, dark gray; weak crumb; few small slickensides; common, fine, carbonized roots; common, very fine-grain, disseminated organic matter; few, thin, coaly laminations; non-calcareous; clear.
2	0.67	0.79	mudstone; 5Y6/1, light olive gray; weak granular; few, prominent, branching, horizontal, carbonized roots; few, small patches of fine-grain pyrite; very weakly calcareous; clear.
3	0.84	1.63	mudstone; 5Y4/1, olive gray; weak blocky; common, large slickensides; common to many, small to large (1-50mm), carbonate nodules, large ones are tuberous, complex, and septarian; few, small patches of fine-grained pyrite; calcareous; gradual.
4	0.66	2.29	mudstone; 5GY5/1, greenish gray; weak blocky; common, large slickensides, some with thin coating of carbonate; common to many, small to large (1-50mm), carbonate nodules, large ones are tuberous, complex, and septarian; few, small patches of fine-grained pyrite; calcareous; clear.
5	0.32	2.61	mudstone; 10R3/4, dark reddish brown; moderate blocky; common, large slickensides; few, distinct, 5GY5/1, greenish gray, vertical mottles after roots; common, medium (5-15mm) carbonate nodules, some with stacked vertical form (rhizocretions) and clay-filled root channels; calcareous; clear.
6	0.20	2.81	sandstone; medium-grain; argillaceous; 5GY5/1, greenish gray; 5cm layer at top very argillaceous; few, vertical, root channels filled with clay; calcareous; abrupt.

PALEOSOL: 2422PV (cont'd)

UNIT	THK.(m)	DPTH(m)	DESCRIPTIONS
7	0.31	3.12	mudstone; 5GY5/1, greenish gray; weak blocky; few, large slickensides; few, prominent, medium, irregular-shaped, 10R3/4, dark reddish brown mottles with indistinct margins; few, vertical cracks (30-50mm long and <2mm wide), filled with silt and very fine-grain sand; weakly calcareous; gradual.
8	0.32	2.43	mudstone; 10R3/4, dark red brown; weak blocky; few large slickensides; few, prominent, fine, 5GY5/1, greenish gray, vertical mottles after roots, some preserve organic matter; common, distinct, fine, 5Y4/1, olive gray mottles surrounding peds; very weakly calcareous; gradual.
9	0.43	2.86	mudstone; 10R3/4, dark red brown; medium platy; few, prominent, medium, irregular-shaped mottles surrounding peds; few, vertical root channels filled with red clay, disrupt general fabric; non-calcareous; gradual.
10	0.53	3.39	shale; 5R3/4, dusky red; fissile; non-calcareous; gradual.

PALEOSOL: 2552BC

Location: Belmont Cty, OH; Goshen Twp.; SW1/4, NE1/4, NE1/4, SEC. 6; Bethesda 71/2' quad; UTM COORD. zone 17, X=499,200E Y= 4,431,200N

UNIT	THK.(m)	DPTH(m)	DESCRIPTIONS
1	0.36	0.36	mudstone; 5GY4/1, dark greenish gray; weak granular; rare, large slickensides; few, carbonized, sub-horizontal root traces; non-calcareous; gradual.
2	1.81	2.17	mudstone; 5GY4/1, dark greenish gray; weak blocky; common, large slickensides; common, tuberous, small to medium (1-15mm) carbonate nodules; rare, vertical, cracks; calcareous; gradual.
3	0.55	2.72	mudstone; 5Y5/1, olive gray; strong blocky; common, large slickensides; common, 5Y3/1, dark olive gray mottles surrounding some peds; few, medium, sub-vertical, carbonized roots near base of unit; calcareous; clear.
4	0.25	2.97	mudstone; carbonaceous; 5Y2/1, olive black; weak blocky; few, small slickensides; few, faint, fine, 5Y4/1, olive gray mottles surrounding some peds; scattered fine-grain organic matter; weakly calcareous; gradual.
5	0.58	3.55	mudstone; 5Y4/1, olive gray; weak blocky; few, large slickensides; weakly calcareous; clear.
6	1.10	4.65	shale; 5GY5/1, greenish gray; sandy; few, 5Y2/1, olive black ,vertical, mottles after root channels filled with clay; common, large patches of net-like veins of carbonate; variably brecciated in lower part with ptygmatically folded cracks.

APPENDIX B

GEOCHEMICAL DATA

RK2402

smpl	depth in core (feet)	depth in core (meters)	depth from top of psol (meters)	Na2O	MgO	Al2O3	SiO2	K2O	CaO	MnO	Fe2O3	Ba	Sr
				weight percent and ppm (ppm in italics)									
R1	238.40	73.24	0.13	1.39	1.89	18.18	63.67	2.90	0.55	*290*	4.26	*500*	*210*
RA	238.55	73.28	0.17	1.05	4.58	13.09	42.51	2.32	13.57	0.13	4.34	*400*	*380*
RB	238.90	73.39	0.28	0.79	5.13	11.77	37.06	2.00	17.32	0.14	3.57	*410*	*410*
R2	239.20	73.48	0.37	0.62	3.45	10.22	31.54	1.39	25.29	0.19	2.92	*250*	*380*
R3	241.00	74.04	0.93	0.98	6.08	9.96	34.63	1.68	19.26	0.15	3.55	*280*	**490*
R4	244.00	74.96	1.85	1.04	5.99	9.96	34.63	1.68	17.30	0.16	3.99	*310*	**490*
R5	248.00	76.19	3.08	0.99	6.09	11.04	36.40	1.99	16.68	0.18	4.43	*380*	**490*
R6	255.00	78.34	5.23	1.01	5.10	12.78	40.31	2.26	14.19	0.18	4.47	*360*	**420*
R7	255.50	78.49	5.38	0.82	2.77	16.23	47.10	2.21	10.54	0.10	4.65	*430*	*300*
R8	259.00	79.56	6.45	0.92	1.73	20.12	57.85	2.57	0.63	*290*	11.07	*440*	*190*
R9	263.30	80.89	7.78	0.83	1.56	20.87	56.62	3.47	1.15	*280*	8.68	*650*	*180*

depth (m)	SiO_2/Al_2O_3	SiO_2/Fe_2O_3	Ba/Sr	$Al_2O_3/(CaO+MgO+Na_2O+K_2O)$	$(Fe_2O_3+MnO)/Al_2O_3$	$(CaO+Mg)/Al_2O_3$
molecular ratios						
0.13	5.94	39.72	1.53	1.62	0.15	0.32
0.17	5.51	26.03	0.68	0.32	0.23	2.77
0.28	5.35	27.62	0.64	0.25	0.22	3.78
0.37	5.24	28.70	0.41	0.18	0.22	5.35
0.93	5.90	25.92	0.37	0.19	0.26	5.06
1.85	5.90	23.07	0.40	0.21	0.27	4.36
3.08	5.60	21.83	0.50	0.22	0.29	4.14
5.23	5.36	23.97	0.54	0.30	0.25	3.03
5.38	4.93	26.92	0.91	0.54	0.19	1.61
6.45	4.88	13.90	1.50	2.05	0.35	0.27
7.78	4.61	17.34	2.24	1.87	0.27	0.29

RK2405

smpl	depth in core		depth from top of psol		weight percent			and ppm (ppm in italics)					
	(feet)	(meters)	(meters)	Na2O	MgO	Al2O3	SiO2	K2O	CaO	MnO	Fe2O3	Ba	Sr
R1	121.60	37.36	0.16	1.40	1.87	18.50	60.64	3.10	0.81	*370*	5.27	*760*	*270*
R2	125.00	38.40	1.20	1.03	2.07	15.02	50.72	2.61	8.39	*610*	3.87	*600*	*310*
R3	128.55	39.49	2.29	2.21	1.45	5.50	18.99	1.03	36.60	0.14	2.29	*140*	*400*
R4	130.20	40.00	2.80	2.29	9.38	7.51	22.13	1.57	20.30	0.25	5.13	*300*	*490*
R5	132.40	40.67	3.47	0.94	6.28	11.98	37.71	2.46	13.54	0.15	4.89	*370*	**450*
R6A	138.00	42.39	5.19	0.89	4.74	13.59	43.02	2.82	11.43	0.13	4.54	*460*	*380*
R6B	142.80	43.87	6.67	0.98	2.62	16.70	49.27	3.44	7.87	0.10	4.82	*660*	*300*
R7	148.10	45.50	8.30	0.89	1.40	21.86	60.70	3.22	1.22	*150*	5.15	*700*	*370*
R8	152.40	46.82	9.62	0.89	1.38	20.89	59.45	2.99	0.27	*190*	8.70	*660*	*370*
R9	156.00	47.92	10.72	0.79	1.40	21.19	60.47	3.08	0.26	*120*	5.90	*690*	*270*
R11	157.90	48.51	11.31	0.74	1.38	19.88	60.02	2.76	0.13	*410*	11.01	*540*	*170*
R12	160.00	49.15	11.95	0.90	1.34	16.69	65.13	2.11	1.80	0.11	6.61	*490*	*140*

molecular ratios

	SiO_2	SiO_2	Ba	Al_2O_3	Fe_2O_3+MnO	CaO+Mg
depth (m)	Al_2O_3	Fe_2O_3	Sr	CaO+MgO+Na_2O+K_2O	Al_2O_3	Al_2O_3
0.16	5.56	30.59	1.83	1.56	0.19	0.33
1.20	5.73	34.81	1.22	0.60	0.17	1.36
2.29	5.86	22.00	0.22	0.07	0.31	12.76
2.80	5.00	11.47	0.39	0.11	0.50	8.07
3.47	5.35	20.51	0.52	0.27	0.28	3.38
5.19	5.01	27.19	1.39	0.64	0.19	1.25
6.67	4.71	31.34	1.20	2.04	0.15	0.26
8.30	4.83	18.17	1.57	2.40	0.27	0.19
9.62	4.84	27.24	1.64	2.46	0.18	0.19
10.72	5.13	14.50	2.10	2.50	0.36	0.19
11.31	6.11	24.13	2.19	1.60	0.27	0.40

RK2408

smpl	depth in core		depth from top of psol										
	(feet)	(meters)	(meters)	Na2O	MgO	Al2O3	SiO2	K2O	CaO	MnO	Fe2O3	Ba	Sr
R2A	290.82	89.34	0.18	1.20	1.90	18.72	63.75	2.92	0.47	*300*	7.24	*570*	*250*
R2B	292.12	89.74	0.58	1.09	1.93	18.60	61.67	2.76	0.50	*320*	8.41	*520*	*250*
R3	292.79	89.95	0.79	0.97	2.12	15.98	52.75	2.29	8.42	*560*	7.31	*490*	*290*
R3A	293.45	90.15	0.99	0.82	2.19	14.49	47.09	2.07	11.91	*600*	6.24	*360*	*280*
R3B	294.12	90.35	1.19	1.01	2.18	17.30	56.60	2.52	5.46	*430*	7.41	*410*	*270*
R4	296.75	91.16	2.00	0.94	2.12	17.68	55.06	2.52	5.30	*410*	8.21	*410*	*280*
R5	298.07	91.57	2.41	0.88	2.05	17.06	53.60	2.36	8.31	*510*	4.85	*410*	*300*
R6	300.71	92.38	3.22	1.14	1.95	19.35	56.64	2.19	3.73	*380*	6.38	*190*	*280*
R7	305.99	94.00	4.84	1.01	1.67	22.65	59.37	1.88	1.08	*190*	7.55	*470*	*240*
R8	310.61	95.42	6.26	0.98	1.54	18.80	59.24	3.02	0.34	*610*	12.70	*570*	*210*
R9	313.91	96.43	7.27	0.87	1.72	18.45	57.20	2.83	5.53	*460*	3.64	*500*	*280*
R10	315.89	97.04	7.88	1.01	1.66	19.08	59.85	3.18	2.94	*360*	7.36	*560*	*260*
R11	318.53	97.85	8.69	0.74	1.31	20.83	58.80	2.97	0.34	*420*	9.45	*630*	*230*
R12	321.17	98.66	9.50	0.95	1.58	21.11	58.84	3.14	0.32	*240*	9.33	*570*	*250*

RK2408

molecular ratios

depth (m)	SiO_2 / Al_2O_3	SiO_2 / Fe_2O_3	Ba / Sr	Al_2O_3 / $CaO+MgO+Na_2O+K_2O$	Fe_2O_3+MnO / Al_2O_3	$CaO+Mg$ / Al_2O_3
0.18	5.78	6.88	1.45	1.74	0.25	0.30
0.58	5.63	5.88	1.35	1.76	0.29	0.31
0.79	5.60	5.81	1.09	0.65	0.30	1.29
0.99	5.52	6.18	0.83	0.47	0.28	1.88
1.19	5.55	6.21	0.99	0.87	0.28	0.89
2.00	5.29	5.73	0.95	0.92	0.30	0.85
2.41	5.33	9.36	0.86	0.70	0.19	1.19
3.22	4.97	8.06	1.15	1.21	0.21	0.60
4.84	4.45	7.97	1.25	2.29	0.21	0.27
6.26	5.35	3.94	1.73	2.00	0.44	0.24
7.27	5.26	13.48	1.11	0.98	0.13	0.78
7.88	5.32	6.89	1.35	1.30	0.25	0.50
8.69	4.79	5.86	1.73	2.49	0.29	0.19

RK2428

smpl	depth in core		depth from top of psol			weight percent		and ppm (ppm in italics)					
	(feet)	(meters)	(meters)	Na2O	MgO	Al2O3	SiO2	K2O	CaO	MnO	Fe2O3	Ba	Sr
R2	233.18	71.63	0.08	1.15	1.30	18.54	66.91	3.33	0.34	*250*	3.35	*240*	*170*
R3	233.84	71.84	0.29	1.12	1.78	19.14	61.71	2.74	0.29	*300*	11.17	*450*	*600*
R3A	234.50	72.04	0.49	1.35	2.17	18.97	64.86	2.60	1.08	*250*	5.94	*410*	*200*
R4	235.16	72.24	0.69	1.32	2.05	18.78	64.13	3.00	0.64	*340*	7.67	*510*	*200*
R5	237.14	72.85	1.30	1.18	2.27	18.08	57.72	2.66	4.87	*450*	6.16	*490*	*220*
R6	239.12	73.46	1.91	1.04	2.16	18.13	58.02	2.98	5.62	*500*	5.35	*520*	*250*
R7	241.76	74.27	2.72	1.13	1.93	20.27	58.28	2.85	4.67	*390*	5.61	*470*	*230*
R8	243.74	74.88	3.33	0.97	1.98	18.08	54.47	2.58	5.83	*580*	9.34	*350*	*240*
R9	246.38	75.69	4.14	1.01	1.65	20.36	60.95	2.67	1.68	*280*	8.23	*480*	*200*
R10	248.36	76.30	4.75	0.91	1.70	16.50	49.41	2.08	11.29	*510*	6.14	*400*	*220*
R11	251.00	77.11	5.56	0.92	1.57	21.90	62.81	3.20	0.35	*230*	6.73	*180*	*170*
R12	252.32	77.51	5.96	1.10	1.62	20.42	61.14	3.26	3.26	*300*	11.04	*560*	*170*
R13	253.64	77.92	6.37	0.92	1.39	20.55	63.80	3.34	0.30	*170*	7.12	*530*	*200*
R14	254.83	78.28	6.73	1.25	2.06	18.08	63.10	3.53	0.49	*310*	8.52	*620*	*180*

RK2428

molecular ratios

depth (m)	SiO_2 / Al_2O_3	SiO_2 / Fe_2O_3	Ba / Sr	Al_2O_3 / $CaO+MgO+Na_2O+K_2O$	Fe_2O_3+MnO / Al_2O_3	CaO+Mg / Al_2O_3
0.08	6.13	14.73	0.90	1.97	0.12	0.21
0.29	5.47	4.56	0.72	1.94	0.38	0.26
0.49	5.81	8.49	1.33	1.52	0.20	0.39
0.69	5.80	6.51	1.59	1.59	0.26	0.34
1.30	5.42	7.80	1.46	0.93	0.22	0.81
1.91	5.43	9.01	1.33	0.88	0.19	0.86
2.72	4.88	9.61	1.28	1.11	0.18	0.66
3.33	5.12	5.14	0.94	0.90	0.34	0.86
4.14	5.08	6.58	1.58	1.73	0.26	0.35
4.75	5.09	7.14	1.15	0.58	0.24	1.51
5.56	4.87	8.65	0.68	2.29	0.20	0.21
5.96	5.08	4.92	2.14	1.33	0.35	0.49
6.37	5.27	7.68	1.72	2.23	0.22	0.20
6.73	5.93	5.64	2.26	1.51	0.30	0.34

RK2432

smpl #	depth in core		depth from top of psol		weight percent and ppm (ppm in italics)								
	(feet)	(meters)	(meters)	Na2O	MgO	Al2O3	SiO2	K2O	CaO	MnO	Fe2O3	Ba	Sr
R1	564.55	173.43	0.06	1.04	1.87	20.00	59.59	3.10	0.72	*210*	4.69	*680*	*210*
R2	566.70	174.09	0.72	0.70	2.42	14.07	43.50	1.84	14.70	*510*	3.98	*310*	*300*
R3	568.80	174.74	1.37	0.73	2.40	15.29	44.89	1.99	12.87	*630*	5.43	*380*	*220*
R4	573.20	176.09	2.72	0.77	2.48	17.00	46.78	2.07	10.88	0.10	7.37	*380*	*240*
R5	577.10	177.29	3.92	0.09	1.68	21.61	59.35	2.80	0.39	*200*	7.52	*460*	*200*
R6	580.65	178.38	5.01	0.93	1.33	21.03	57.76	3.44	0.31	*180*	9.14	*610*	*170*
R7	582.50	178.94	5.57	0.96	2.44	14.00	41.82	2.30	2.59	0.42	28.06	*500*	*150*
R8	584.50	179.56	6.19	0.64	1.52	17.46	50.54	2.91	8.40	*460*	4.30	*500*	*210*
R9	586.90	180.30	6.93	0.77	1.85	19.91	60.55	3.44	0.58	0.10	7.11	*670*	*160*
R10	590.50	181.40	8.03	0.90	1.64	17.49	50.33	3.66	5.57	*800*	8.21	*620*	*290*
R11	596.65	183.29	9.92	0.93	1.71	17.38	57.50	2.06	3.22	0.20	7.79	*130*	*210*

molecular ratios

depth (m)	$\frac{SiO_2}{Al_2O_3}$	$\frac{SiO_2}{Fe_2O_3}$	$\frac{Ba}{Sr}$	$\frac{Al_2O_3}{CaO+MgO+Na_2O+K_2O}$	$\frac{Fe_2O_3+MnO}{Al_2O_3}$	$\frac{CaO+MgO}{Al_2O_3}$
0.06	5.06	33.77	2.01	1.80	0.15	0.30
0.72	5.25	29.06	0.66	0.39	0.19	2.34
1.37	4.99	21.99	1.11	0.47	0.23	1.93
2.72	4.67	16.88	1.00	0.58	0.29	1.53
3.92	4.66	20.99	1.47	2.65	0.22	0.23
5.01	4.66	16.81	2.23	2.29	0.28	0.19
5.57	5.07	3.96	1.74	0.94	1.34	0.78
6.19	4.91	31.23	1.51	0.75	0.16	1.09
6.93	5.16	22.64	2.60	1.86	0.24	0.29
8.03	4.89	16.31	1.35	0.89	0.31	0.82
9.92	5.62	19.64	3.89	1.25	0.31	0.59

RK2552

smpl #	depth in core		depth from top of psol			weight percent		and ppm (ppm in italics)					
	(feet)	(meters)	(meters)	Na2O	MgO	Al2O3	SiO2	K2O	CaO	MnO	Fe2O3	Ba	Sr
R1A	341.81	105.00	0.15	1.13	1.55	19.05	63.14	3.26	0.35	*380*	6.61	*500.00*	*270.00*
R2	342.47	105.21	0.36	1.17	1.67	19.09	61.20	2.75	0.23	*260*	5.65	*460.00*	*400.00*
R3	343.77	105.61	0.76	0.78	1.75	16.70	55.76	2.82	5.44	*660*	4.74	*480.00*	*170.00*
R4	345.11	106.02	1.17	0.92	1.75	17.66	56.39	2.92	3.50	*520*	8.10	*580.00*	*160.00*
R5	347.75	106.83	1.98	0.96	1.82	17.85	55.94	2.91	4.53	*500*	6.61	*460.00*	*170.00*
R6	349.73	107.44	2.59	0.82	1.82	17.22	53.38	2.56	5.75	*630*	7.68	*480.00*	*190.00*
R7	350.39	107.64	2.79	0.91	1.74	17.63	52.68	2.44	6.76	*550*	7.05	*420.00*	*200.00*
R8	352.37	108.25	3.40	0.81	1.78	18.54	54.37	2.35	5.44	*430*	7.03	*450.00*	*180.00*
R9	354.35	108.86	4.01	0.98	1.64	19.81	57.37	2.37	3.76	*350*	7.02	*420.00*	*170.00*
R10	355.01	109.06	4.21	0.95	1.49	20.72	58.88	2.33	1.77	*370*	8.03	*400.00*	*160.00*
R11	360.29	110.68	5.83	0.89	1.36	21.15	59.08	2.39	0.53	*340*	9.79	*570.00*	*140.00*
R12	362.93	111.49	6.64	0.95	1.40	20.61	60.25	2.91	0.39	*320*	10.26	*490.00*	*140.00*
R13	364.91	112.10	7.25	0.89	1.18	20.46	59.18	2.80	1.38	*300*	6.60	*540.00*	*150.00*
R14	366.89	112.71	7.86	0.82	1.24	20.77	60.59	2.79	0.65	*230*	7.49	*550.00*	*140.00*
R15	368.21	113.11	8.26	0.70	1.30	20.66	58.50	2.76	0.38	*310*	10.80	*500.00*	*170.00*
R16	370.49	113.81	8.96	1.02	1.48	20.58	61.40	3.51	0.34	*260*	7.11	*670.00*	*140.00*
R17	371.51	114.13	9.28	0.92	1.19	19.15	62.73	2.94	0.32	0.11	6.81	*700.00*	*130.00*

RK2552

molecular ratios

depth (m)	SiO_2 / Al_2O_3	SiO_2 / Fe_2O_3	Ba / Sr	Al_2O_3 / $CaO+MgO+Na_2O+K_2O$	Fe_2O_3+MnO / Al_2O_3	CaO+MgO / Al_2O_3
0.15	5.63	25.38	1.17	1.92	0.23	0.24
0.36	5.44	28.79	0.73	2.00	0.19	0.24
0.76	5.67	31.27	1.79	0.90	0.19	0.86
1.17	5.42	18.50	2.38	1.14	0.30	0.61
1.98	5.32	22.49	1.76	1.02	0.24	0.72
2.59	5.26	18.48	1.62	0.90	0.29	0.87
2.79	5.07	19.87	1.32	0.85	0.26	0.95
3.40	4.98	20.57	1.56	1.01	0.25	0.78
4.01	4.92	21.74	1.60	1.31	0.23	0.55
4.21	4.83	19.49	1.66	1.87	0.25	0.34
5.83	4.74	16.05	2.58	2.50	0.30	0.21
6.64	4.94	15.54	2.26	2.30	0.32	0.21
7.25	4.98	24.19	2.34	2.05	0.21	0.27
7.86	4.90	21.29	2.57	2.39	0.23	0.21
8.26	4.93	14.77	1.87	2.54	0.34	0.19
8.96	4.95	22.43	3.00	2.09	0.22	0.21
9.28	5.32	23.42	3.35	2.31	0.24	0.19

Core #	Smple	Depth (m)	Ca/Sr
2402		0.13	41.0015
2405		0.16	47.3755
2432		0.06	52.3415
2408		0.18	29.3732
		0.58	31.3506
2428		0.08	31.9285
		0.29	11.3677
2552		0.15	20.2849
		0.36	9.0815

APPENDIX C

CORE LOCATIONS, COAL THICKNESS, AND CUMULATIVE THICKNESS OF LOW-CHROMA UNITS AS PERCENTAGE OF TOTAL PROFILE THICKNESS (%LC)

NOTE

1. For sample identification with respect to geographic location, paleosol, and profile unit (i.e., horizon) the following alpha-numeric code is used. For exmaple:

(location)	(paleosol)	(profile unit)
2432	RK	2

refers core 2432, RK refers to the sub-Ames paleosol, and 2 refers to unit 2 in the profile. Other paleosol symbols include;

BC = sub-Brush Creek paleosol, and
PV = sub-Portersville paleosol.

core no.	UTM coordinates x	y	coal*** thknss	%lc	lithology**
705	523646	4447570	0	*	o
706	520616	4444200	0	*	o
2071	500275	4420920	0	*	o
2072	506038	4429020	0	*	o
2073	484330	4417970	0	*	o
2074	511049	4427710	0	*	o
2173	498540	4385800	20	45	c
2174	489550	4391750	0	55	s
2175	488350	4407300	0	11	lm
2176	456560	4382780	45	82	c
2177	444710	4402100	0	98	s
2178	445110	4386150	0	*	lm
2179	475250	4399600	0	17	lm
2181	467200	4380800	0	36	s
2197	483200	4372010	0	42	s
2386	471120	4379790	0	52	s
2387	472100	4384080	0	24	lm
2388	474050	4383150	0	58	s
2401	455820	4377820	0	100	s
2402	453720	4389820	31	67	c
2403	456050	4396130	0	45	s
2404	470330	4391670	47	100	c
2405	469400	4395340	33	72	c
2406	463370	4402720	15	68	c
2407	467590	4402110	0	21	lm
2408	473410	4404210	0	37	lm
2409	479150	4403020	0	12	s
2410	479360	4410180	28	91	c
2411	475420	4412060	0	9	lm
2412	470000	4410000	0	41	s

average %lc relative to lithology of overlying strata

lmst	sh	coal	
11	55	45	
17	98	82	
24	36	67	
21	42	100	
37	52	72	
9	58	68	
12	100	91	
56	45	72	
8	12	38	
34	41	82	
3	44	61	
42	36	100	
13	11		
26	41		
15	90		
	49		
	46		
n=15	n=17	n=12	
21.87	50.35	73.17	mean %lc
14.75	25.19	19.45	s.d.

core no.	UTM coordinates x	y	coal*** thknss	%lc	lithology**
2413	464280	4407400	0	12	lm
2418	473720	4417590	0	44	s
2419	479840	4417610	0	36	s
2420	487020	4415700	0	56	lm
2421	498360	4407630	0	11	s
2422	490820	4420260	0	8	lm
2423	482030	4424110	0	34	lm
2425	494840	4426320	0	3	lm
2426	506430	4417490	0	41	s
2427	468530	4414320	0	42	lm
2428	449350	4394230	0	90	s
2429	457300	4403430	31	72	c
2430	509110	4400400	0	49	s
2431	503240	4493640	13	38	c
2432	497090	4394000	23	82	c
2551	486450	4432020	0	13	lm
2552	499200	4431200	0	26	lm
2553	480740	4437040	47	61	c
2554	511890	4412720	0	46	s
2559	487630	4438820	0	15	lm
2562	513307	4437920	26	100	c
2622	502788	4401760	0	*	o
				n=44	
				47	mean % lc
				28.63	s.d.

*** core descriptions not sufficient to permit calculation of %lc**

**** o=other, c=coal, s=shale, lm=limestone**

***** coal thickness in centimeters**

VITA

Michael R. Caudill was born in Louisa, Kentucky on March 17, 1953. He graduated from Fort Gay High School in Fort Gay, West Virginia in May of 1971. He entered Marshall University in the Fall of 1977 and graduate in May, 1982 (B.Sc. Geology). In September, 1983, he entered Ohio University. His thesis research focused on the sedimentology and provenance of Pennsylvanian-age strata in southeastern New Brunswick, Canada. In September, 1985, before completing his Master's degree, Michael was employed as a Project Geologist by the Ohio Geological Survey and conducted detailed field mapping in the Ohio coal fields. He remained at the Ohio Survey until the summer of 1991, during which time he completed his Master's degree in Geology in December 1989. He entered the Ph.D. program in the Fall of 1991.